

**Role of Residual Bitumen on the Solvent Removal from Alberta Oil Sands  
Gangue**

by

**Siddhant Panda**

A thesis submitted in partial fulfillment of the requirements for the degree of

**Master of Science**

**in**

**Chemical Engineering**

Department of Chemical and Materials Engineering  
University of Alberta

© Siddhant Panda, 2015

## **Abstract**

Non-aqueous extraction technologies are currently being investigated as an alternative to the conventional water based process for extracting bitumen from oil sands. The reduced dependence on fresh water and land for creation of tailing ponds makes non-aqueous technologies a greener alternative. The recovery of solvent from the extracted waste termed as 'gangue' to industrially as well as environmentally acceptable limits remains a major challenge.

Preliminary drying experiments under ambient conditions of the gangue obtained from rich grade ore extraction using cyclohexane exhibited an interesting albeit unexpected physical process. The residual bitumen in the gangue migrated along with the solvent (cyclohexane) to the top of the bed forming a dark bitumen enriched top layer. The deposition of bitumen in the pores could hinder the solvent connectivity and removal from the bed. Understanding the effect of this bitumen migration process on solvent recovery was vital. The residual bitumen and initial cyclohexane composition in extracted gangue were highly variable. To gain an insight into the residual bitumen-solvent interaction during the gangue drying process a control was needed on the composition of the components making up the gangue. An experimental protocol was developed to prepare control samples termed henceforth as 'reconstituted gangue'. These reconstituted gangue samples were representative of the extracted gangue samples obtained after the non-aqueous extraction process.

Reconstituted gangue samples were prepared with residual bitumen as would be expected in extracted gangue for bitumen recoveries in the range 84-96%. Two initial solvent contents of 12 and 8% by net weight of gangue were selected. The water

content was kept constant. The drying experiments were performed with reconstituted gangue inside a fume-hood under ambient conditions for 2 hrs. Three bed heights of 0.6,1 and 1.4 cm were chosen for sample packing. The drying curves had two stages, a fast drying stage and a slow drying stage separated by a breakpoint termed as 'transition time'. It was concluded that the transition time needed to be reached before ending the drying process so as to obtain residual cyclohexane content < 600 ppm. For any bed height, for reconstituted gangue samples with initially 12% cyclohexane, the samples with highest residual bitumen content had the highest final pore volume saturation in the top layer with bitumen, lowest initial 10 min flux and the maximum delay in transition time to occur. Exactly opposite observations were seen with the samples with the lowest residual bitumen content.

Higher bitumen migration was observed for reconstituted gangue samples with 12% initial cyclohexane compared to 8% initial cyclohexane. An initial flux reduction was also seen in reconstituted gangue samples with 8% initial cyclohexane with increase in residual bitumen content though not as obvious as for the 12% initial cyclohexane samples. For reconstituted samples with 8% initial cyclohexane content, the delay in transition time with increase in residual bitumen content though apparent wasn't gradual as in samples with 12% initial cyclohexane but more like a step change after a significant increase in residual bitumen content. For achieving the goal residual cyclohexane content of <260 ppm in 2 hr of drying at ambient conditions the residual bitumen content should be <1.8 wt. % and the bed height <1 cm.

## **Acknowledgements**

During the course of this thesis I have been assisted, guided, motivated and inspired by many wonderful individuals for which I am extremely grateful.

I would like to start with thanking my supervisor Dr. Phillip Choi for his continuous guidance, support and belief in me. His support and innovative approach to problems has helped me deal with the various huddles faced during this thesis. I have learnt from him the importance of having an inquisitive mind in research.

I am grateful to Dr. Murray Gray for getting me involved in this very interesting research project. His challenging questions and insightful responses to my queries helped me gain a better understanding of the work. His wisdom and guidance were vital in helping me complete my thesis.

I am thankful to Dr. Qi Liu for his practical ideas and suggestions to improve the work carried out in this thesis. Dr. Liu also helped me develop an understanding of the mass migration process that was studied here.

I am thankful to Dr. Krupal Pal for her perennial support, lab training sessions and advice that has helped me write this thesis. Dr. Pal showed great patience in dealing with all the day to day project queries I had. The brainstorming sessions we had, to understand the various aspects of this project were highly enjoyable.

I am thankful to Dr. Natalia Semagina, a member of my thesis supervisory committee for her comments that helped me revise my thesis.

I am thankful to intern student Sumeet Merzara for his dedication and sincerity while performing experiments - some of which were incorporated in this thesis.

I would like to thank Dr. Xiaoli Tan, Dr. Abolfazl Noorjahan, Richard Renaud and Lawrence Ejike for their valuable inputs during the group presentations.

I would like to acknowledge the excellent lab technicians at IOSI- Jeremiah Bryksa, Lisa Brandt, Yahui Zhang and Brittany Mackinnon led by Research Associate- Dr. Xiaoli Tan for all the lab equipment setups, trainings and assistance provided by them.

I am thankful to Dr. Cheng Wang from Dr. Thomas Etsell's lab for helping perform the surface tension measurement experiments.

Finally I would like to acknowledge and thank Institute for Oil Sands Innovation (IOSI), Natural Resources Canada (NRCan) and Natural Sciences and Engineering Research Council (NSERC) for funding this project.

# Table of Contents

<b><u>1. Introduction .....</u></b>	<b><u>1</u></b>
1.1 Commercial Extraction Methods .....	1
1.2 Shortcomings of the Aqueous Extraction Method .....	2
1.3 Non-aqueous Extraction Methods .....	3
1.4 Research Goal.....	6
<b><u>2. Drying in Porous Media.....</u></b>	<b><u>8</u></b>
2.1 Liquid Films in Porous Media and their Effect on Drying .....	8
2.2 Drying of Solutions .....	12
2.3 Wettability of Oil Sands Solids.....	15
2.4 Viscosity .....	15
<b><u>3. Methodology.....</u></b>	<b><u>16</u></b>
3.1 The Need for Preparing Synthetic or 'Reconstituted' Gangue .....	16
3.2 Selection Criteria for Composition of Samples Prepared.....	16
3.3 Materials used.....	18
3.4 Protocol – Preparation of Reconstituted Gangue Sample.....	19
3.4.1 Addition of Bitumen .....	20
3.4.2 Addition of Water .....	21
3.4.3 Addition of Solvent .....	22
3.5 Sample Packing.....	23
3.6 Drying Conditions .....	23
3.7 Analytical Techniques.....	26
3.7.1 Residual Solvent Measurement with QICMS .....	26
3.7.2 Bitumen Content Analysis using Elemental Analysis Equipment .....	27
3.8 Wettability Determination.....	28
<b><u>4. Drying and Residual Solvent Content.....</u></b>	<b><u>29</u></b>

4.1 Drying Curve Analysis .....	29
4.1.1 Plotting the Weight Loss Data .....	29
4.1.2 Initial Flux Determination.....	30
4.1.3 Breakpoint or Transition Time Determination .....	31
4.1.4 Final Flux Determination .....	34
4.2 Drying Curves for Extracted Gangue .....	35
4.3 Drying Comparison: Extracted and Reconstituted Gangue .....	37
4.4 Representation of Results .....	40
4.5 Drying of Reconstituted Gangue with 12 and 8% Cyclohexane .....	40
4.5.1 Drying Studies at a Bed Height of 0.6 cm .....	40
4.5.2 Drying Studies at a Bed Height of 1 cm.....	47
4.5.3 Drying Studies at a Bed Height of 1.4 cm .....	54
4.5.4 The Slow Drying Stage and Final Flux .....	61

## **5. Bitumen Migration Studies ..... 64**

5.1 Bitumen Migration and Volatile Loss in Pictures .....	64
5.2 Visual Observations during Drying .....	65
5.3 Bitumen Migration Analysis Methods .....	68
5.3.1 Enrichment Ratio .....	69
5.3.1.1 Enrichment Ratio Comparison for Reconstituted and Extracted Gangue .....	70
5.3.1.2 Enrichment Ratio Comparison for Reconstituted Gangue with Bitumen, Water and 12 or 8% Cyclohexane .....	70
5.3.2 Bitumen Migration Fraction (BMF) .....	74
5.3.2.1 Bitumen Migration Fraction Comparison for Reconstituted and Extracted Gangue .	76
5.3.2.2 Bitumen Migration Fraction for Reconstituted Gangue with Bitumen, Water and 12 or 8% Cyclohexane.....	76
5.4 Pure Cyclohexane and Cyclohexane-Bitumen Solution Drying.....	80
5.5 Pore Volume Saturation with Bitumen .....	84
5.6 Sorptivity Studies .....	87
5.7 Proposed Mechanism of Drying .....	91

## **6. Conclusions ..... 94**

Future Recommendations .....	99
------------------------------	----

---

**References ..... 102****Appendix A ..... 110**

Appendix A.1- Calculations for Reconstituted Gangue Preparation .....	110
Appendix A.2- Calculations for Ratio of Soxhlet Gangue: Cyclohexane-Bitumen Solution in Reconstituted Gangue .....	111
Appendix A.3 – Calibrations of QICMS .....	112
Appendix A.4 – Wettability Determinations using Film Flotation Measurements	115

**Appendix B ..... 116**

Appendix B.1 – Transition Time Interval Determination .....	116
Appendix B.2 –Piecewise Regression Approach .....	122
Appendix B.3-Drying Comparison: Lamp and no Lamp Drying .....	124
B.3.1. Enrichment Ratio Comparison for Lamp and no Lamp Drying Runs .....	127
B.3.2 Bitumen Migration Fraction Comparison for Lamp and no Lamp Drying Runs ....	127

**Appendix C ..... 128**

Appendix C.1 – Development of the Final Equation of Bitumen Migration Fraction .....	128
---	-----

**List of Figures**

Figure 1. 2-D pore network structure showing gas invading the liquid filled pore.  
The gas-liquid interface rests at the ingress of a throat..... 9

Figure 2 (A). The porous bed has 3 regions- gas filled, liquid film and liquid filled.  
(B) Magnified image of a small section of porous bed with 3 different kind of pores.  
..... 11

Figure 3. Flowsheet for synthetic 'reconstituted' gangue preparation ..... 19

Figure 4. The experimental setup. 1-Temperature/Humidity probe, 2- Lamps, 3-  
Balance readings, 4- Camera, 5-CPU and 6- Blackened reflection blocker..... 24

Figure 5. Sample representation of weight loss data. CH = cyclohexane, W = water and 1 cm is the sample bed height. All the samples had 3.7% water on a solvent free weight basis.....	29
Figure 6. Average initial flux determination. ....	30
Figure 7. Transition from fast drying stage to slow drying stage. The boxed area is the region/interval where the breakpoint lies.....	32
Figure 8. Piecewise regression fit in the transition time interval with 95 percent confidence interval for the breakpoint estimated.....	33
Figure 9. Average final flux determination. ....	34
Figure 10. Drying curves for extracted gangue.....	35
Figure 11. Dimensionless drying curves for extracted gangue. ....	36
Figure 12. Extracted and reconstituted gangue drying curves. ....	38
Figure 13. Cumulative weight loss curves for bed height 0.6 cm, 12% cyclohexane, 0.5-2% Bit.C and 3.7% water.....	41
Figure 14. Cumulative weight loss curves for bed height 0.6 cm, 8% cyclohexane, 0.5-2% Bit.C and 3.7% water.....	41
Figure 15. Initial drying flux comparison at different cyclohexane (CH) contents, bed height= 0.6 cm.....	43
Figure 16. Transition time comparison at different cyclohexane (CH) contents, bed height= 0.6 cm.....	44
Figure 17. Residual cyclohexane content (ppm) vs Bit.C% for a bed height of 0.6 cm, 12% CH.....	46
Figure 18. Residual cyclohexane content (ppm) vs Bit.C% for a bed height of 0.6 cm, 8% CH. ....	46

Figure 19. Cumulative weight loss curves for bed height 1 cm, 12% cyclohexane, 0.5-2% Bit.C and 3.7% water.....	48
Figure 20. Cumulative weight loss curves for bed height 1 cm, 8% cyclohexane, 0.5-2% Bit.C and 3.7% water.....	49
Figure 21. Initial drying flux comparison at different cyclohexane (CH) contents, bed height= 1 cm .....	50
Figure 22. Transition time comparison at different cyclohexane (CH) contents, bed height= 1 cm .....	51
Figure 23. Residual cyclohexane content (ppm) vs Bit.C% for a bed height of 1 cm, 12% Cyclohexane (CH).....	53
Figure 24. Residual cyclohexane content (ppm) vs Bit.C% for a bed height of 1 cm, 8% cyclohexane (CH) .....	53
Figure 25. Cumulative weight loss curves for bed height 1.4 cm, 12% cyclohexane and 3.7% water.....	55
Figure 26. Cumulative weight loss curves for bed height 1.4 cm, 8% cyclohexane and 3.7% water.....	55
Figure 27. Initial drying flux comparison at different cyclohexane (CH) contents, bed height= 1.4 cm.....	57
Figure 28. Residual cyclohexane content (ppm) vs Bit.C% for a bed height of 1.4 cm, 12% cyclohexane initially.....	58
Figure 29. Residual cyclohexane content (ppm) vs Bit.C% for a bed height of 1.4 cm, 8% cyclohexane initially .....	59
Figure 30. Residual cyclohexane content (ppm) vs duration of slow drying stage .	60
Figure 31. Drying curves for showing the effect of water during the slow drying stage, CH = Cyclohexane, W = Water.....	62

Figure 32. Bitumen migration leading to thicker dark top layer.....	64
Figure 33. The top layer stays the same thickness, the middle lighter layer increases in thickness.....	64
Figure 34. The gangue bed at the end of drying. Sample: 1% Bit.C, 12% CH, 3.7% W, bed height = 1 cm.....	64
Figure 35. A cross section of the top view image for: A) Reconstituted sample with bitumen, 12% cyclohexane and water B) Reconstituted sample with bitumen, 8% cyclohexane and water .....	67
Figure 36. Enrichment ratio comparison at different cyclohexane (CH) contents, bed height= 0.6 cm.....	71
Figure 37. Enrichment ratio at different cyclohexane contents, bed height= 1 cm	72
Figure 38. Enrichment ratio comparison at different cyclohexane contents, bed height= 1.4 cm.....	73
Figure 39. Bitumen migration fraction comparison at different cyclohexane contents, bed height= 0.6 cm.....	77
Figure 40. Bitumen migration fraction comparison at different cyclohexane contents, bed height= 1 cm .....	78
Figure 41. Bitumen migration fraction comparison at different cyclohexane contents, bed height= 1.4 cm.....	78
Figure 42. Cyclohexane-Bitumen solution drying, showing thin liquid film rising ...	81
Figure 43. Drying curves for cyclohexane, 5.30 and 15.70 wt. % initial bitumen ..	82
Figure 44. Drying flux plots for cyclohexane, 5.30 and 15.70 wt. % initial bitumen ..	83
Figure 45. Final vs initial pore saturation vol. % in the top layer with bitumen .....	85

Figure 46. Viscosity of toluene-bitumen mixture vs toluene weight fraction. The experimental viscosity values are from Guan [50] .....	90
Figure 47. Calibrations for volume in the range 0.2-0.8 ul.....	113
Figure 48. Calibrations for volume in the range 0.2-30 ul.....	114
Figure 49. Calibrations for volume in the range 30-75 ul.....	114
Figure 50. Cumulative weight loss vs time plot .....	117
Figure 51. MSE vs start time for a 30 min moving linear fit. ....	117
Figure 52. High MSE data range (70-100 min).....	119
Figure 53. Low MSE data range (90-120 min).....	119
Figure 54. MSE vs start time for a 40 min moving linear fit. ....	120
Figure 55. MSE vs start time for a 20 min moving linear fit. ....	121
Figure 56. MSE vs start time for a 10 min moving linear fit. ....	121
Figure 57. Piecewise regression fit in the transition time interval. The transition time interval was obtained using the procedure given in Appendix B.1 .....	123
Figure 58. Lamps and without lamps drying curves. ....	125

## List of Tables

Table 1. Mass fractions and weights used for recovery calculations.....	18
Table 2. The bitumen associated C contents (weight %) of extracted gangue. ....	37
Table 3. Initial flux, transition time and final flux .....	38

Table 4. Initial flux and final flux for drying curves of samples with 0.5% Bit.C, 12% CH, with and without water and drying curve for water.....	62
Table 5. Enrichment ratio of extracted and reconstituted gangue. ....	70
Table 6. Top layer weight comparisons for 12 and 8% cyclohexane containing samples.....	72
Table 7. Bitumen migration fraction of extracted and reconstituted gangue.....	76
Table 8. Composition of Reconstituted gangue.....	111
Table 9. Ratio of Soxhlet gangue: Cyclohexane bitumen solution in Reconstituted gangue .....	112
Table 10. Initial flux, transition time, final flux comparison (lamps and no lamps) .....	126
Table 11. Enrichment ratio comparison (lamps and no lamps) .....	127
Table 12. BMF comparison (lamps and no lamps).....	128

# 1. Introduction

Oil sands aka tar sands are deposits of unconsolidated sand containing high molar weight and extremely viscous petroleum referred to as bitumen [1]. Canada and Venezuela are two of the world's largest oil sands reserves. The largest deposit of oil sands in Canada lies in Alberta with proven reserves of 168 billion barrels, making it the third largest crude oil reserve in the world as of now [2]. About 3% of the oil sands area comprising 20% of the oil sands reserves in Alberta can be mined, the rest being too deep for mining applications [2]-[4]. In the year 2014, 2.3 million barrels per day of crude bitumen was produced in Alberta. Surface mining and in situ productions accounted for 45% and 55% of the net production respectively [5]. Bitumen is upgraded to synthetic crude oil and diesel. Off-gases and mixtures of alkanes and alkenes in gaseous form are also produced that acts as feed for the petrochemical industry of Alberta [5].

## 1.1 Commercial Extraction Methods

Steam assisted gravity drainage (SAGD) method is employed for oil sands reserves deemed too deep for mining operations. This method involves using steam to heat the bitumen in a horizontal well to a temperature where it can flow by gravity to a lower well. This is followed by pumping the bitumen to the surface [4]. The impact on surface for SAGD operations is similar to conventional oil operations [4] .

This thesis is based on extraction of oil sands obtained from the mineable reserves of oil sands. Clark's hot water extraction process, the basis for current extraction

technologies for mineable oil sands reserves was first implemented on a large scale by Suncor Energy Inc. (Then Great Canadian Oil Sands) in 1967 [1].

The first step for the hot water extraction process involves open pit mining of the oil sands reserves. The oil sands lumps are next crushed and mixed with hot water. This is the conditioning step. Further the oil sands slurry is passed through to hydro-transport pipelines or tumblers where bitumen is released from the sand. With the slurry chemical additives may be added. Bitumen is aerated in the hydro-transport pipelines. Finally the slurry is passed onto separation vessels where the aerated bitumen rises up and is skimmed and collected. [1]

Typically bitumen recovery in commercial applications is in the range 88-95% [1].

## 1.2 Shortcomings of the Aqueous Extraction Method

Oil sands extraction process using the convention method is made possible due to the hydrophilic nature of the sand grains in oil sands [6]. This ability to use water to extract the oil sands also has been the dominant cause for most of the issues facing the conventional extraction process today. The extraction of bitumen from oil sands requires huge amounts of fresh water withdrawal from Athabasca River. The year 2013 saw almost 103 million m<sup>3</sup> of water withdrawn from the Athabasca River [7]. Excess water withdrawal might affect the ecological sustainability of the river [8].

Tailings, the waste generated after bitumen extraction in the conventional method is composed mainly of sand, water and clay with some residual bitumen. Tailings also contain toxic chemicals and can't be discharged directly into a water body or ground surface [9]. To effectively contain tailings in the form of tailings ponds, large dam or

dyke systems need to be built [10]. The total area occupied by tailing ponds and associated dykes was 220 km<sup>2</sup> in 2013 [11]. The bottom layer in the tailings pond takes decades to settle and dry out making land reclamation extremely difficult [9]. More than \$1 billion has been invested by oil sands operators for the development of tailings reduction technology [9]. The tailing ponds by themselves also pose a risk to surrounding wildlife especially to waterfowls due to the toxic nature of chemicals present [9]. Due to the nature of current technologies for oil sands extraction the need for tailings ponds would always be there [12].

### 1.3 Non-aqueous Extraction Methods

Non aqueous extraction technologies can reduce the fresh water demand greatly and remove the need for the creation of tailings ponds. These potential advantages along with higher potential bitumen recovery is what has motivated the development of solvent based oil sands extraction technologies in the past [13].

Coulson[14] outlined the primary basis of operation for most solvent based extraction processes i.e. choosing solvents capable of dissolving most of the bitumen. It was advised to take precautions to avoid solvent losses if low boiling liquid hydrocarbons such as benzene, xylene etc. were used. Higher boiling petroleum fractions such as naptha, kerosene and gas oil were recommended to reduce overall solvent losses and still achieve satisfactory recoveries. Aromatic or olefinic solvents due to better solubility of the constituents of bitumen were recommended over paraffinic solvents.

For solvent based extraction processes to be economical a high degree of solvent recovery from the fines and coarse waste solids needs to be maintained [15]. Hanson et al. [15] achieved this using toluene and other aromatic solvents. Their process

involved heating up the solvent though and seemed to have a high energy consumption. Aiming to reduce the losses of the solvent and lower the energy consumption yet achieving high yields of tar or bitumen, Blaine et al. [16] patented the use of trichloroethylene at a typical temperature of 300 °F and pressure of 50 Psig. Bitumen yields of over 99 vol. % were achieved with solvent losses less than 0.5 vol. %.

Benzene, toluene and kerosene along with other solvents as potential bitumen extraction solvents were studied by Leung et al. [17]. Solvents with either high aromatic compound content or low boiling point were determined to be good solvents for bitumen. Meadus et al. [13] found kerosene and naptha preloaded with bitumen for enhanced aromatic content (to improve solvency) were satisfactory solvents for dissolving bitumen and extracting it from oil sands. They used a slowly rotating cylindrical mill having iron rods acting as the mixing medium.

Despite all these advances in solvent extraction methods none could be established commercially. The major factor being the difficulty in removing the solvents from the extracted waste of oil sands coupled with sustaining a high bitumen recovery [8].

Increased concerns about the sustainability of Athabasca River and detrimental impact of tailings ponds on environment has renewed the interest in solvent based extraction processes in the recent years [8]. Wu and Dabros [18] developed a light hydrocarbon solvent based extraction process. The solvent-bitumen solution was separated from the solids by either regular pressure filtration or centrifugal filtration. Finally the solvent which stayed behind in the filter cake was evaporated under vacuum conditions. Of all the solvents tested which included toluene, cyclo-pentane,

hexane, n-pentane, mixture of n-pentane and cyclo-pentane; cyclo-pentane was stated as the best solvent. This was based on its high bitumen recovery and low boiling point. The bitumen recoveries using cyclo-pentane for both high and low grade ores were comparable to the conventional water based process.

Hooshiar et al. [19] used 4 different ratios of toluene to heptane to observe their effect on recovery for good and poor processing ores. The extraction procedure involved tumbling action and agitations via rotary mixer for better solvent-bitumen interactions. The bitumen recovery from poor processing ore was found to decrease with decrease in toluene amount. The extraction procedure was carried out at room conditions and produced bitumen with less than 0.5 wt. % solids and water. The total bitumen recovery achieved for both the types of ores was higher than 96%.

Nikakhtari et al. [8] carried out extractions using various pure solvents and blends following a lab scale extraction process similar to Hooshiar et al. [19]. They came up with the conclusion that cyclohexane was a potential solvent for extracting bitumen from oil sands. This conclusion was based on the high bitumen recovery (>94%) , low amounts of fines migrating to the bitumen product and rapid drying achieved from the spent waste termed as 'gangue' [8].

Though the fine migration to the bitumen product as observed by Nikakhtari et al. [8] was low , it was still higher than the maximum allowable solid concentration for pipeline transport. Solvent mixtures of cycloalkanes and n-alkanes were prepared and studied by Pal et al. [20] to observe the effect of solubility parameter of the solvent mixture on the fine solids migrating to the bitumen product. The fine solids migrating to the bitumen product at any given solubility parameter was found to be

sensitive to the solvent mixtures composition which was unexpected. Cycloalkane/n-pentane blends were found to have the lowest amount of fines migrating to the bitumen product.

Richard [21] worked with the gangue produced from the extraction process described in Nikakhtari et al. [8] and Pal et al. [20]. The effect of temperature and pressure on the removal of cyclohexane was studied. An initial cyclohexane content of  $11.8 \pm 2.1$  wt. % or  $118,000 \pm 21000$  ppm was reported for the extracted gangue from rich grade ore. Alberta regulations for water based extraction processes requires that less than 4 volumes of solvent remains in the tailings per thousand volumes of extracted bitumen [22]. This was considered as a benchmark for the dried waste of the solvent based extraction process. 4 volumes of solvent/1000 volumes of bitumen for an average grade ore with 10 wt.% bitumen translated to about 260 mg residual solvent/1 kg of gangue [8], [21]. Cyclohexane release mass flux (from gangue) was found to increase with increasing temperature and a decrease in pressure. Migration of residual bitumen in the rich grade gangue bed was observed which formed a dark top layer enriched with bitumen. The effect of this bitumen migration on solvent removal from the gangue bed wasn't discussed.

## 1.4 Research Goal

Bitumen deposition and migration could possibly hinder the solvent connectivity in the bed affecting the solvent removal efficiency from the gangue. The research goal for this thesis hence was to investigate the effect of residual bitumen and initial cyclohexane in gangue samples on the recovery of cyclohexane while drying under ambient conditions.

Ultimately this knowledge can help with the modelling of the drying process of the spent waste of cyclohexane based extraction process and serve as a guideline for designing an effective drying technique that can be utilized by the industry.

Because the use of both high temperature and vacuum was energy intensive, bitumen migration phenomena inside the porous gangue bed and its effect on drying was studied under ambient conditions.

## 2. Drying in Porous Media

### 2.1 Liquid Films in Porous Media and their Effect on Drying

A porous media can be considered to be a network of pores connected to each other by throats [23]–[27]. Throats are narrower and generally have higher capillary forces compared to pores [25]. In three dimensional space, pores can be thought as spheres and throats as cylinders [25]. Drying in porous media involves displacement of the evaporating fluid by a non-wetting gas/air [28], [29]. When the capillary forces dominate over viscous forces, the displacement pattern of the subsiding liquid interfaces can be described well by the theory of invasion percolation [25], [29]. Capillary number is defined as the ratio of viscous forces to surface tension forces, it is used to identify if capillary forces are dominant [23].

Invasion percolation theory describes the displacement process to be taking place at constant flow rate [25]. In drying the pore throat invaded by air at each time step is that with the least capillary resistance i.e. having a wider diameter [25], [30]. The theory of invasion percolation in a stabilizing gradient is used to describe the displacement pattern if viscous forces or/and gravity forces in the liquid and gas phases become significant [30], [31].

Prior to Yiotis et al.[26] studies related to modelling of drying processes didn't incorporate the effect of liquid films on drying. To understand how drying in porous media was assumed and modelled before, we refer to Yiotis et al. [27] . In this study [27], the porous medium was modelled as a 2D network of pores with only a single permeable side as shown in Figure 1.

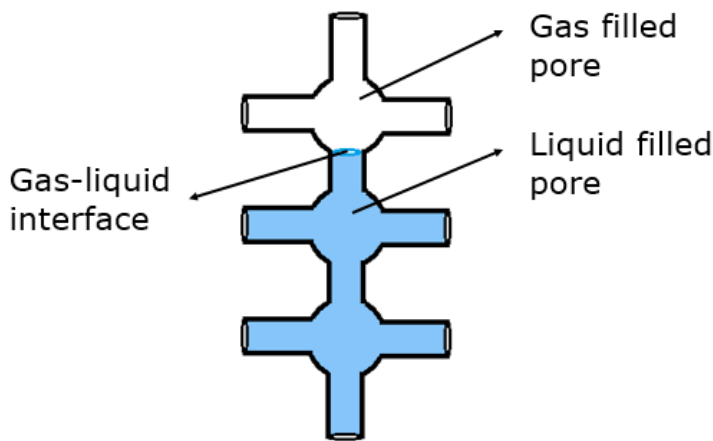


**Figure 1. 2-D pore network structure showing gas invading the liquid filled pore. The gas-liquid interface rests at the ingress of a throat.**

The pore bodies act as repositories for both the gas and liquid phases. They are assumed to have no flow or capillary resistance. The throats are the capillary barriers and control the flow and mass transfer occurring. The presence of a stationary gas-liquid interface at the ingress of a throat neighboring a liquid pore (Refer Figure 1) leads to the development of an interfacial pressure difference ( $P_c$ ) which can be estimated by equation (1) –

$$P_c = \frac{2\gamma}{r} \quad (1)$$

Where  $\gamma$  is the surface tension of the fluid and  $r$  is the throat radius.

The gas-liquid interface remains immobile until the threshold capillary pressure given by (1) is surpassed by the pressure difference between the two pores. Once surpassed, the interface recedes instantly due to the assumptions of null throat volume and capillary resistance inside the pore bodies.

On the contrary, Yiotis et al. [26] reported that in realistic pore geometries the displacement of meniscus (gas-liquid interface) should be followed by liquid films formation along the surface of the pore. Their study involved macroscopic films in capillary porous media which provide hydraulic conductivity for the falling liquid and can hence help in the transport of mass to the evaporating surface. Further transport of mass into the gas phase is assumed by diffusion.

To calculate the pressure in liquid films Yiotis et al. [26] used Young-Laplace's equation as shown in equation (2) which relates the pressure difference ( $\Delta P$ ) between two phases,

$$\Delta P = \gamma \left( \frac{1}{R_1} + \frac{1}{R_2} \right) \quad (2)$$

Where  $\gamma$  is the surface tension of liquid film,  $R_1$  and  $R_2$  are the two principal radii of curvature.

The pressure in the liquid film ( $P_l$ ) is given by –

$$P_l = P_g - P_c = -\frac{\gamma}{r} \quad (3)$$

Where  $P_g$  is the gas phase pressure,  $P_c$  is the capillary pressure and  $r$  is the radius of curvature which is a function of time and position/distance. A decrease in film radius can be expected when a film gets closer to the evaporating surface. This leads to the generation of a flow upwards driven by capillarity.

The pore structure inside a porous bed as described by Yiotis et al.[26] with only a single open boundary (top) is shown in Figure 2. There can be disconnected liquid clusters present in the liquid film region.

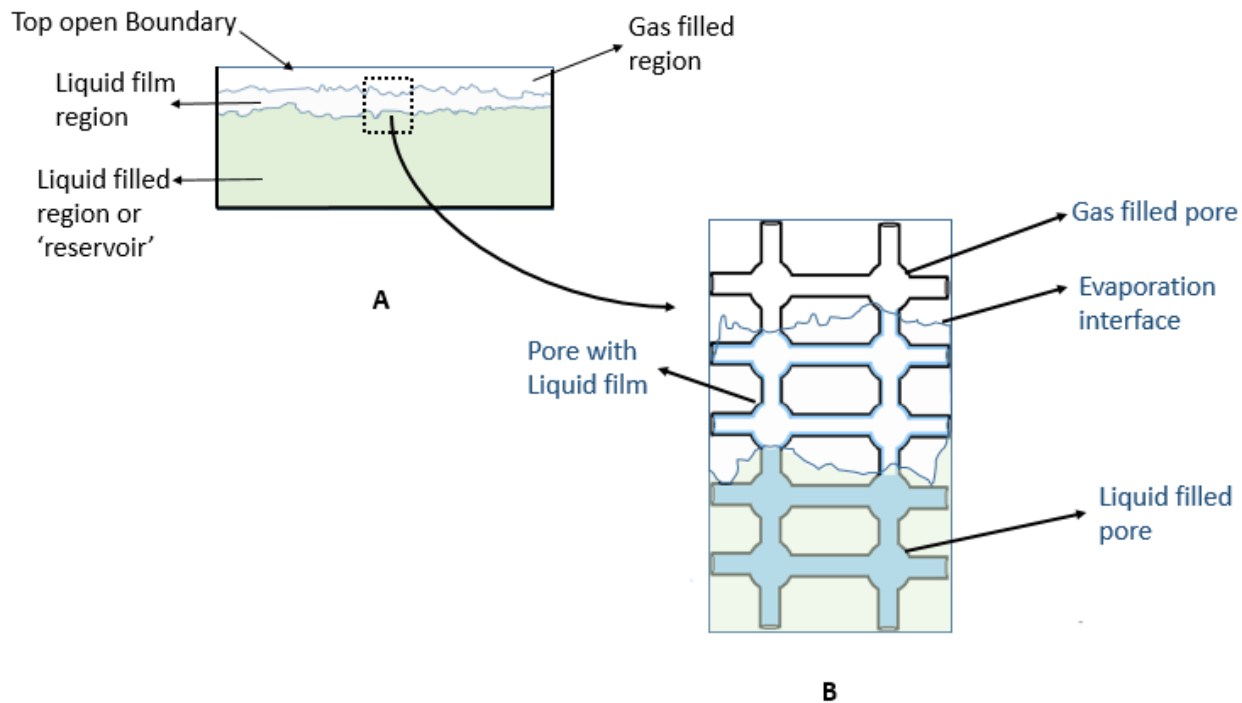


**Figure 2 (A).** The porous bed has 3 regions- gas filled, liquid film and liquid filled. **(B)** Magnified image of a small section of porous bed with 3 different kind of pores.

Yiotis et al.[26] concluded liquid film flow to be a major transport mechanism providing liquid to the evaporating surface in capillary porous media. The nearly constant drying rate during stage 1 of evaporation is due to the existence of these hydraulic connections maintained by liquid films between the liquid filled interior region (Reservoir in Figure 2) and the evaporating surface [32]–[37]. Liquid films when present lead to much faster drying rates [33], [38], [39]. All the evaporation takes place near the film tips where large concentration gradients exist [26]. The fine pores at the surface of porous media act as the preferred locations for liquid

vaporization during the stage 1 of evaporation [37]. The gas phase in the pores below remains saturated and very little/no evaporation takes place there [26]. If film flow dominates, the temperature effects (due to non-isothermal conditions) become trivial [26] . The liquid connection to the top is broken when the upward capillary forces are balanced by the gravitational forces acting downwards. This causes the gas-liquid interface to regress into the porous media [36].

Presence of liquid films can be neglected in non-wet porous media [33], [39], [40] and stage 1 of evaporation is expected to be non-existent in them [33]. The primary means of mass loss in non-wet porous media is through vapor diffusion (no associated liquid flow) [33]. Progressively shorter duration of stage 1 evaporation of water has been observed with increase in hydrophobic fractions of sand grains [33], [36]. These studies indicate capillary forces to weaken with increase in hydrophobicity of particles.

## 2.2 Drying of Solutions

Thick liquid films play an important role in the drying of salt water solutions and in the transport and distribution of dissolved salt in capillary/hydrophilic porous media [39], [41], [42] . An analogy has been made between dissolved salt migration during drying of salt solution in porous bed and bitumen migration observed during the drying of cyclohexane extracted gangue [21]. Bitumen migration and its effect on solvent recovery is the crux of this work. A study of salt migration in porous beds it seems can provide us with some insight into the solvent recovery from gangue.

NaCl ions present inside the pore space fraction occupied by liquid phase can move by diffusion (Brownian movement) and by advection. Brownian motion will tend to

distribute the ions uniformly whereas convection/advection tends to transport the ions with the bulk liquid to the evaporation surface [39]. Convective transfer of ions can lead to their high concentration at the surface of the porous structure, with salt crystallization occurring when concentration is sufficiently high [39], [43], [44]. NaCl crystallization can occur at the surface of porous media(efflorescence) or inside the porous media (subflorescence) [43].

Peclet number ( $Pe$ ) is used for determining which of diffusive or convective transport is dominant [37], [39], [43], [45] and is given by -

$$Pe = \frac{V * l}{D} \quad (4)$$

Where  $V$ ,  $l$  and  $D$  represents the average interstitial velocity, characteristic length of the pore space and effective salt diffusion coefficient respectively.

$Pe$  greater than 1 indicates that the rate of transport by advection to be greater than that by diffusion and gives rise to a higher salt concentration near the porous sample surface [39]. Salt deposition is seen preferentially in the fine pores at the surface when these pores are supplied with fluid due to capillary liquid flow [37].

As the liquid films in the porous media recede from the surface to inside the material during evaporation, subflorescence can be formed [39].

In concentrated salt solutions drying in saturated porous media, the solution flow to the evaporative surface can lead to high salt concentrations near the surface. At these high concentrations, chemical potential of solution near the surface is reduced with respect to the interior bulk solution and can limit the drying [44]. Once the saturation

salt concentration is reached near the top, the chemical potential for water becomes constant and excess salt precipitates out [44]. This process is expected to continue till a continuous hydraulic connection to the surface of porous media exists [44].

Slower drying rate at higher salt concentrations has also been attributed to the reduction in sorptivity [46]. Sorptivity is a property which expresses the propensity of a material to absorb and transmit fluids by capillarity [46], [47]. It depends both on the material and fluid and is given by –

$$S = \left(\frac{\sigma}{\mu}\right)^{\frac{1}{2}} S' \quad (5)$$

Where  $\sigma, \mu$  are the surface tension of fluid (mN/m) and its viscosity (cP) respectively.  $S'$  is the intrinsic sorptivity of the material. Hence using different fluids the sorptivity with respect to the material would scale with  $\left(\frac{\sigma}{\mu}\right)^{\frac{1}{2}}$  [46], [47].

Bitumen migration in cyclohexane extracted gangue drying studies [21] indicates that liquid films (Cyclohexane possibly since it can dissolve bitumen) might exist in the porous gangue bed all the way to the surface. Since hydraulic connectivity has the connotation of liquid water films, and gangue bed contains both solvent and water, with solvent possibly forming liquid films the term 'capillary connectivity' will be used instead.

To validate the hypothesis of presence of liquid films, the wettability of the solids constituting the gangue needs to be measured. Bitumen that migrates in the gangue bed is the residual bitumen. The residual bitumen content in the gangue depends on the efficiency of bitumen recovery using the lab scale process [8]. Since varying

residual bitumen content can affect the viscosity and surface tension of bitumen-fluid solution inside the pores of gangue, different sorptivities can be expected.

## 2.3 Wettability of Oil Sands Solids

Oil sands solids are composed of two main fractions namely coarse solids (106-250 µm) and fines (<45 µm). Dang-Vu et al. [48] worked on the determination of most sensitive method for wettability characterization of these 2 fractions. The solids were isolated following water based extraction in a Denver cell. Water drop penetration time and Contact angle measurements worked best with fines [48]. For coarse solids, Film flotation technique and particle partition measurements gave the best results[48].

Recently Wang et al. [49] determined wettability of fine solids obtained from Alberta oil sands by non-aqueous (solvent based) extraction [49]. They stated that Non-aqueous extraction has higher bitumen recovery compared to water based processes which can render fines more hydrophilic. Hence they argued the applicability of wettability characterization techniques stated in [48] to their solids. Film flotation method was deemed most appropriate by them for assessing the hydrophobicity/hydrophilicity of fine solids.

## 2.4 Viscosity

The viscosity of bitumen-toluene mixtures have been experimentally determined for toluene weight fractions 0.05-0.60 [50]. To approximate bitumen-cyclohexane viscosity ratios at different weight fractions we can use bitumen-toluene viscosity ratios at these weight fractions as a first approximation.

### 3. Methodology

#### 3.1 The Need for Preparing Synthetic or ‘Reconstituted’ Gangue

The extracted gangue samples contain cyclohexane along with residual bitumen and connate water. The residual bitumen, cyclohexane and fines contents of this extracted gangue are difficult to control as the batch varies with each extraction [21]. Conducting drying studies with an initial product this variable is prone to give us non comparable results. A controlled or ‘reconstituted gangue’ can provide us with an insight into the complex interplay between the solvent, residual bitumen and fines during the gangue drying process.

Replicating the extracted gangue by creating a reconstituted gangue for systematic drying studies can be challenging [21]. The goal ergo, wasn’t achieving the perfect imitation of extracted gangue but to create a starting material with controlled parameters that could somehow reflect the drying behaviour of extracted gangue. Further the insight achieved would be helpful in the development of a model on solvent recovery from gangue which requires a systematic study on the effects of varying solvent and residual bitumen contents.

#### 3.2 Selection Criteria for Composition of Samples Prepared

The composition of reconstituted gangue samples prepared was based on gangue obtained from non-aqueous extraction of rich grade Athabasca oil sands ore. The cyclohexane content of extracted gangue varies from 8-18% by weight with a mean and standard deviation of  $11.8 \pm 2.1\%$  [21]. Based on this, reconstituted samples with about 8 and 12% by weight of cyclohexane were prepared. A constant water

content of 3.7% by weight (on cyclohexane free basis) was maintained. The water content is within the range of what has been reported previously by [8] and [51].

0.5 to 2.0 wt. % bitumen associated carbon or bitumen carbon (Bit.C that corresponds to 0.6-2.4 wt. % bitumen) on a dry gangue weight basis, was added to the Soxhlet sand (Soxhlet gangue) to prepare the reconstituted gangue. Bitumen associated carbon refers to the organic carbon whose source is bitumen. The sources of carbon in the samples prepared are bitumen and inorganic materials. Hence subtracting the inorganic C wt. % in the prepared samples from the net measured C wt. % in the sample gave us the Bit.C%. The inorganic C wt. % in the samples was the C wt. % of the Soxhlet gangue used to prepare the reconstituted gangue.

Bitumen recoveries of greater than 90% has been achieved previously for rich grade ore with cyclohexane as solvent [8]. Reduction in bitumen recovery can be expected when scaling up the process to industrial scale. Hence the bitumen added to prepare reconstituted gangue was so as to correspond with residual bitumen in extracted gangue when recoveries in the range 84-96% are achieved.

The equation used to calculate bitumen recovery as mentioned in [8] is as follows-

$$\text{Bitumen Recovery \%} = (1 - A * B) * 100 \quad (6)$$

$$\text{with } A = \frac{W_t - W_s}{(W_o - W_s)(W_b - W_t + W_s)} \quad (7)$$

$$\text{and } B = (W_b - W_o + W_s) - \frac{M_c}{M}(W_b - W_c + W_s) \quad (8)$$

Where  $W_t$ ,  $W_s$ ,  $W_o$ ,  $W_b$ ,  $W_c$  are the mass fractions of C in dried gangue, Soxhlet gangue, oil sands ore, bitumen and dried centrifuge solids respectively.  $M$  and  $M_c$  represent the mass of ore and centrifuge solids.

The calculations of recovery done here was based on –

**Table 1. Mass fractions and weights used for recovery calculations**

$W_t * 100$	$W_s * 100$	$W_o$	$W_b$	$W_c$	$M$	$M_c$
0.83/1.33/1.83/2.33	0.33	0.11	0.84	0.22	150.00 g	0.23 g

The values for  $W_s$ ,  $W_o$ ,  $W_b$ ,  $M$  are from reported values [8] while for  $W_c$  and  $M_c$  the values used are in the mentioned range. The range of  $W_t - W_s$  values in Table 1 coincide with 0.5-2 wt. % Bit.C. It should be noted that the values used here are so as to get a rough estimate of recovery. 0.5% Bit.C corresponds to a very high recovery of 96% whereas 2% Bit.C corresponds to a low recovery of about 84%.

### 3.3 Materials used

The sample of rich grade oil sands ore used was provided by Syncrude Canada Ltd. The bitumen and water contents of rich grade ore as measured by dean stark extractions was  $13.5 \pm 1.1$  wt.% and  $3 \pm 0.9$  wt.% ( $n=6$  for both). The fines content of the ore was measured by particle size analyzer to be  $11.2 \pm 0.7$  wt. % ( $n=3$ ). The remainder of mass was coarse solids. Toluene (Certified ACS grade, Fischer Scientific, USA) was used for the Dean Stark extraction of the oil sands ore to obtain the coarse and fine solids which make up the Soxhlet gangue. The Soxhlet gangue was coated with Athabasca bitumen provided by Syncrude. Cyclohexane (Certified ACS grade,

Fischer Scientific, USA) and demineralized water were added to prepare the reconstituted gangue.

### 3.4 Protocol – Preparation of Reconstituted Gangue Sample

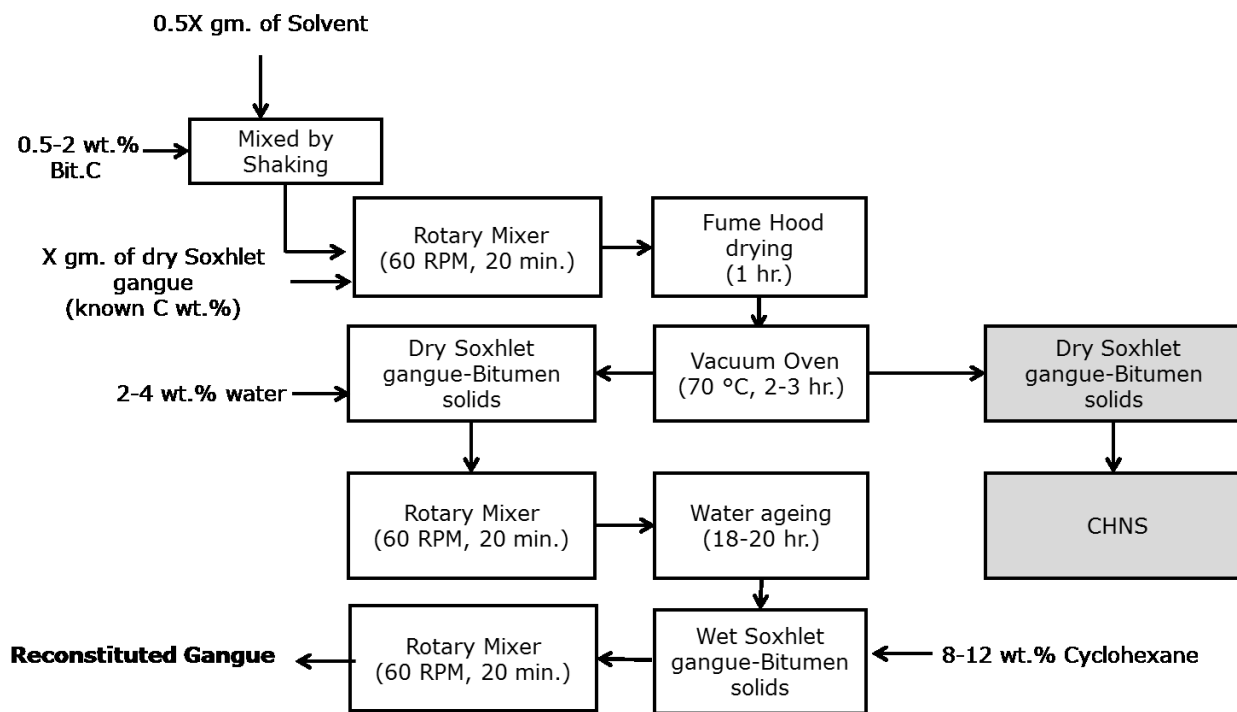


**Figure 3. Flowsheet for synthetic 'reconstituted' gangue preparation**

The above figure shows the protocol developed to prepare the 'reconstituted' gangue in this study. All of the steps shown in the flowsheet were carried out at room temperature ( $21 \pm 1$  °C) and ambient pressure conditions and will be explained in detail below.

While preparing the protocol it was assumed that the residual bitumen, initial water and cyclohexane in the extracted gangue is distributed uniformly. This is a valid assumption considering that the steps involved in non-aqueous extraction of bitumen

involves mixing and sieving [8] that should form an almost homogeneous product (i.e. uniformly distributed bitumen, water and cyclohexane in gangue).

### 3.4.1 Addition of Bitumen

The clean sand (Soxhlet gangue) used for reconstitution was obtained from complete drying of the Soxhlet sand collected after the Dean stark extraction procedure of rich grade ore with toluene. The Soxhlet gangue can be expected to contain no organic carbon content due to the exhaustive nature of the procedure. Previously it has been reported that using cyclohexane the fines migrating to the bitumen product was < 0.7 wt. % of the initial ore for low-medium fines rich grade ore as used in our case [8], [52] and can be as high as 1.3 wt.% of initial ore for high fines medium grade ore. The rest of the solids are retained in the extracted gangue. Hence in our case, the use of Soxhlet gangue to prepare reconstituted gangue is justified since it is made up of almost the same composition of coarse and fine solids as in the extracted gangue. About 50-250 g of Soxhlet gangue was used for reconstituted gangue preparation per batch. 0.5\* Soxhlet gangue weight of cyclohexane was mixed with the required 0.5-2.0 wt. % Bit.C to form the cyclohexane-bitumen solution. Teflon bottles were used to store the Soxhlet gangue and cyclohexane-bitumen solution.

To add the residual bitumen to the Soxhlet gangue during reconstituted gangue preparations it needs to be mixed with cyclohexane which can dissolve it and allow for its uniform distribution in the gangue. It might be argued that the cyclohexane-bitumen solution in required final ratio or amounts can be added directly to the Soxhlet gangue. Though this seems less complicated compared to all the steps mentioned in the protocol, it would have required us to mix Soxhlet gangue:

cyclohexane-bitumen solution in the ratio 6-11:1 (On weight basis, depending on the composition of reconstituted gangue, refer Appendix A.2). We cannot possibly expect a uniform mixture of Soxhlet gangue and solution at this high a ratio. This is why sand: cyclohexane-bitumen solution used in the protocol was much lower i.e. 2:1. At this ratio we achieved a proper washing of Soxhlet gangue with the solution to form slurry. The mixing was done using a rotary mixer at 60 rpm for 20 min. The next step in protocol involved drying off most of the solvent from the slurry. The slurry was poured into a sieve bottom/large glass beaker and was continuously mixed manually during its drying inside a fume-hood. This step ensured uniform bitumen distribution in gangue. An alternate to this was to dry the solution till we achieved the required ratio of sand: solution i.e. 6-11:1. This however was difficult to perform owing to the bitumen migration taking place during excess solvent removal by drying which had to be negated by continuous mixing. Mixing was vital to bitumen distribution in the sample but made it difficult to monitor the solvent losses.

To ensure complete cyclohexane removal, the product from the previous step was put into a vacuum oven at 70 °C for 2-3 hr. The bitumen coated Soxhlet gangue produced from this step was called Dry Soxhlet gangue bitumen solids or DSBS. Some of the DSBS was used for elemental analysis using the CHNS. For more on the CHNS analysis please refer to section 3.7.2.

### 3.4.2 Addition of Water

It was important to ensure that the water added to reconstituted gangue behaved somewhat similar to the dispersed connate water in the extracted gangue. The water ageing step mentioned in Figure 3 was to give water time to enter into the pores of

the Soxhlet gangue. Connate water prior to non-aqueous extraction is in close contact with the bitumen and sand particles constituting oil sands. The extraction procedure can disperse the water and change the pre-existing interaction of water with the sand and bitumen particles and this step was expected to replicate this dispersion of water in gangue.

The water addition step begins with adding the required wt. % of water to the DSBS put inside a Teflon bottle. The product formed from this step was called wet Soxhlet gangue bitumen solids or WSBS. Please note: The wt. % for Bit.C and water was based on DSBS and WSBS weights respectively and not the net weight of Reconstituted gangue. Refer Appendix A.1 for details. The Teflon bottle was sealed with para-film and placed on a rotary mixer for 20 min at 60 rpm. This step ensured water got mixed with the DSBS properly. The WSBS was next water aged in the Teflon bottle for 18-20 hr.

### 3.4.3 Addition of Solvent

The final solvent addition and mixing step was to spread and mix the solvent uniformly to form the reconstituted gangue. 8/12 wt. % of Cyclohexane was added to the WSBS in a Teflon bottle. The Teflon bottle was placed on the rotary mixer for 20 min at 60 rpm. The Reconstituted gangue formed was collected in glass jars and sealed with para-film.

The reconstituted gangue was kept inside a freezer to avoid solvent losses. The freezer was at a temperature of -13 °C.

### **The samples prepared were as follows –**

Based on the protocol the reconstituted gangue samples were prepared for 12% and 8% solvent with 0.5, 1, 1.5 and 2% residual Bit.C% combination. The water content was constant in all the samples, 3.7%. In order to study the drying mechanism in detail, solvent only samples were also prepared.

### **3.5 Sample Packing**

A gangue sample (extracted or reconstituted) can be considered to be Soxhlet gangue with bitumen, cyclohexane and water in its pores. The packing procedure for drying experiments was so as to spread 15.2/25.2/35.2  $\pm$  0.4 g of reconstituted gangue samples evenly in the glass petri-dish to give a sample depth of 0.6/1/1.4  $\pm$  0.05 cm respectively. The bulk density of Soxhlet gangue in the drying experiments was 1140  $\pm$  170 kg/m<sup>3</sup>. Pycnometry experiments were carried out with cyclohexane and the particle density of Soxhlet gangue was determined to be 2540 kg/m<sup>3</sup>. The pore fraction in the gangue bed was calculated to be 0.55  $\pm$  0.07. Nikakhtari et al. [51] have reported a similar bulk density and pore fraction for extracted rich grade gangue samples used in their packed bed drying study. No bed shrinkage was observed during drying. This can be explained by the high coarse solids content in the reconstituted samples, similar to what has been reported by Nikakhtari et al. [51] for their extracted gangue samples.

### **3.6 Drying Conditions**

The drying experiments were performed in a fume-hood. The sash height of the fume-hood was kept constant to maintain constant flow conditions. The setup designed for performing the drying experiments is shown in Figure 4. The blackened light reflection

blocker further limited the air flowing into the balance chamber where the experiments were performed. The temperature and humidity inside the balance chamber were measured with a temperature/humidity probe (1166121, Fisher Scientific, No.: CON4189) placed 12-14 cm above the balance bottom. Two lamps were used for illumination purposes i.e. to obtain brighter images during drying. The lamps were placed facing the front edge of the balance chamber at a distance of about 30 cm from it.

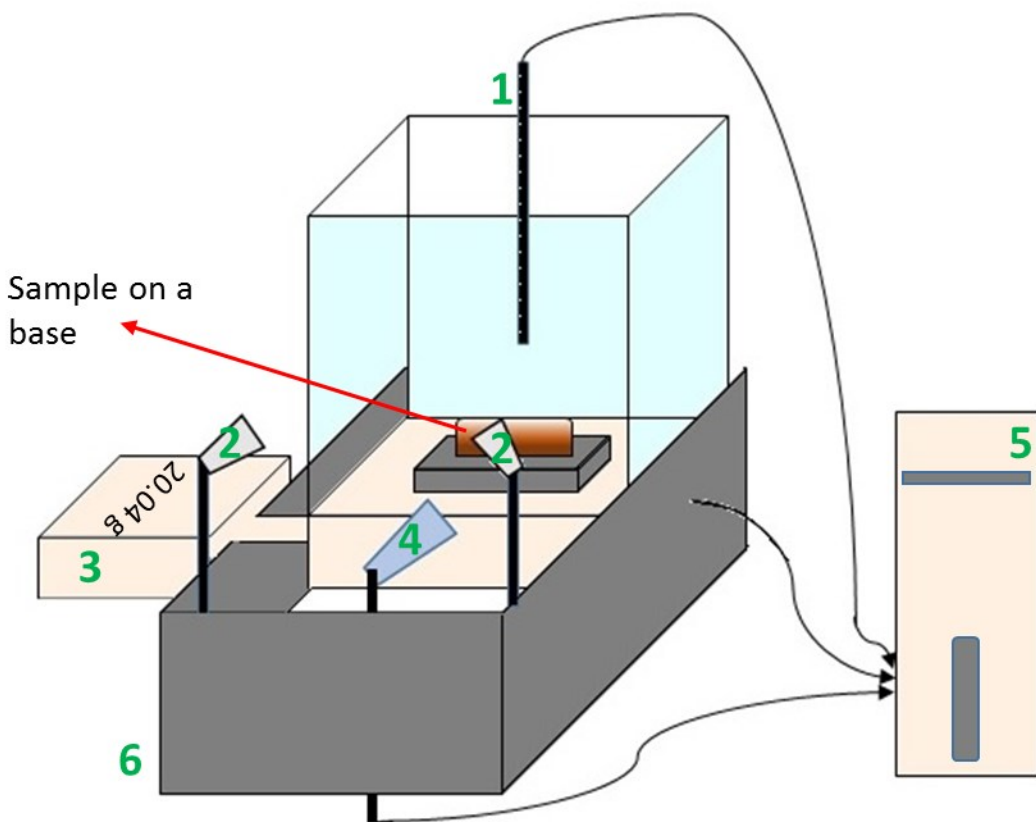


**Figure 4. The experimental setup. 1-Temperature/Humidity probe, 2- Lamps, 3-Balance readings, 4- Camera, 5-CPU and 6- Blackened reflection blocker.**

The Reconstituted gangue jars prior to drying runs were taken out of the freezer and thawed at room conditions for  $12 \pm 2$  min. After thawing, the gangue sample was

packed into a glass petri-dish (OD 60 mm and height 15 mm, 50 mm ID, PYREX®, CLS316060). The packing weights and density maintained were discussed in the section 3.5. The petri-dish was next loaded onto the balance inside the fume-hood at room temperature ( $21 \pm 1$  °C) and ambient pressure. The airflow over the sample inside the balance chamber was measured to be  $V_x = 0.03\text{-}0.08$  m/s and  $V_y = 0.01\text{-}0.04$  m/s. The balance was connected to a computer and weight readings were obtained using Mettler Toledo software every 20 seconds.

After loading the sample, the two lamps were switched on. The lamps slightly increased the temperature inside the chamber and consequently the drying flux. Lamps and no lamps drying have been compared in Appendix B.3. Each sample was dried for 2 hours. The glass petri-dish helped us to observe the bitumen migration taking place during the drying experiments. Drying images were continuously captured by a camera, placed facing the front edge of the balance chamber. Images were captured at an interval of 1 min. For some experiments, Top view of the samples were captured.

Due to bitumen migration two distinct layers, a darker coloured top layer and a comparatively lighter coloured bottom layer were formed. The top and bottom layers were separated and collected in glass tubes. The top layer was scraped off from the sample bed and packed into one of the tubes. About 4-6 g of bottom layer was packed into another tube. The process of scraping off the top layer and packing into the glass tube took  $8 \pm 3$  min. The packing of the bottom layer into the glass tube took about  $3 \pm 1$  min. The end of glass tubes were sealed with glass wool to prevent sand and fine particles from entering into the capillary sampling unit of the mass spectrometer (HPR-20, QIC Mass Spectrometer, Warrington, England) during residual solvent

analysis. To prevent solvent losses prior to connecting the glass tubes with the mass spectrometer unit, the tubes were sealed with parafilm and placed inside a freezer maintained at -13 ° C. The sealed glass tubes were thawed for 1-3 min before making the connection with the mass spectrometer unit. Further the carbon content analysis of the mass spectrometer dried top and bottom layers was done using an elemental analyzer (Flash 2000 CHNS-O Analyzer, Thermo Scientific).

### 3.7 Analytical Techniques

#### 3.7.1 Residual Solvent Measurement with QICMS

The glass tube with the collected sample (top and bottom layer) was placed inside a heating unit (Short Path Thermal Collection System, Scientific instrument Services Inc., Rigoes, NJ). The temperature was maintained at 21-80 °C. The carrier gas (high purity nitrogen) was introduced to one end of the glass tube (placed inside the heating unit) and carried the desorbed solvents through the other end of the glass tube to the heated capillary sampling inlet line. A carrier gas flow rate of  $18 \pm 1.5$  mL/min was maintained. The pressure of the mass spectrometer (HPR-20, QIC Mass Spectrometer or QICMS, Warrington, England) was adjusted to  $2 \times 10^{-6}$  torr and maintained at this reading throughout the duration of the solvent analysis.

The QICMS was calibrated to convert the mass spectrometer response at the end of analysis to cyclohexane content in  $\mu\text{l}$  (Appendix A.3). The cyclohexane volume obtained was divided by the mass of sample inserted to give the residual cyclohexane content in ppm.

### 3.7.2 Bitumen Content Analysis using Elemental Analysis Equipment

The top and bottom layers after the QICMS analysis were stored in separate glass vials and homogenized by mixing thoroughly. Next 4 sub samples (15-20 mg each) from each layer were carefully weighed in tin boats/capsules and placed inside the autosampler unit of the elemental analyzer (Flash 2000 CHNS-O Analyzer, Thermo Scientific).

At a preset time, based on the sequence of loading, a sub sample was dropped into the quartz combustion reactor placed inside a furnace at a temperature of 900 °C. When the tin boat/capsule came in contact with oxygen in the immensely oxidizing environment of the reactor a strongly exothermic reaction was triggered. Temperature as high as approximately 1800 °C was reached causing sample combustion to occur instantly. The combustion products formed were transported across the reactor where the oxidation was completed. The Nitrogen oxides and sulfur trioxides possible formed were reduced to nitrogen and sulfur dioxide gases. The gas mixture from the combustion reactor comprising of  $CO_2$ ,  $N_2$ ,  $H_2O$ , and  $SO_2$  were next separated in a chromatographic column. Finally the eluted gases were passed onto a TCD (thermal conductivity detector). The TCD generates electric signals which was processed by the Eager Xperience software to provide us with the percentages of Carbon, Hydrogen, Nitrogen and sulfur present in the sub-sample.

From dropping of a sub-sample into the reactor till obtaining the C, H, N and S percentages took approximately 12 min. The CHNS analysis of Soxhlet gangue gave us the inorganic carbon content that will be present in the reconstituted gangue formed using it. The organic/bitumen associated carbon content (Bit.C) in the

layers/dry Soxhlet bitumen solids was determined by subtracting this inorganic carbon content from the net carbon content obtained from the CHNS.

### 3.8 Wettability Determination

The wettability of Soxhlet gangue and DSBS was measured using film flotation technique described in [49]. Dry solids were sprinkled gently on the surface of methanol-water solutions with varying surface tension depending on methanol vol. %. The mean critical surface tension of solids was calculated based on the weight % of particles floating at the surface of the probing solutions prepared. This technique can also indicate if the solid particles are heterogeneous. The steps followed in this technique have been discussed in detail in Appendix A.4.

## 4. Drying and Residual Solvent Content

### 4.1 Drying Curve Analysis

#### 4.1.1 Plotting the Weight Loss Data

The sample was loaded onto a balance which was set to send data to a computer every 20 seconds. Cumulative weight loss vs time graph was plotted from this data, as shown in Figure 5. This way of representing weight loss data was found to be useful in comparing samples with different compositions of solvent and bitumen.

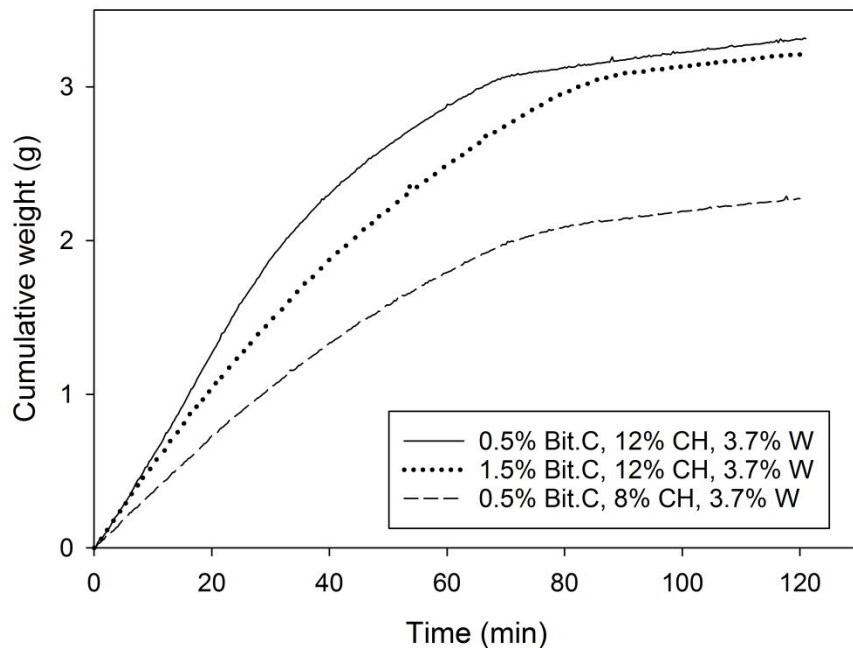


**Figure 5. Sample representation of weight loss data. CH = cyclohexane, W = water and 1 cm is the sample bed height. All the samples had 3.7% water on a solvent free weight basis.**

#### 4.1.2 Initial Flux Determination

The initial 10 min of cumulative weight loss vs time data was fit using linear regression. The R squared (Coefficient of determination) for the linear fit in most cases was 0.99 or higher indicating that the linear model fit the data well. The slope obtained from linear regression was used to evaluate the average initial drying flux (i.e. during the 1<sup>st</sup> 10 min.). The average initial flux was obtained by –

*Average initial flux*

$$= \frac{\text{Slope of linear regression fit (in the 1}^{\text{st}} \text{ 10 min)}}{\text{Petridish Top Area} (= 19.64 \text{ cm}^2)} \quad (9)$$

Initial flux comparison was used to quantitatively compare the initial drying behaviour of the reconstituted gangue samples.

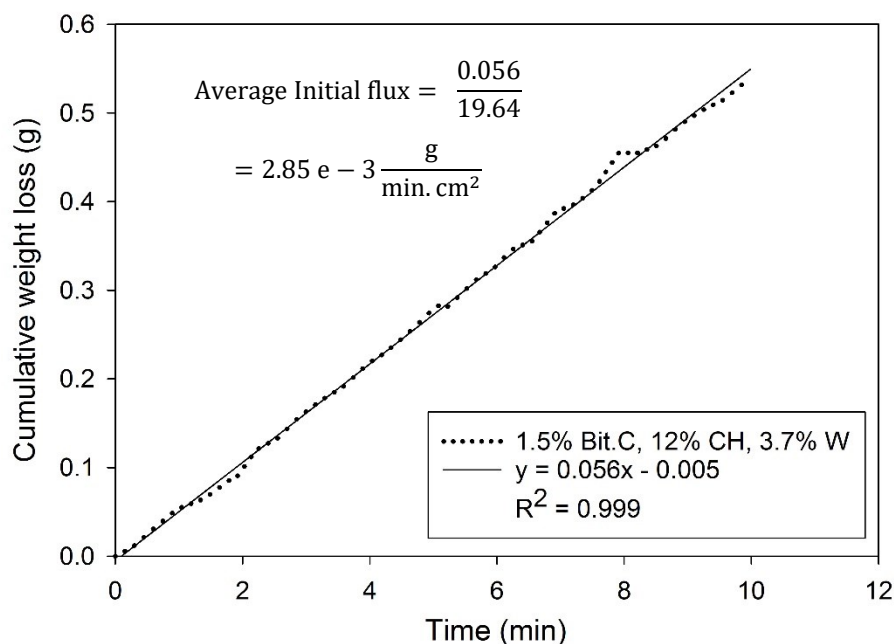


**Figure 6. Average initial flux determination.**

#### 4.1.3 Breakpoint or Transition Time Determination

The sample drying curves shown in Figure 5 can be roughly divided into two intervals/stages from visual observation. A fast drying stage (Refer Figure 7) and a slow drying stage. These two stages are separated by a breakpoint which lies somewhere in the boxed region shown in Figure 7. This breakpoint will be alternatively termed as 'Transition time' since it denotes the transition from the fast drying stage to the slow drying stage. To determine this breakpoint, piecewise regression approach was used in a statistically determined region called henceforth the 'Transition time interval' (Please refer Appendix B.1 for determination of Transition time interval).

A piecewise linear regression model is used in cases where both the single linear model and nonlinear model are inappropriate [53]. The piecewise model is continuous and consists of two straight lines (linear regression models) for two different x bounds separated by a structural break/ breakpoint [53], [54]. The justification of using a piecewise regression model over a single linear model is the reduction in error (Mean square error) of the curve fit [53].

Mean square error (MSE) of a model fit to data is given by –

$$MSE = \frac{1}{n} \sum_{k=1}^n (\tilde{Y}_k - Y_k)^2 \quad (10)$$

Here  $Y_k$  is the observed value at any given  $X_k$  and  $\tilde{Y}_k$  is the corresponding value predicted by a model fitting the data ( $\tilde{Y} = f(X)$ ).

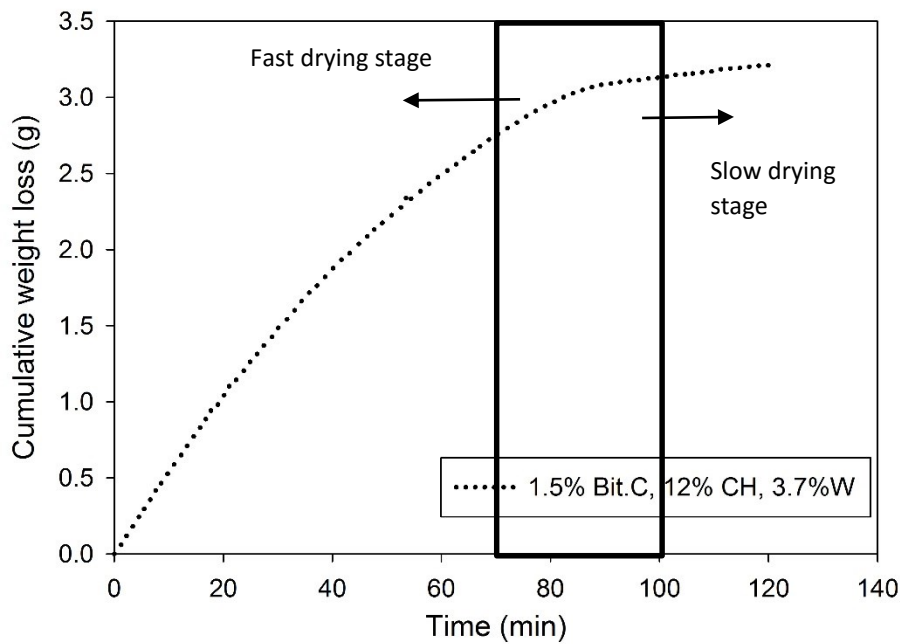


**Figure 7. Transition from fast drying stage to slow drying stage. The boxed area is the region/interval where the breakpoint lies.**

The determination of breakpoint/ transition time for slow drying stage using piecewise regression fit in the transition time interval needed the application of nonlinear iterative least square regression technique. The function *nlinfit* in MATLAB R2015a was used for this purpose (Please Refer Appendix B.2 for more details). The 95 percent confidence interval for the breakpoint of a piecewise regression model has been previously estimated using a technique called bootstrapping [53]. Bootstrapping involves creating new data sets (Bootstrap samples) from the original dataset (original sample) [55]. A bootstrap sample thus created can be defined as a random sample of same size as the original sample, containing data points drawn with replacement from the data set of original sample [55].

The bootstrap samples created ( $n=2000$ ) were further analyzed for determination of the same parameters (including breakpoint) as the original sample. Using the breakpoint estimates obtained for the bootstrap samples the 95 percent BCa (Bias corrected and accelerated) confidence interval for the breakpoint of the original piece wise model was estimated.

Bootstrapping was performed for the data in the transition time interval using the *bootstrp* and *bootci* functions in MATLAB R2015a. The *bootci* function along with providing us with the parameter estimates for the bootstrap samples can provide us with the 95% BCa confidence interval. Figure. 8 shows us the results of piecewise regression fit followed by bootstrapping in the transition time interval.

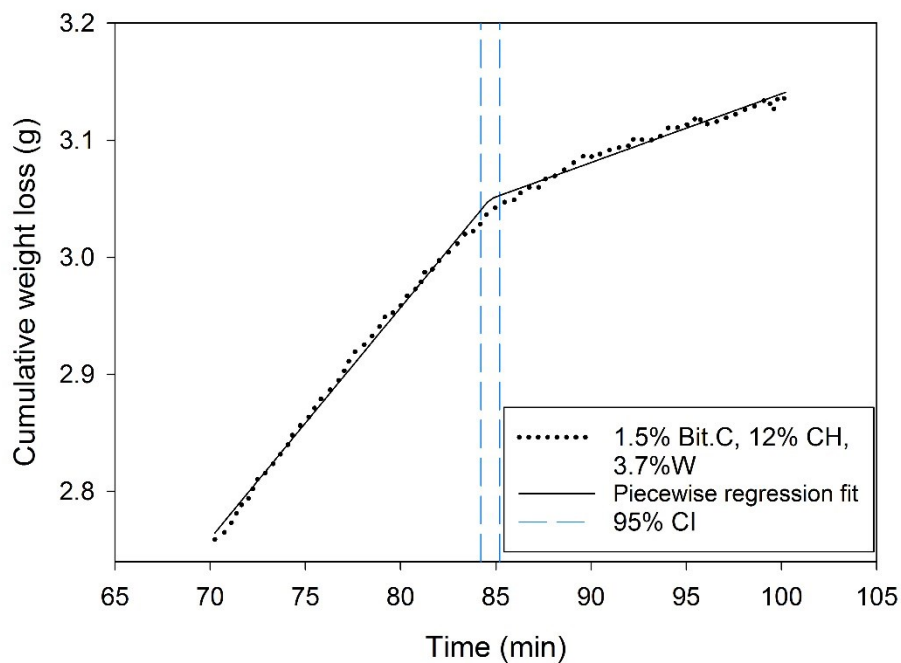


**Figure 8. Piecewise regression fit in the transition time interval with 95 percent confidence interval for the breakpoint estimated.**

#### 4.1.4 Final Flux Determination

The slope of linear regression fit of cumulative weight loss vs time data starting from breakpoint/transition time till the end of drying (slow drying stage) gives the average final drying rate. In the slow drying stage, unlike in the fast one a linear regression fit has a good visual fit for the entire data range (Figure 9). This was probably because of an almost constant drying flux in this stage. The average final flux, similar to average initial flux was calculated as follows:

$$\text{Average final flux} = \frac{\text{Slope of linear regression fit (after breakpoint)}}{\text{Petridish Top Area} (= 19.64 \text{ cm}^2)} \quad (11)$$

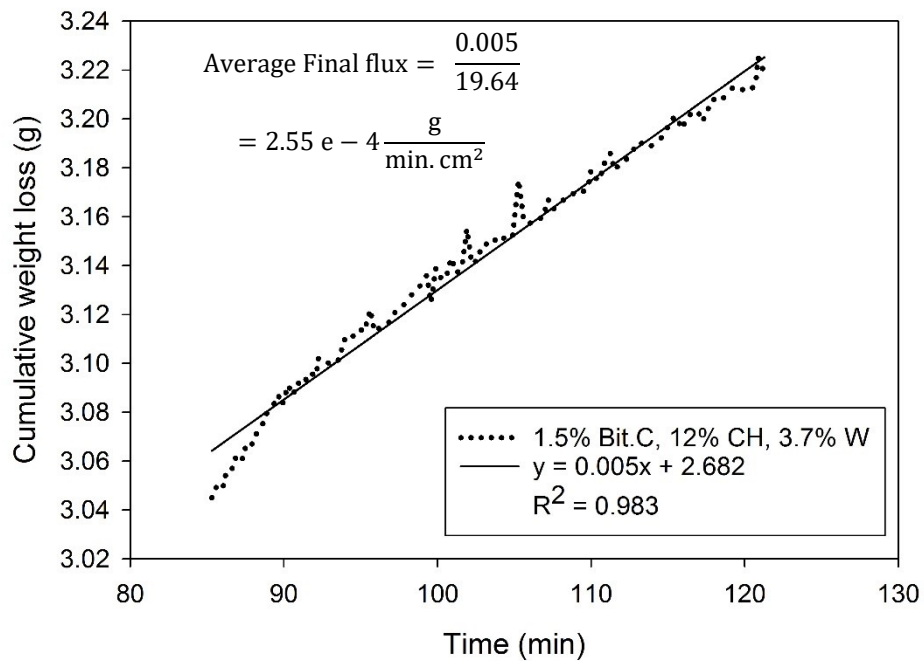


**Figure 9. Average final flux determination.**

For bed heights of 0.6 cm, in some cases the final stage is followed by an even slower drying stage. In such cases the duration of the slow drying stage is considered to be from transition time till the beginning of this extremely slow drying stage.

## 4.2 Drying Curves for Extracted Gangue

The cumulative weight loss vs time plots for two extracted gangue samples are shown in Figure 10 below. The gangue samples were extracted from rich grade Athabasca oil sands ore using cyclohexane as solvent. Samples were collected from two separate extraction experiments and therefore the composition (residual bitumen and solvent) varies in each case. The procedure followed for extraction was the same as mentioned in Nikakhtari et al. [8].

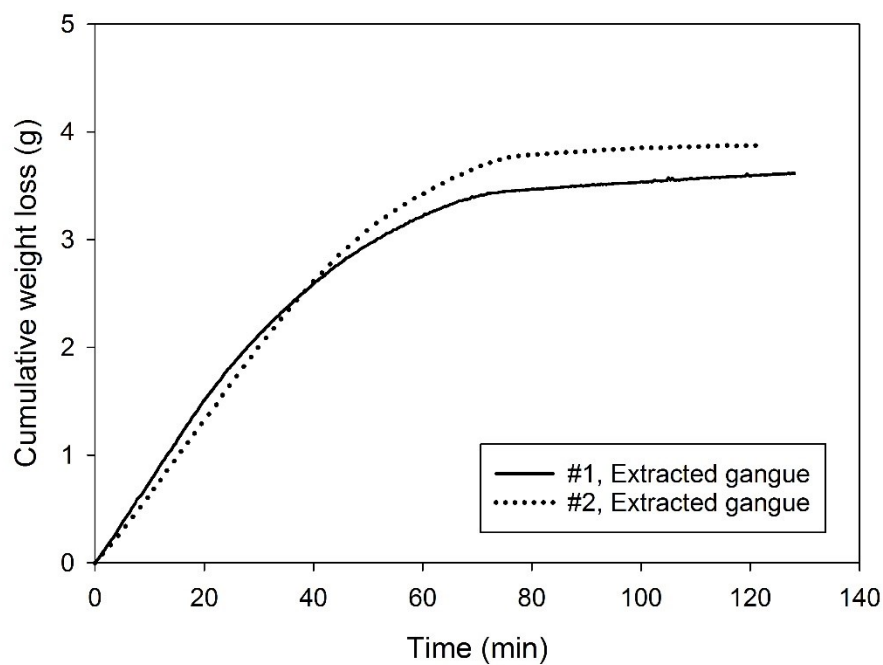


**Figure 10. Drying curves for extracted gangue.**

Nikakhtari et al. [8] performed some drying experiments on extracted gangue samples and concluded that the slow drying stage is dominated by water evaporation. The drying before the slow drying regime has been reported as to be solvent dominated. They came up with this conclusion from studying their dimensionless weight curves. The experimental data sets were plotted as dimensionless weight curves and it confirmed that the slow drying stage in the dimensionless weight curve (Figure 11) was the same as the slow drying stage in the cumulative weight curve.

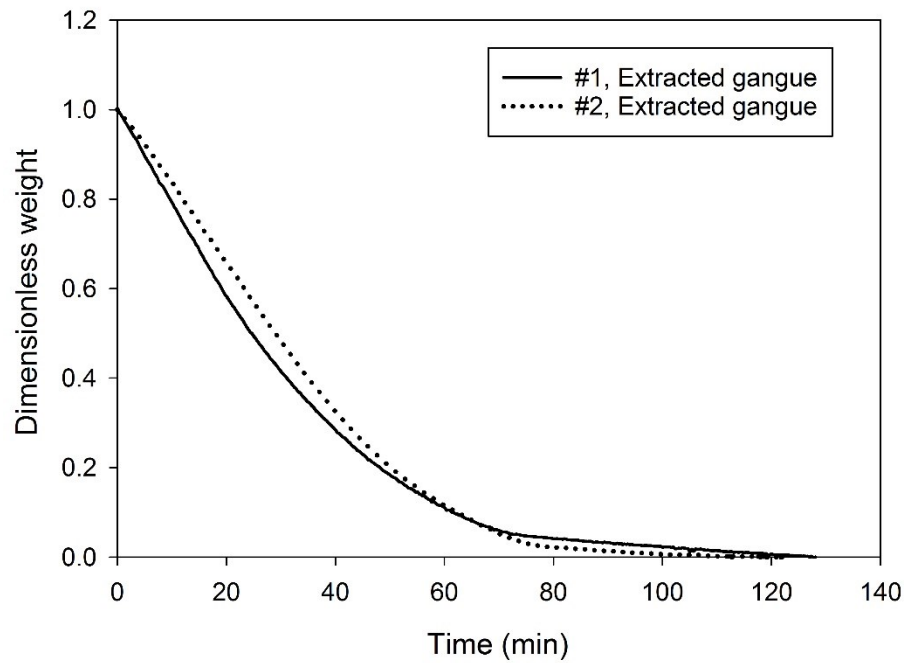


**Figure 11. Dimensionless drying curves for extracted gangue.**

The break point/transition time remains similar if the data is represented in terms of dimensionless weight or cumulative weight loss curves. On the basis of what has been reported for extracted gangue, the extrapolation of the water dominant drying stage could give us an estimate of the initial water content (wt.%) and consequently the cyclohexane content [8]. This is based on an assumption of no cyclohexane and

water interaction during drying. Following this method of volatile content estimation, the cyclohexane content of #1 and #2, *Extracted rich gangue* was estimated to be about 12.5-13% and 14-14.5% respectively. The weight % of water lost during 120 min of drying was estimated as 1.5-2% on a cyclohexane free basis in gangue.

The initial Bit.C (Bitumen associated Carbon) content of the extracted gangue samples is shown in Table 2. The bitumen associated carbon content was determined by the elemental analysis technique.

**Table 2. The bitumen associated C contents (weight %) of extracted gangue.**

Sample name	Bit.C %
# 1, Extracted rich gangue	0.58
#2, Extracted rich gangue	0.26

#### 4.3 Drying Comparison: Extracted and Reconstituted Gangue

The drying behaviour of extracted gangue samples was compared with reconstituted gangue (Figure 12) having a similar composition of *0.5% Bit.C, 12/14% Cyclohexane and 3.7% water* for a bed height of 1 cm.

The drying curves for the extracted and reconstituted gangue samples appear similar visually (similar trend, fast stage followed by a slower drying stage).

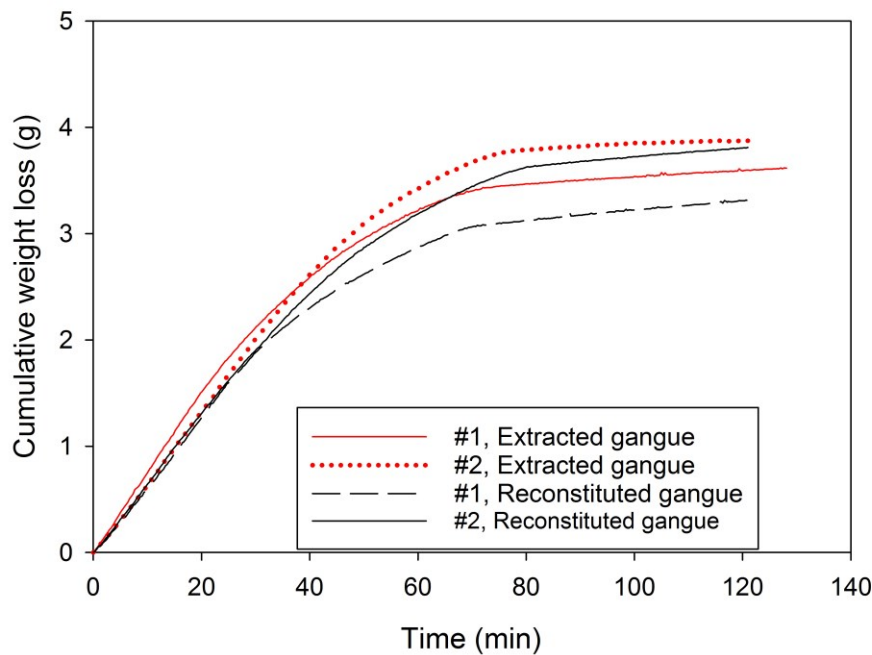


**Figure 12. Extracted and reconstituted gangue drying curves.**

The initial flux, transition time and final flux for the drying curves is shown in Table 3.

**Table 3. Initial flux, transition time and final flux**

Sample name	Initial flux (g/min.cm <sup>2</sup> )	Transition time(95% confidence) (min)	Final flux (g/min.cm <sup>2</sup> )
# 1, Extracted gangue	3.87 e-03	67.6-69.3	1.68e-04
#2, Extracted gangue	3.26 e-03	73.5-74.5	1.73e-04
#1, Reconstituted gangue	3.10 e-03	68.1-68.9	2.44e-04
#2, Reconstituted gangue	3.32 e-03	77.5-78.5	2.19e-04

Table 3 reports that, the initial drying flux range for reconstituted gangue was similar to that obtained for extracted gangue. The final flux for all samples was an order of magnitude lower than initial flux. As mentioned before the slow stage of drying is dominated by water drying. The higher final flux for Reconstituted gangue sample was hence possibly due to lower RH conditions i.e. 12-16% RH compared to RH conditions of 25-55% during extracted gangue drying runs. When reconstituted gangue drying runs were repeated at 38-39% RH conditions, final flux value similar to extracted gangue samples was observed ( $1.78e-04$  g/min.cm<sup>2</sup>). The 95% BCa confidence interval for transition time is comparable for extracted and reconstituted gangue (Table 3).

Based on the above comparison it is confirmed that the reconstituted gangue with similar bitumen and solvent content as the extracted gangue replicates its drying behaviour. Other comparisons of extracted and reconstituted gangue based on the bitumen migration behaviour, which supports this statement further have been made in Chapter 5.

After verification of drying behavior of samples, reconstituted gangue samples with *0.5-2% Bit.C, 12 or 8% cyclohexane and 3.7% water* were prepared. The main purpose in preparing reconstituted gangue sample is to obtain gangue sample with more controlled initial parameters.

Based on the volatile estimation method the cyclohexane content in the reconstituted samples with 12%, 8% cyclohexane was reported as  $10.90 \pm 0.4\%$  and  $7.4 \pm 0.4\%$  respectively. The estimated cyclohexane content of 14% cyclohexane sample (#2, Reconstituted gangue) was 13.6%. The solvent being volatile, it is difficult to

precisely control its concentration, however the concentration remained relatively similar for all the experiments. The water content for both 8 and 12 % samples was estimated as  $3.5 \pm 0.2\%$  on a dry gangue basis.

#### 4.4 Representation of Results

Experiments were conducted in triplicates for every individual sample composition at any bed height. In this thesis, while comparing the drying curves for different compositions of reconstituted gangue only a single curve for any particular composition will be shown. This drying curve shown for any particular composition is depictive of the general drying trend at that composition in reconstituted gangue.

#### 4.5 Drying of Reconstituted Gangue with 12 and 8% Cyclohexane

The net cumulative weight loss of 8 % cyclohexane, 0.5-2% Bit.C and 3.7% water samples was lower compared to 12 % cyclohexane, 0.5-2% Bit.C and 3.7% water samples owing to the lower solvent content. Further in this chapter, comparison has been carried out based on the drying bed height.

##### 4.5.1 Drying Studies at a Bed Height of 0.6 cm

In this section the drying behaviour of reconstituted gangue samples with 12% cyclohexane, 0.5-2% Bit.C and 3.7% water has been compared with 8% cyclohexane, 0.5-2% Bit.C and 3.7% water at bed height of 0.6 cm. The drying curves obtained has been shown in Figure 13 and 14.

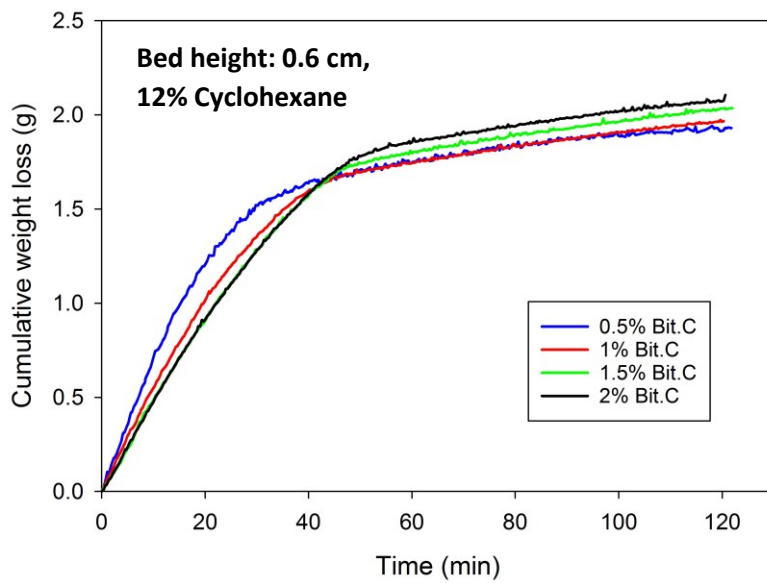


**Figure 13. Cumulative weight loss curves for bed height 0.6 cm, 12% cyclohexane, 0.5-2% Bit.C and 3.7% water**

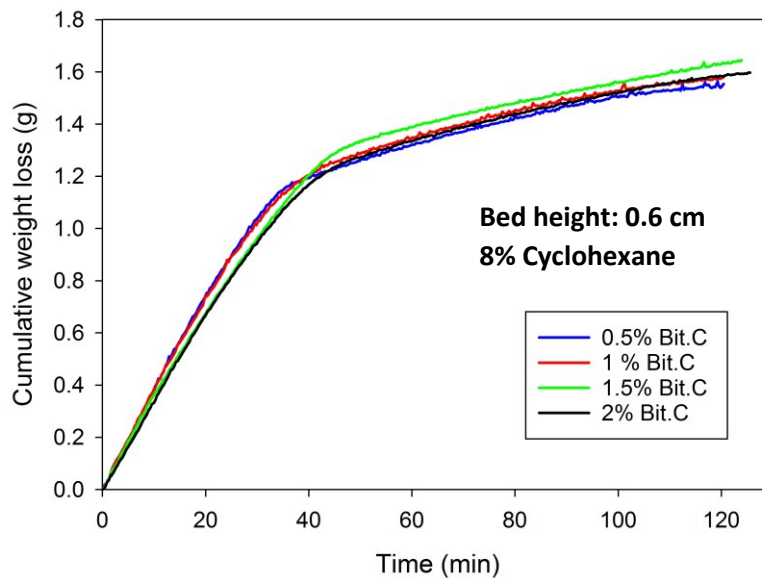


**Figure 14. Cumulative weight loss curves for bed height 0.6 cm, 8% cyclohexane, 0.5-2% Bit.C and 3.7% water**

At the bed height of 0.6 cm, for the reconstituted gangue samples with 12% initial cyclohexane, we observe a very short overlap time in the curves initially. Thereupon 0.5% Bit.C sample seems to have a shorter duration of the fast drying stage (Transition time appears to be reached sooner) compared to the higher Bit.C% samples. The 1.5 and 2% Bit.C samples actually have a complete overlap in the fast drying stage suggesting identical drying behaviour.

For samples with 8% initial cyclohexane content as can be observed in Figure 14, the overlap time of the curves initially is much more compared to what was observed for 12% initial cyclohexane content samples. The longer the initial overlap, the longer the samples under study have identical initial drying characteristics. Also unlike in 12% initial cyclohexane content samples, 8% initial cyclohexane sample with 0.5% Bit.C don't seem to have a significantly shorter duration of fast drying stage.

Next, the initial flux of the 0.5-2% Bit.C samples with 3.7% water and the different solvent contents were compared as shown in Figure 15.

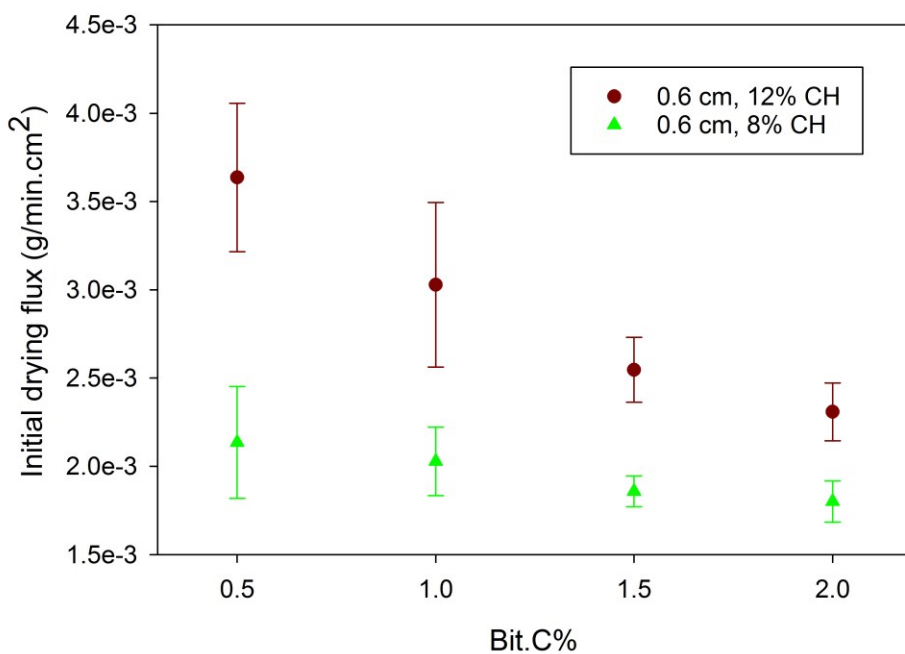


**Figure 15. Initial drying flux comparison at different cyclohexane (CH) contents, bed height= 0.6 cm**

Samples with 12% initial cyclohexane content showed a reduction in initial flux with an increase in Bit.C%. This reduction was especially evident while comparing the lowest and highest Bit.C% samples. The 1.5 and 2% Bit.C samples had similar initial drying flux as was expected looking at their overlapping drying curves.

In contrast to 12% initial cyclohexane containing samples, the samples with 8% initial cyclohexane did not show any significant initial flux variations with Bit.C%. This was again expected due to the longer duration of initial overlap in the samples with different Bit.C%. 8% initial cyclohexane samples also had a much lower initial flux compared to 12% samples for any Bit.C%. Though, gradually with an increase in Bit.C% the difference in initial flux was reduced for the two different initial solvent contents. Lower solvent content can limit the capillary connectivity, leading to fewer

continuous liquid clusters existing throughout the bed. The lower initial flux for 8% cyclohexane samples might be due to a reduction in capillary connectivity for volatiles to the top of the bed where they diffuse into the surrounding air.

The comparison of transition time was also made and has been shown in Figure 16.

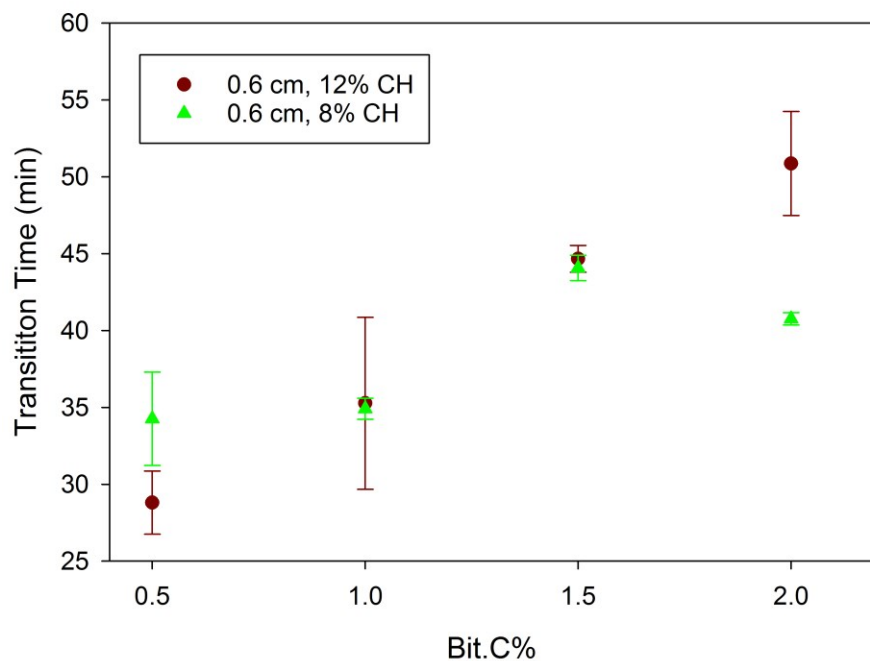


**Figure 16. Transition time comparison at different cyclohexane (CH) contents, bed height= 0.6 cm**

The transition time and the 95% BCa confidence interval was determined for the drying curves using the procedure described in section 4.1.3. The mean and standard deviation of transition time for each Bit.C% was plotted vs Bit.C% at bed heights of 0.6 cm.

For 12% initial cyclohexane samples a trend is seen, that of increasing transition time with an increase in Bit.C%. This revealed that with an increase in Bit.C% the overall drying process during the fast drying stage was slowed down.

8% initial cyclohexane samples with 0.5% Bit.C had a higher transition time compared to the 12% initial cyclohexane sample with same Bit.C%. The transition time measurements at 1 and 1.5% Bit.C point out to the fact that 8% initial cyclohexane samples even though contained lower cyclohexane initially as compared to 12% samples, due to the flux reduction took same/similar time for drying in the fast drying stage. An increase in transition time is seen when comparing 0.5% Bit.C samples to 1.5 or 2% Bit.C samples.

Hence it can be concluded that the overall drying during the fast drying stage even for 8% cyclohexane sample is a function of Bit.C% (albeit a weak function).

The duration of slow drying stage (2hr – transition time) at a bed height of 0.6 cm was very long i.e. >65 min as can be seen from the transition time plot.

The residual cyclohexane content in the top and bottom layers for 12 and 8% cyclohexane containing samples have been shown in Figure 17 and Figure 18 respectively.

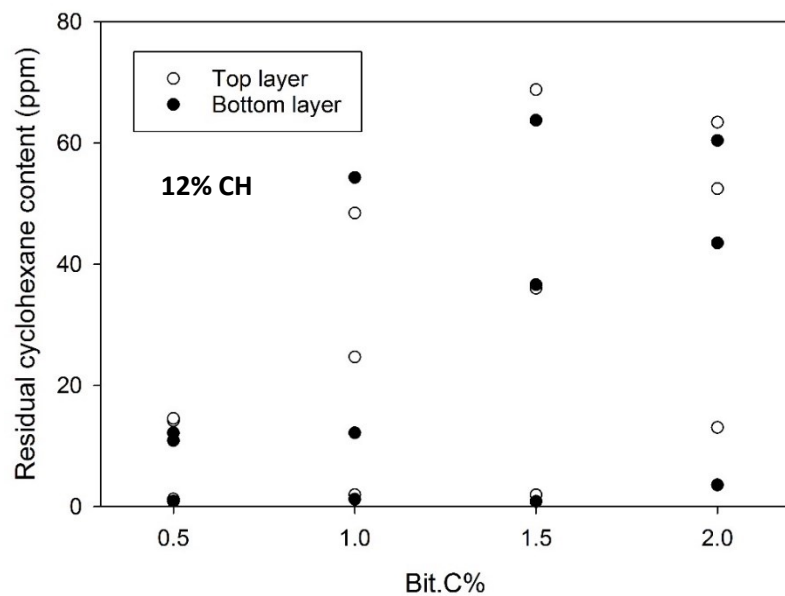


**Figure 17. Residual cyclohexane content (ppm) vs Bit.C% for a bed height of 0.6 cm, 12% CH**

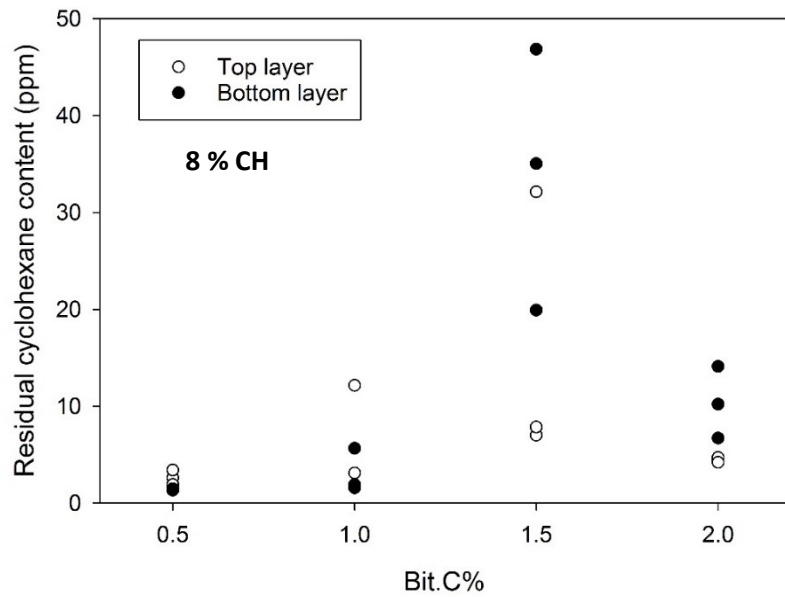


**Figure 18. Residual cyclohexane content (ppm) vs Bit.C% for a bed height of 0.6 cm, 8% CH.**

The residual cyclohexane content values plotted here are not absolute. As mentioned before the top layer took about  $8 \pm 3$  min for packing and the bottom layer about  $3 \pm 1$  min. There would definitely be some cyclohexane losses during the packing of these layers. These losses will be low if the slow drying stage has begun since the solvent losses are diffusion limited during the final stage (Section 4.5.4). The residual cyclohexane content values can be said to be indicative of whether or not we can dry the sample to below 260 ppm in the 2hrs of drying + the sampling time. Since the bottom layer had a lower packing time it can be expected to have residual solvent content comparable to what we would expect at the end of 2 hr of drying. Nevertheless, the residual cyclohexane content for both the layers shown here can be considered as roughly what can be expected from the sample when it was dried for 2 hrs + sampling time.

As can be seen from Figs 17 and 18, residual cyclohexane content of < 80 ppm was observed for both 12 and 8% initial cyclohexane containing samples. A conclusive trend wasn't observed in any of the cases, though residual cyclohexane content of < 20 ppm was observed for samples with 0.5% Bit.C.

#### 4.5.2 Drying Studies at a Bed Height of 1 cm

In this section the drying behaviour of reconstituted gangue samples with 12% cyclohexane, 0.5-2% Bit.C and 3.7% water has been compared with 8% cyclohexane, 0.5-2% Bit.C and 3.7% water at bed height of 1 cm. The effect of the presence of bitumen in the overall drying behaviour was studied by comparing the above mentioned drying curves with 12% cyclohexane, 0% Bit.C and 3.7% water and 8% cyclohexane, 0% Bit.C and 3.7% water samples. Since ideally 0% Bit.C

cannot be achieved by extraction, we mainly focus on the initial flux obtained for these samples and the transition time obtained without delving any deeper. The bed height of 1 cm, was chosen for studying these 'ideal' samples.

The drying curves obtained have been shown in Figs. 19 and 20.

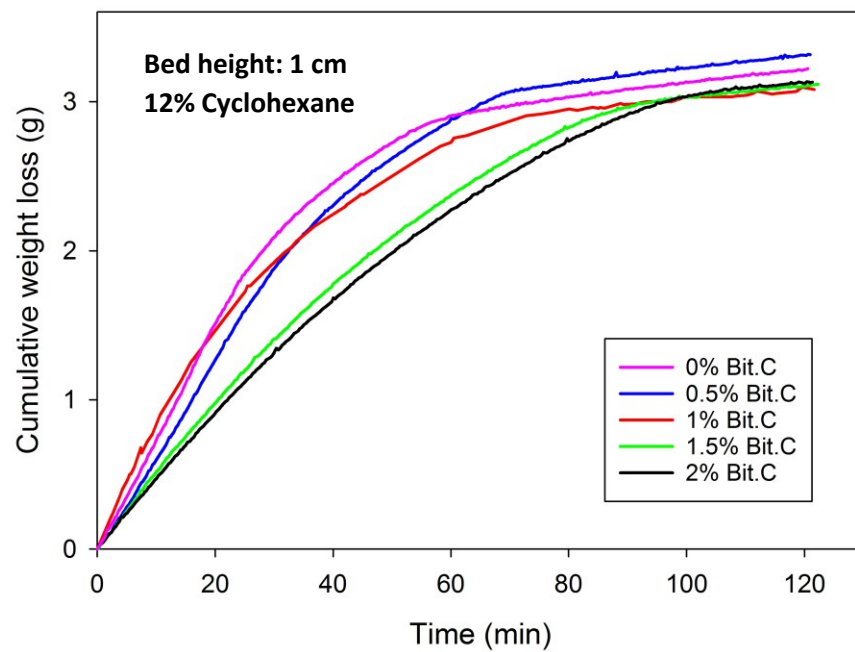


**Figure 19. Cumulative weight loss curves for bed height 1 cm, 12% cyclohexane, 0.5-2% Bit.C and 3.7% water**

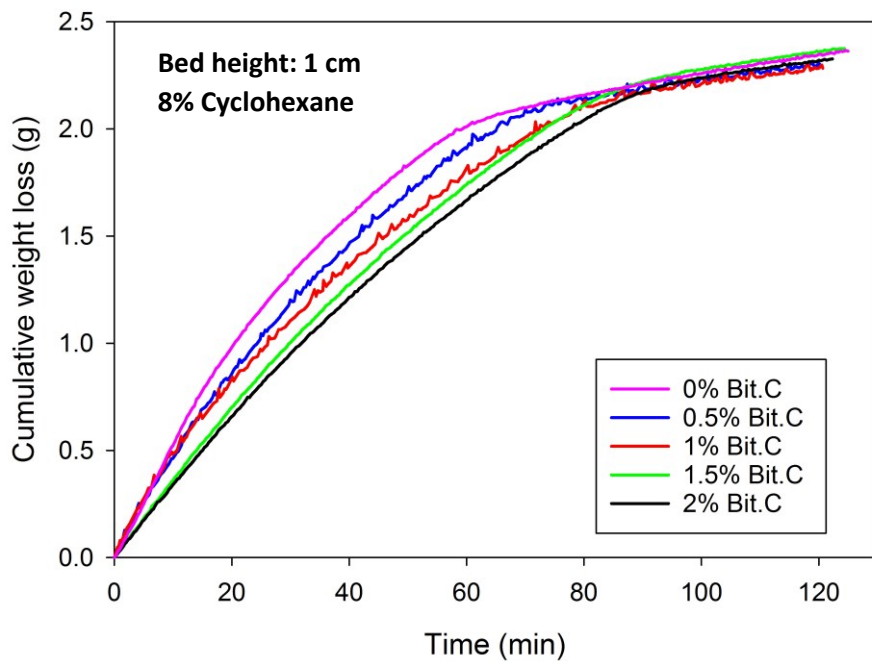


**Figure 20. Cumulative weight loss curves for bed height 1 cm, 8% cyclohexane, 0.5-2% Bit.C and 3.7% water**

For 12% initial cyclohexane containing samples, the initial overlap for the samples with different Bit.C% was for a short duration. 0-1% Bit.C samples had very similar looking curves and could not be distinguished based on Bit.C%. The 1.5 and 2% Bit.C samples had a longer duration for fast drying stage compared to 0-1% Bit.C samples.

At the bed height of 1 cm, 8% cyclohexane containing samples have a similar short initial overlap time as 12 % cyclohexane containing samples. Unlike at bed height of 0.6 cm, we can make out that with an increase in Bit.C% the overall drying time for the fast drying stage is delayed.

For both the solvent contents the samples with 0% Bit.C seem to have a shorter duration of fast drying stage.

To examine the initial drying characteristics of 12 and 8% initial cyclohexane samples with 0-2% Bit.C and 3.7% water the initial flux was plotted as shown Figure 21.

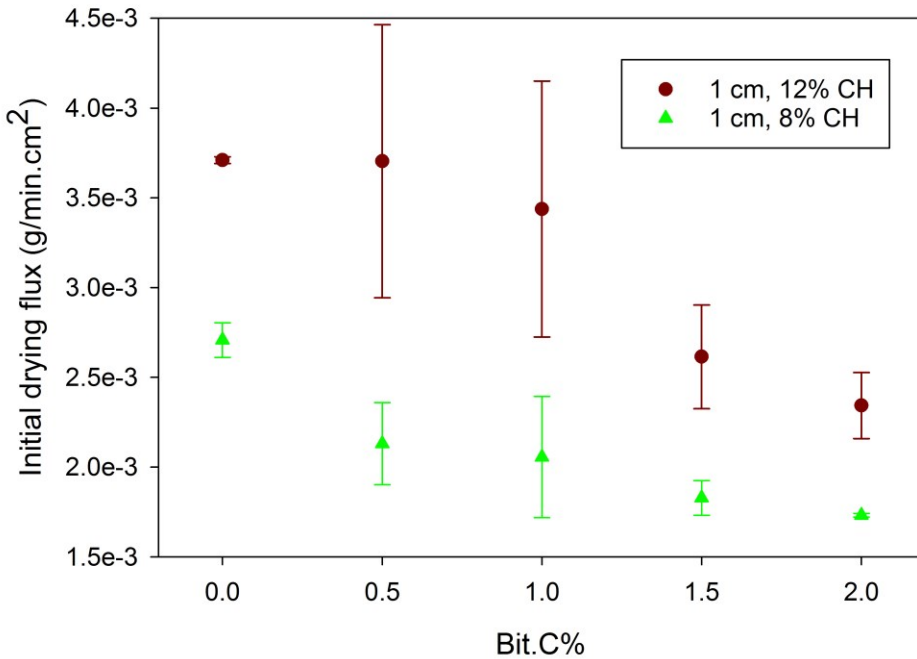


**Figure 21. Initial drying flux comparison at different cyclohexane (CH) contents, bed height= 1 cm**

For samples with 12% initial cyclohexane, 0-1% Bit.C samples had a very similar mean initial drying flux. Similar to what was observed for a bed height of 0.6 cm, a drop in initial flux is evident while comparing the samples with the lowest and highest Bit.C%. The low deviation in initial drying flux for samples with 0% Bit.C might be due to absence of bitumen (Clean system). The presence of bitumen in the system might be causing the initial flux to vary leading to the high deviations seen in 0.5 and 1% Bit.C samples.

In the 8% initial cyclohexane containing samples, a noticeable drop in flux is seen while comparing 0% Bit.C samples with 0.5 and 1% Bit.C samples which have

comparable initial flux range. A slight drop in initial flux is seen while comparing the lowest and highest Bit.C% samples as opposed to no visible trend for bed height of 0.6 cm. Like for a bed height of 0.6 cm, 8% initial cyclohexane samples had a much lower initial flux compared to 12% samples at any particular Bit.C%. A reduction in initial drying flux with Bit.C% for both the initial cyclohexane contents (especially 12% cyclohexane samples) at bed height of 1 cm indicates an apparent impact of bitumen on the initial solvent removal process.

The transition time was also compared for the different solvent contents as has been shown in Figure 22.

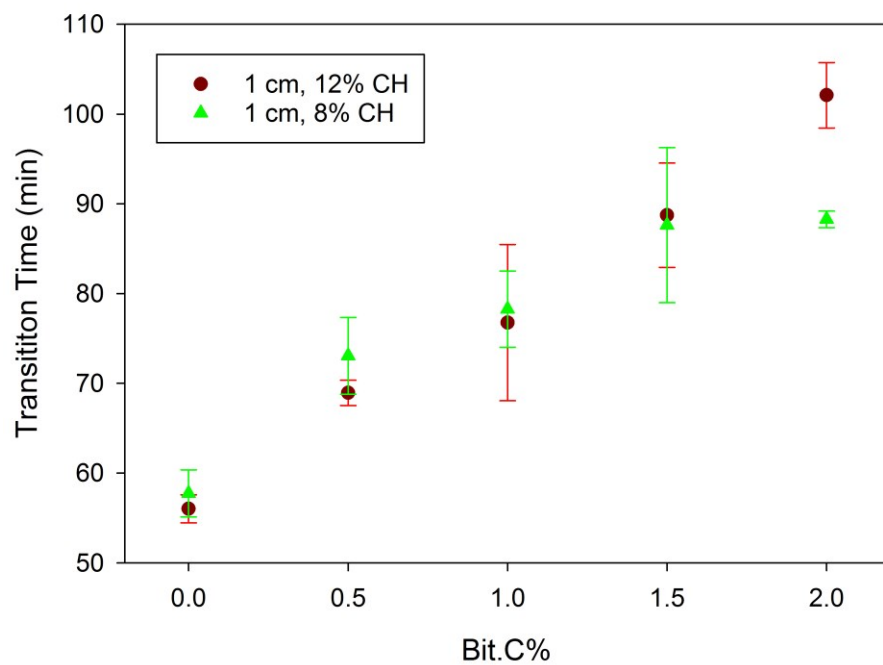


**Figure 22. Transition time comparison at different cyclohexane (CH) contents, bed height= 1 cm**

The mean and standard deviation of transition time for each Bit.C% was plotted vs Bit.C% at bed heights of 1 cm.

The presence of bitumen even as low as 0.5% (Bit.C) can cause a significant increase in the time to reach transition as can be seen from Figure 22. For both 8 and 12% cyclohexane samples the same trend of increase in transition time was observed with an increase in Bit.C%. The transition time was highly comparable for 8 and 12 % initial cyclohexane contents, at any particular Bit.C% in the range 0-1.5 %. Samples with 12% initial cyclohexane seem to have an increase in transition time as the Bit.C% increases from 1.5 to 2% unlike in 8% cyclohexane samples where the transition time stays the same.

Looking at the transition time plots at the different Bit.C% it can be verified as stated before that the overall drying process during the fast drying stage for both 8 and 12% cyclohexane samples is a function of Bit.C%. The transition time at a bed height of 1 cm was noticeably higher compared to the same sample dried having a bed height of 0.6 cm for any particular Bit.C% and initial cyclohexane content. This was conceivable considering 1 cm samples had higher mass and hence higher cyclohexane content to begin with.

The residual cyclohexane content in the top and bottom layers for samples with 0.5-2% Bit.C and 12 or 8% initial cyclohexane has been shown in Figs. 23 and 24 respectively. 0% Bit.C samples residual content wasn't of interest since it's a hypothetical product of an ideal extraction with 100% bitumen recovery.

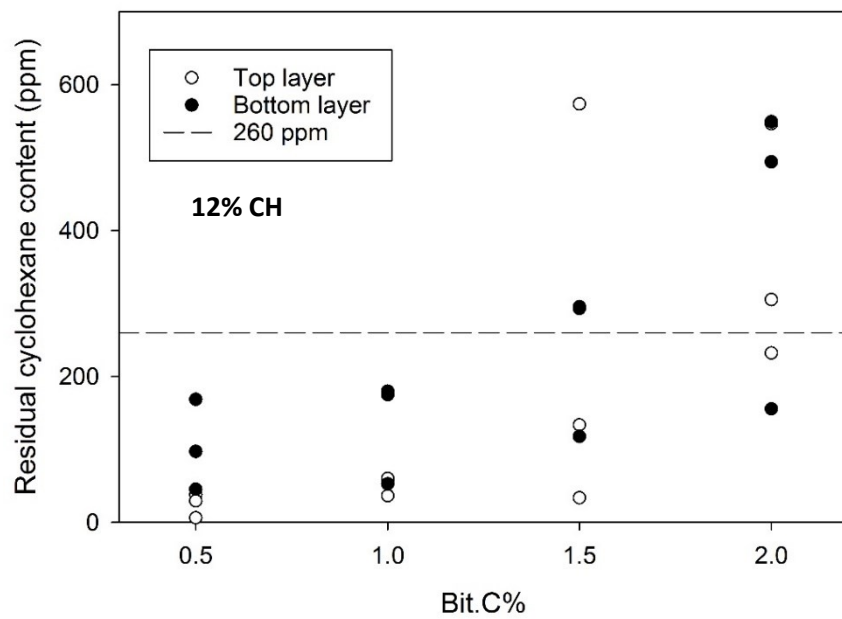


**Figure 23. Residual cyclohexane content (ppm) vs Bit.C% for a bed height of 1 cm, 12% Cyclohexane (CH)**

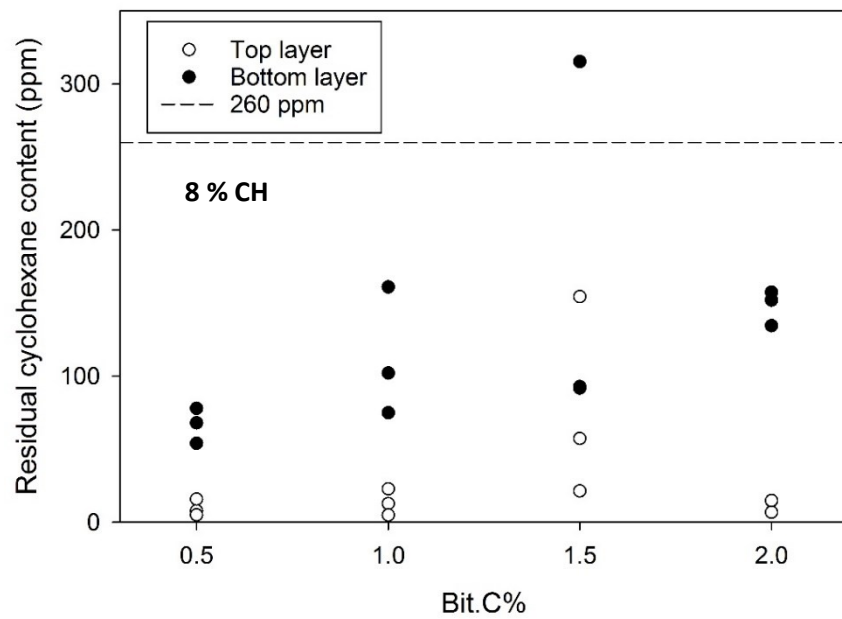


**Figure 24. Residual cyclohexane content (ppm) vs Bit.C% for a bed height of 1 cm, 8% cyclohexane (CH)**

Clearly at a bed height of 1 cm we have a higher residual cyclohexane content in the samples compared to what was observed for the lower bed height of 0.6 cm. The bottom layer in most cases had a higher residual cyclohexane content compared to the top layer.

Looking at Figures. 23 and 24 , it can be said for certain that for most cases the samples with 1.5 and 2% Bit.C have a higher residual cyclohexane content in the bottom layer compared to the samples with 0.5% Bit.C. This was something not observed for a bed height of 0.6 cm.

For samples with 12 and 8 % cyclohexane content initially, if the Bit.C% was  $\geq$  1.5% (Bitumen wt. %  $\geq$  1.8), the residual solvent content could exceed 260 ppm. The reduction in the overall drying in the fast drying stage as was being observed with an increase in Bit.C% seems to be detrimental to the solvent recovery process from gangue at a bed depth/height of 1 cm and Bit.C% of 1.5 or more. Opposed to this was 0.5% Bit.C samples (bitumen recovery of >95%) which had solvent content <200 ppm in all cases. It seems that the solvent recovery process is highly dependent on the efficiency of bitumen recovery from gangue.

#### 4.5.3 Drying Studies at a Bed Height of 1.4 cm

In this section the drying behaviour of reconstituted gangue samples with 12% cyclohexane, 0.5-2% Bit.C and 3.7% water has been compared with 8% cyclohexane, 0.5-2% Bit.C and 3.7% water at bed height of 1.4 cm.

The drying curves obtained have been shown in Figures 25 and 26.

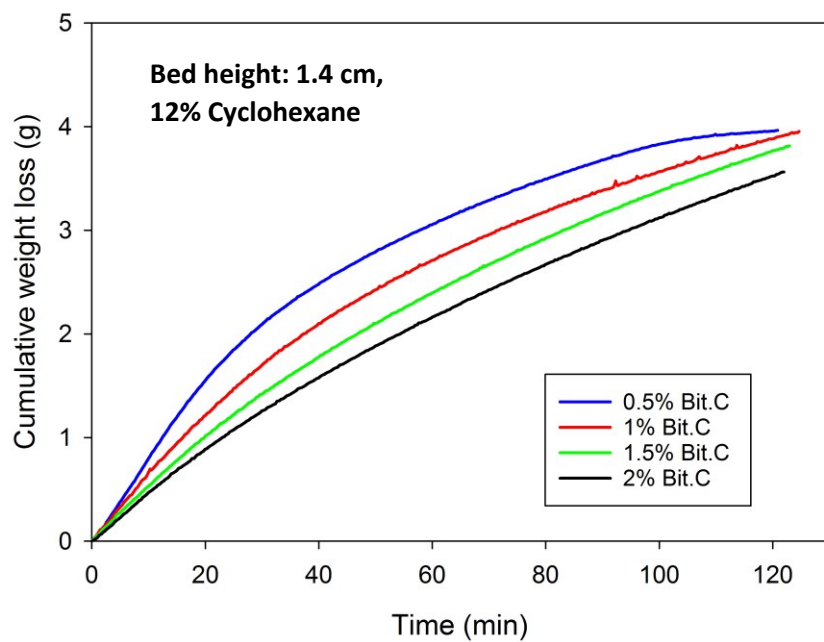


**Figure 25. Cumulative weight loss curves for bed height 1.4 cm, 12% cyclohexane and 3.7% water**

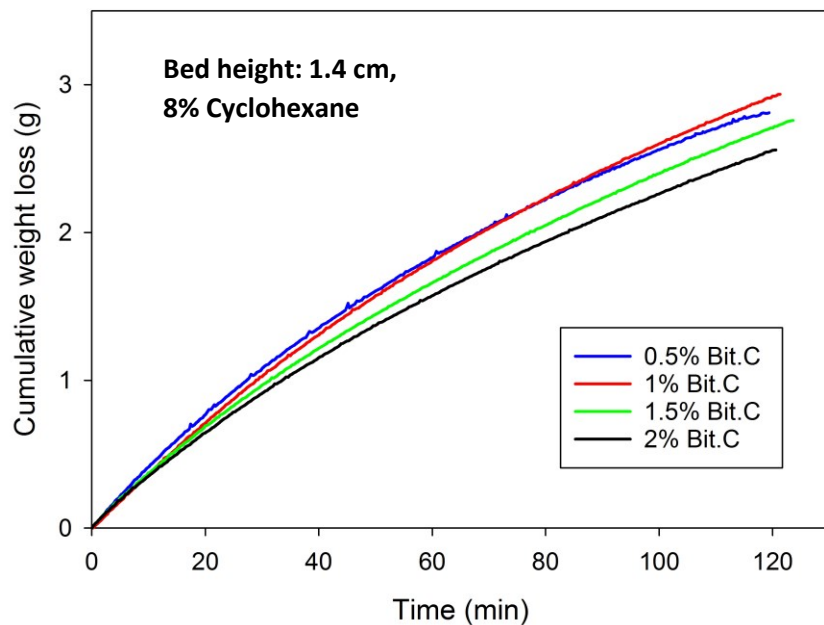


**Figure 26. Cumulative weight loss curves for bed height 1.4 cm, 8% cyclohexane and 3.7% water**

For 12% initial cyclohexane containing samples, all the drying curves seem distinct. There's also a clear progression in the curves, with 0.5% Bit.C sample having the maximum cumulative weight loss at any point of time followed progressively by 1, 1.5 and 2% Bit.C (A vertical line drawn at any time shows lower cumulative weight loss at higher Bit.C %). The transition time was only reached for 0.5% Bit.C samples, again indicating a shorter overall fast drying stage. Transition time was also reached for 1 of the 1% Bit.C samples (not shown in the curves comparison). 2 hr of drying it seems wasn't enough for reaching the slow drying stage for samples with higher Bit.C% of 1.5 and 2%.

For 8% cyclohexane containing samples the same progression as seen above was observed. Though unlike in the case of 12% cyclohexane samples, 0.5 and 1% Bit.C samples weren't very distinct and showed overlaps over long periods of time.

The initial flux of the 0.5-2% Bit.C samples with 3.7% water and the different solvent contents were also compared as shown in Figure 27.

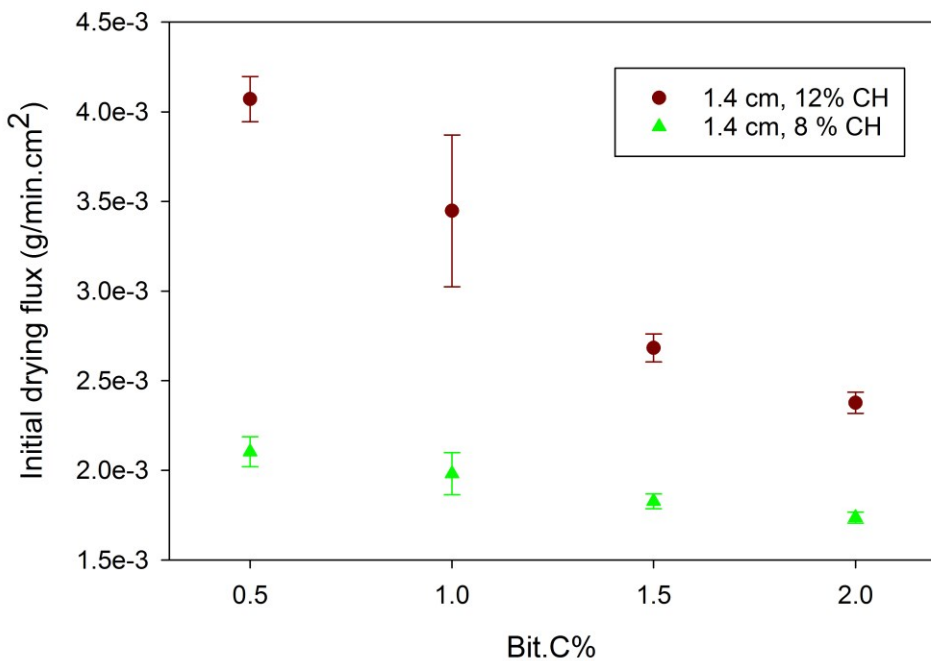


**Figure 27. Initial drying flux comparison at different cyclohexane (CH) contents, bed height= 1.4 cm**

For samples with 12% cyclohexane, there was a clear decrease in the initial drying flux with an increase in Bit.C%. Even with an increase in Bit.C% from 0.5 to 1% a decrease in initial drying flux was observed unlike for bed heights 0.6 and 1 cm. The reduction in mean flux value of 2% Bit.C samples as compared with 0.5% Bit.C samples was about 42 %.

In the 8% initial cyclohexane containing samples, a drop in initial flux was also seen while comparing the lowest and highest Bit.C% samples although compared to 12% cyclohexane samples it was much lower. Similar to what was observed for bed heights of 0.6 and 1 cm, 8% cyclohexane samples had a much lower initial flux compared to 12% cyclohexane samples at any particular Bit.C% under study. The reduction in the

value of mean flux for 2% Bit.C samples as compared with 0.5% Bit.C samples was about 17%.

0.5% Bit.C samples with 12 or 8% initial cyclohexane reached the transition time before the end of drying. Apart from these samples, as mentioned before for 1 of the drying experiments with *1% Bit.C, 12% cyclohexane and 3.7% water*, transition was reached with a transition time of 111.5 min. The transition time for *0.5% Bit.C, 12% cyclohexane and 3.7% water* and for *0.5% Bit.C, 8% cyclohexane and 3.7% water* was  $102.2 \pm 6.7$  min and  $112.3 \pm 2$  min respectively. All of these transition times were reached very close to the end of drying i.e. 2 hr. Figures. 28 and 29 show the residual cyclohexane content in the two different layers for samples with 0.5-2% Bit.C and 12 or 8% initial cyclohexane respectively.

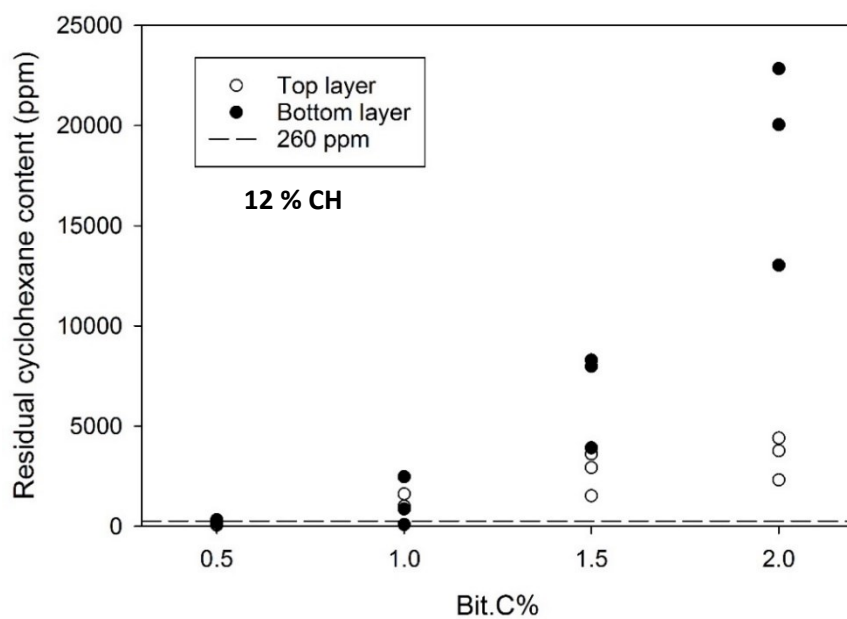


**Figure 28. Residual cyclohexane content (ppm) vs Bit.C% for a bed height of 1.4 cm, 12% cyclohexane initially**

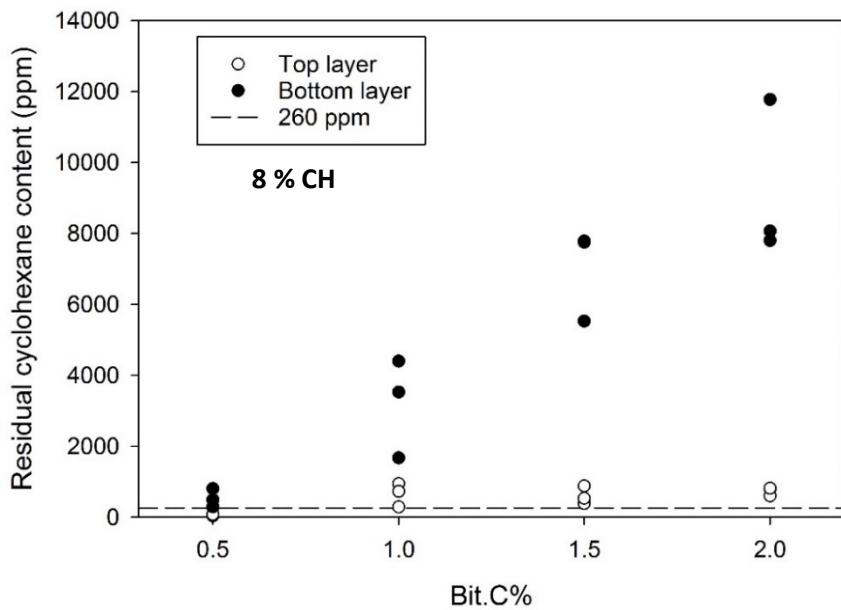


**Figure 29. Residual cyclohexane content (ppm) vs Bit.C% for a bed height of 1.4 cm, 8% cyclohexane initially**

A clear trend is seen at a bed height of 1.4 cm, which is increasing bottom layer residual cyclohexane content with Bit.C%. The residual cyclohexane content in most cases was > 260 ppm.

For samples with 12% initial cyclohexane, the residual cyclohexane content in the bottom layer seems to be increasing exponentially with an increase in Bit.C%. Samples with 0.5% Bit.C where transition time was reached before the drying ended at 2 hr had a solvent content near 260 ppm.

The residual cyclohexane content in samples with 8% initial cyclohexane seems to be increasing linearly with Bit.C%. Again for 0.5% Bit.C samples where transition time was reached low residual cyclohexane content of < 600 ppm was obtained.

Looking at the high values of residual cyclohexane content obtained for 1-2% Bit.C samples it can be considered reasonable to avoid such large bed height dimensions

for optimizing cyclohexane recovery from gangue. A possible link of the transition time and residual solvent content was also suspected and investigated as shown in the figure below.

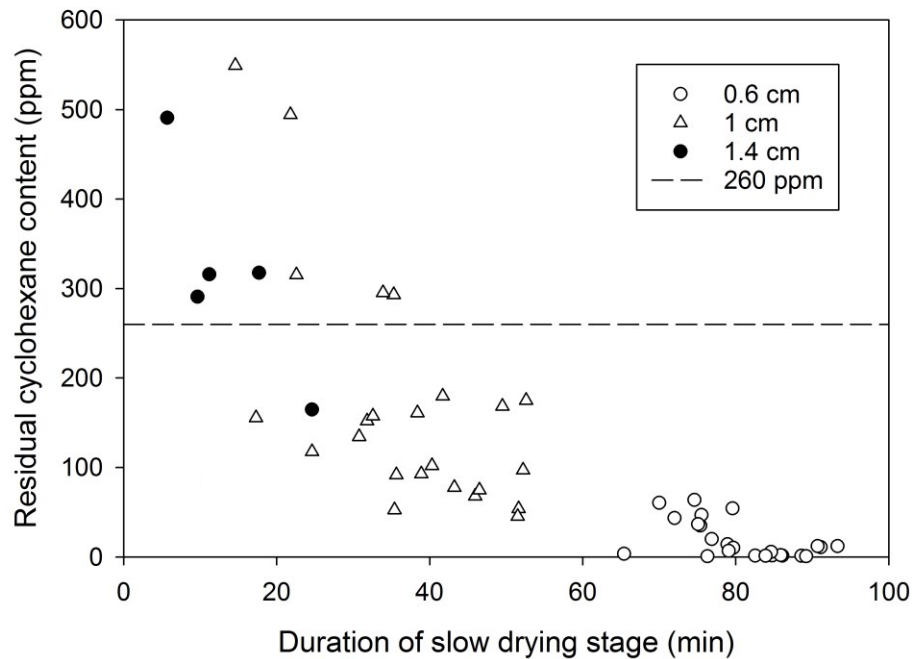


**Figure 30. Residual cyclohexane content (ppm) vs duration of slow drying stage**

The plot of residual cyclohexane content in the bottom layer vs the duration of slow drying stage i.e. (2 hr – Transition time) gives an overview of the residual cyclohexane content at bed heights 0.6 and 1 cm. Bottom layer was chosen since it usually contains as much or more residual cyclohexane content compared to the top layer. If the slow drying stage had begun (transition time reached) prior to 2 hr of drying, residual cyclohexane content of < 600 ppm was observed. This information points to the fact that the fast drying stage is the stage where cyclohexane mainly evaporates. Longer the duration of the

slow drying stage (Conversely sooner is the transition time reached) lesser would be the residual cyclohexane content in the sample. For duration of slow drying stage < 40 min residual cyclohexane content of >260 ppm can be expected.

#### 4.5.4 The Slow Drying Stage and Final Flux

Some tests were performed to verify that the slow drying stage was indeed dominated by water evaporation. This was based on previous observations with extracted gangue [8] as reported in Section 4.2.

In the figure below drying curves for reconstituted samples with 0.5% Bit.C, 12% cyclohexane, *with and without water* have been compared. The purpose of this comparison was to isolate the effect of water in the drying process during the slow drying stage. Reconstituted sample with water only (3.7% W) has also been plotted. The bed height studied was 1 cm.

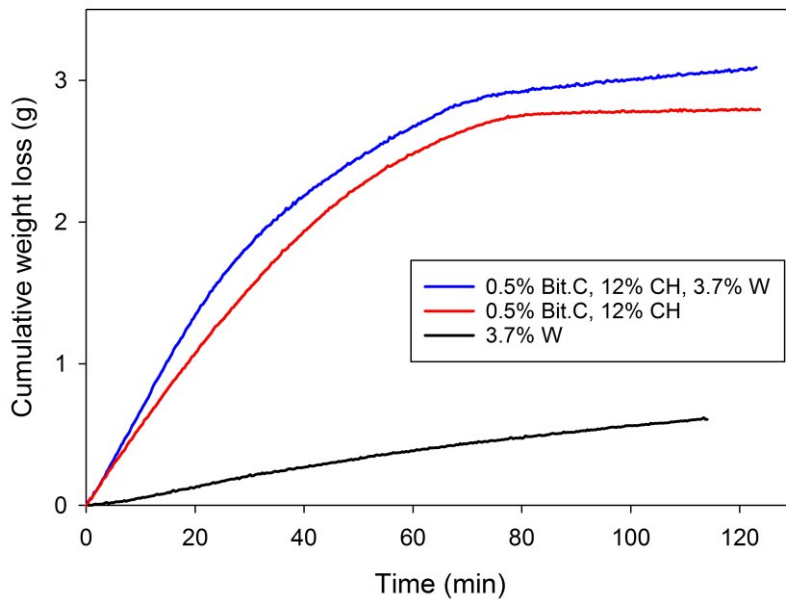


**Figure 31. Drying curves for showing the effect of water during the slow drying stage, CH = Cyclohexane, W = Water**

**Table 4. Initial flux and final flux for drying curves of samples with 0.5% Bit.C, 12% CH, with and without water and drying curve for water**

Sample name	Initial flux (g/min.cm <sup>2</sup> )	Final flux (g/min.cm <sup>2</sup> )
0.5% Bit.C and 12% CH	2.85e-03	4.58e-05
0.5% Bit.C, 12% CH and 3.7%W	3.45e-03	1.99e-04
3.7% W	2.60e-04	1.99e-04 <sup>A</sup>

<sup>A</sup> Water drying curves don't have a breakpoint, the final flux for it refers to: from the later of the transition times in the above two samples till the end of drying. The samples with water were dried under similar RH conditions.

As can be seen from Table 4, the final flux was as low as 4.58e-05 g/min.cm<sup>2</sup> in the absence of water in reconstituted gangue sample. Since there were no other volatiles

in the system, this low final flux was due to the residual cyclohexane being lost probably by diffusion inside the porous gangue bed as reported previously [8]. The addition of water into the system caused the final flux to increase to 1.99e-04 g/min.cm<sup>2</sup>. This is an order of magnitude increase in the flux. The final flux in the reconstituted gangue sample with water (0.5% Bit.C, 12% CH, 3.7% W) is very similar (in the case above, the same) with what was observed for reconstituted sample with only water (3.7% W) in it. What these results indicate is that indeed the slow drying stage is dominated by water drying. The cyclohexane loss during the slow drying stage seems to be diffusion limited.

The effect of relative humidity on the final drying flux wasn't studied in detail since studying the removal of water from the gangue was not the focus of this thesis.

The final drying flux i.e. the flux during the slow drying stage varied from 1.73-2.70 e-04 g/min.cm<sup>2</sup>. There was no visible trend in the final drying flux with respect to the initial Bit.C% or initial cyclohexane content in the samples.

## 5. Bitumen Migration Studies

### 5.1 Bitumen Migration and Volatile Loss in Pictures

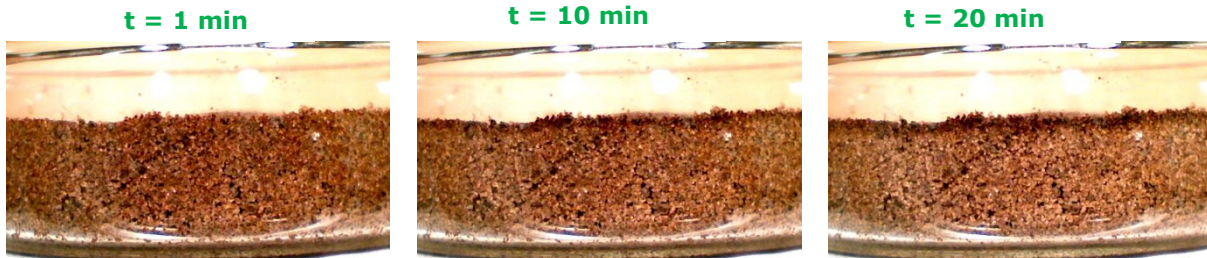


**Figure 32.** Bitumen migration leading to thicker dark top layer.

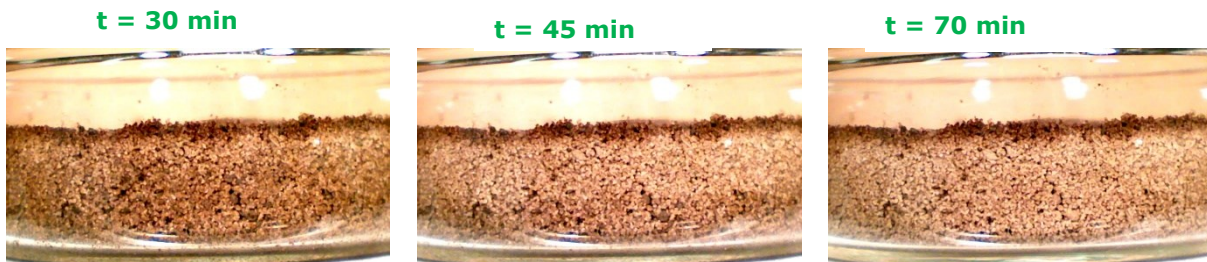


**Figure 33.** The top layer stays the same thickness, the middle lighter layer increases in thickness.



**Figure 34.** The gangue bed at the end of drying. Sample: 1% Bit.C, 12% CH, 3.7% W, bed height = 1 cm

The above images show the typical bitumen migration and the associated volatile (cyclohexane and water) loss during the drying of *12% cyclohexane, 0.5-2% Bit.C and 3.7% water* containing reconstituted gangue. The pictures were taken using the Point 2 View USB Document camera. The contrast of the original pics was enhanced by 30 (with 0 being no enhancement and 100 maximum) using the picture editing feature in Microsoft office 2010.

## 5.2 Visual Observations during Drying

Initially the reconstituted gangue bed looks uniformly wet and of the same color throughout as seen in Figure 32 at time of 1 min. Further with an increase in time we observe that a thin layer of the bed from top becomes darker (Figure 32, time = 10 min). This darkening of the top layer is due to the deposition of bitumen migrating with cyclohexane from inside the bed as reported before [21]. Bitumen is soluble in cyclohexane and can be considered as the non-volatile solute in the cyclohexane-bitumen solution. It is akin to salt in salt-water solution drying inside a porous bed. Bitumen migration process is hence paralleled with salt migration as mentioned earlier in Chapter 2. Bitumen migration like salt migration might be manifested by the existence of liquid connectivity to the top of the bed via liquid films. Though alike in these aspects, these two processes have some noticeable differences.

Salt migration involves efflorescence formation at the top surface [37], [39], [41], [43], [45], [46] and accompanying bed growth in a direction opposite to the source material [37], [39], [43], [44], [46], [56]. Bitumen migration on the other hand doesn't lead to bed growth or efflorescence formation as can be seen from Figs. 32, 33 and 34. Bitumen deposition seems to occur sub surface.

Until the entire bed has a wet appearance, the extent of bed from the top that gets darker increases with time (Figure 32, time = 20 min). Cyclohexane carries the bitumen from inside the bed probably via liquid films to the top of the bed. Cyclohexane is lost via diffusion to the surrounding air, bitumen the non-volatile solute stays behind in the pores near the top of the bed. This leads to the top of the bed having a darker appearance.

A visual cue for identifying that the entire bed is wet is the non-existence of a lighter colored layer underneath the top layer (Refer Figure 33, time = 30 min). The thickness of the top layer ceases to increase once the lighter colored layer starts to be seen underneath the dark top layer. The lighter colored layer may be dried up pores, indicating a discontinuity in capillary connectivity to the top of the bed. As time progresses, the extent of this lighter colored layer increases (Figure 33, time = 45 min) indicating that the pores with liquids/liquid films (Figure 2) have gone deeper inside the bed.

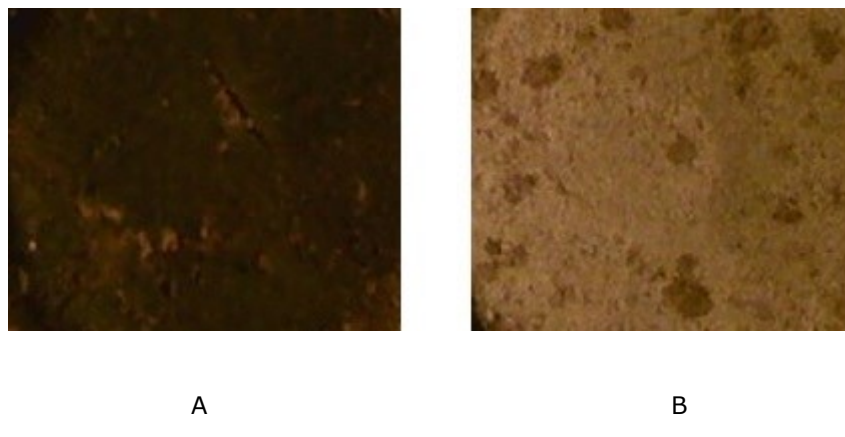


**Figure 35. A cross section of the top view image for: A) Reconstituted sample with bitumen, 12% cyclohexane and water B) Reconstituted sample with bitumen, 8% cyclohexane and water**

Figure 35, shows the typical top view images obtained when drying reconstituted samples with 12 and 8% cyclohexane, bitumen and water. The Point 2 View USB Document camera was mounted overhead of the sample to obtain these images.

In Figure 35 A, we see a uniformly dark top surface due to bitumen deposition for 12% cyclohexane, bitumen and water containing samples. For samples with lower solvent content i.e. 8% cyclohexane with bitumen and water, dark discrete patches are formed on the top (Figure 35 B) instead of a uniformly dark top surface. The side view images for 8% cyclohexane, bitumen and water containing samples didn't show a distinct dark top layer.

The observation of dark discrete patches indicates that the capillary connectivity to the top of the bed for 8% cyclohexane, bitumen and water containing samples was limited. These dark spots might be the location of finer pores which like in salt migration [37] are the preferred locations for liquid (cyclohexane) vaporization due to existence of capillary connectivity.

### 5.3 Bitumen Migration Analysis Methods

The CHNS analysis of the top and bottom layers obtained after drying experiments for reconstituted gangue samples gave us the average C% in each of these layers. Since bitumen was the only organic carbon source in reconstituted gangue hence the initial Bit.C% (Bitumen associated C %) is given by the following –

$$\text{initial Bit.C\%} = (x_i - x_s) \quad (12)$$

Where,  $x_i$  is the initial C% in the reconstituted gangue obtained by CHNS analysis of the DSBS solids and  $x_s$  is the inorganic C% in reconstituted gangue obtained by CHNS analysis of Soxhlet gangue.

The initial Bit.C% of reconstituted samples can vary by as much as 20% of the reported values (0.5-2).

The Bit.C % in the top and bottom layers is given by –

$$\text{Top layer Bit.C\%} = (x_{TL} - x_s) \quad (13)$$

$$\text{Bottom layer Bit.C\%} = (x_{BL} - x_s) \quad (14)$$

Where  $x_{TL}$  and  $x_{BL}$  are the C% of top and bottom layers collected after 120 min of drying followed by QICMS analysis. The values are obtained by the CHNS analysis of the respective layer.

For reconstituted samples with 8% cyclohexane, bitumen and water, the top layer refers to the dark patches formed at the surface as shown in Figure 35B. These patches were scraped off for CHNS analysis. For the reconstituted samples with 12%

cyclohexane, bitumen and water the top layer is the darker layer formed at the top as shown in Figure 34.

### 5.3.1 Enrichment Ratio

Enrichment ratio defined as the ratio of bitumen wt.% in the top layer to the bitumen wt.% in the initial gangue sample has been said to be an effective parameter for representing bitumen migration [21]. Bitumen wt.% in a sample as mentioned in [21] can be given by-

$$\text{Bitumen\%} = \frac{\text{Bit.C\%}}{0.833} \quad (15)$$

0.833 being the mass fraction of carbon in bitumen [57].

Alternatively enrichment ratio can be defined as –

$$\text{Enrichment ratio} = \frac{\text{Bit.C\% in the top layer}}{\text{Bit.C\% in the gangue sample initially}} \quad (16)$$

$$= \frac{(x_{TL} - x_s)}{(x_i - x_s)} \quad (17)$$

Bitumen migration leads to higher Bit.C% in the top layer than initially. Thus bitumen migration to the top layer can be indicated by an enrichment ratio greater than 1 [21].

### 5.3.1.1 Enrichment Ratio Comparison for Reconstituted and Extracted Gangue

Enrichment ratio of extracted gangue (#1) and most comparable reconstituted gangue sample (#2) has been shown in Table 5.

**Table 5. Enrichment ratio of extracted and reconstituted gangue.**

Sample name	Enrichment ratio
Extracted gangue	3.91
Reconstituted gangue	4.30

As can be seen from Table 5, similar enrichment ratio can be obtained for the, *Extracted* and *Reconstituted gangue* samples with similar initial compositions. This is another validation (apart from drying behaviour mentioned in Chapter 4) of reconstituted gangue behaving similar to extracted gangue.

### 5.3.1.2 Enrichment Ratio Comparison for Reconstituted Gangue with Bitumen, Water and 12 or 8% Cyclohexane

An enrichment ratio of greater than 1 was obtained for drying experiments carried out with reconstituted gangue samples with 12 or 8% cyclohexane, 0.5-2% Bit.C and 3.7% water.

For both 12 and 8% cyclohexane containing reconstituted samples, a higher enrichment ratio was obtained for 0.5% Bit.C samples compared to the 1.5 and 2% Bit.C samples at any specific bed height

The comparison of enrichment ratio for 12 and 8% cyclohexane containing samples at the different bed heights has been shown in Figure 36, 37 and 38.

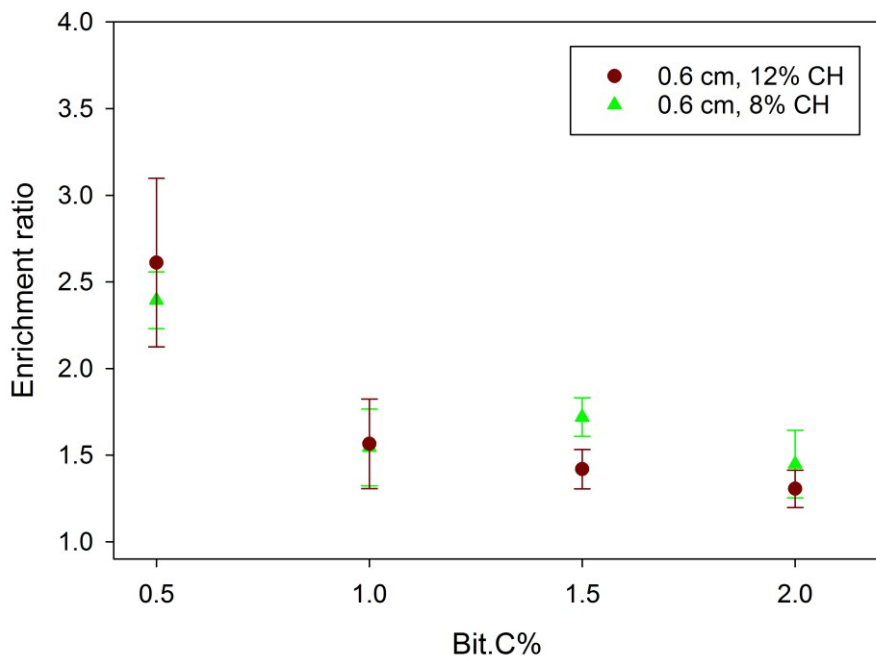


**Figure 36. Enrichment ratio comparison at different cyclohexane (CH) contents, bed height= 0.6 cm**

Similar numbers for enrichment ratio was observed for 12 and 8% cyclohexane containing reconstituted samples at a bed height of 0.6 cm. The weight of top layer for 8 and 12% initial cyclohexane containing samples is shown in Table 6. For the same enrichment ratio a heavier top layer indicates a higher bitumen migration. For e.g. 2% Bit.C samples with initial 12% initial cyclohexane had a much heavier top layer compared to 2% Bit.C samples with 8% initial cyclohexane samples. This implies 2% Bit.C samples should have a higher bitumen migration even though not directly evident from the enrichment ratio values.

**Table 6. Top layer weight comparisons for 12 and 8% cyclohexane containing samples.**

Sample name	Top layer weight (g)	
	12% cyclohexane and	8% cyclohexane and
	3.7% water	3.7% water
0.5% Bit.C	1.91 ± 0.64	1.11 ± 0.26
1% Bit.C	2.82 ± 0.63	2.01 ± 0.29
1.5% Bit.C	3.70 ± 0.42	2.06 ± 0.18
2% Bit.C	4.68 ± 1.00	1.32 ± 0.26

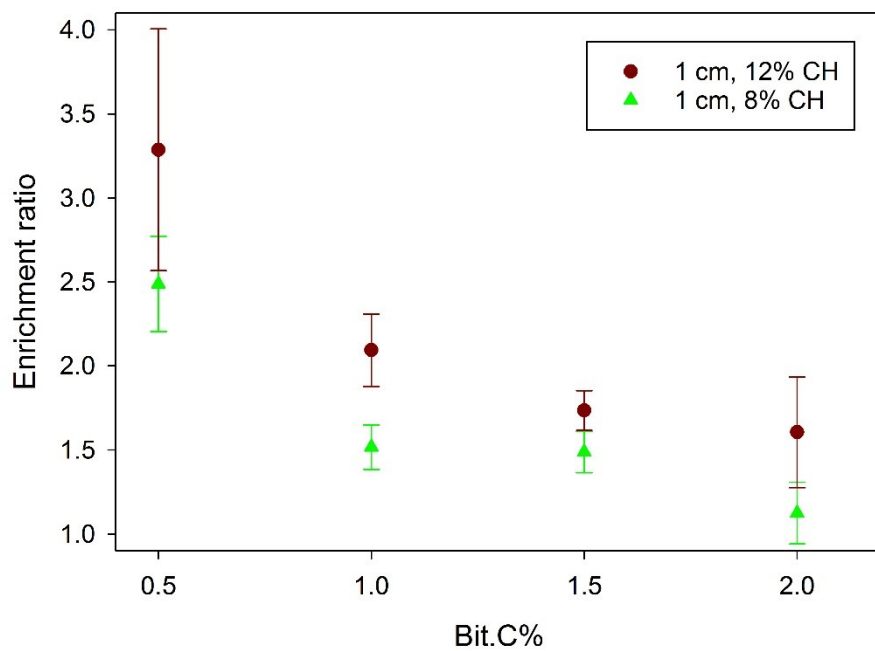


**Figure 37. Enrichment ratio at different cyclohexane contents, bed height= 1 cm**

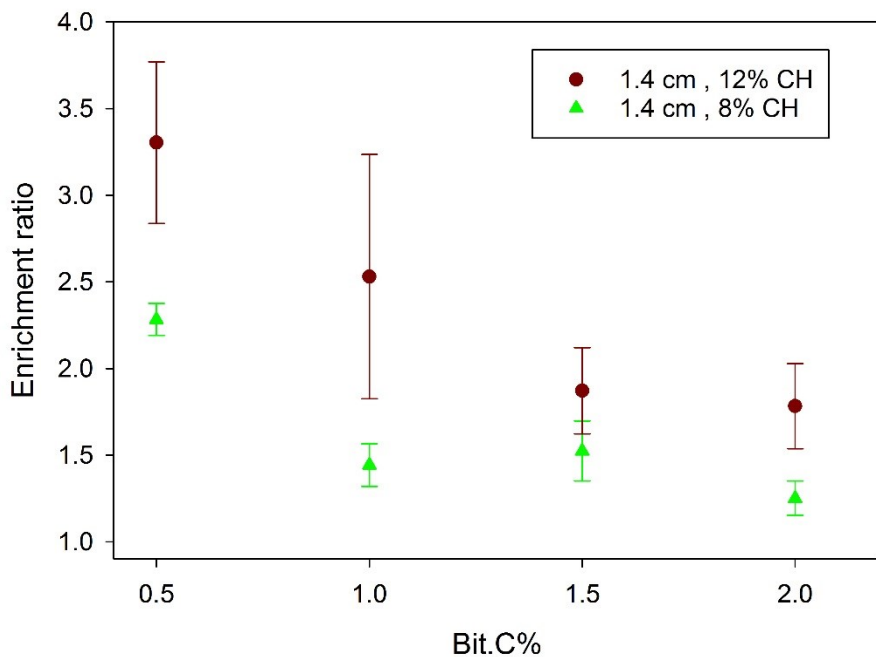


**Figure 38. Enrichment ratio comparison at different cyclohexane contents, bed height= 1.4 cm**

As can been seen from the Figs. 37 and 38, reconstituted samples containing 12% cyclohexane had a higher enrichment compared to 8% cyclohexane samples for the different Bit.C% tested (for bed heights 1 and 1.4 cm). These observations indicate a reduction in bitumen migration with a drop in solvent content. For samples with 2% Bit.C and 8% cyclohexane initially, the enrichment ratio for bed heights 1 and 1.4 cm in some experiments was very close to 1, indicating negligible bitumen migration.

Because enrichment ratio isn't sensitive to the top layer weight collected, for certain cases (same enrichment ratio but different weights) it might lead us to misleading conclusions for bitumen migration. Enrichment ratio though, can be said to be an

estimate of the quality of migration. To explain this further we have to understand how bitumen migration differs in 12 and 8% initial cyclohexane containing samples.

In 8% initial cyclohexane containing samples, fewer top pores will have bitumen deposition (dark patches) compared to 12 % initial cyclohexane containing samples (dark layer). These dark patches as seen above, in some cases for a bed height of 0.6 cm have similar enrichment compared to the top layer of 12% cyclohexane containing samples. For similar initial Bit.C%, same values of enrichment ratio in 8 and 12% samples means the Bit.C% in the dark patches is equal to the Bit.C% in the dark top layer of 12% cyclohexane containing samples. Hence we can say that in a micro scale in the finer pores where bitumen has deposited (in 8% cyclohexane containing samples) the quality of bitumen migration (Bit.C%) is similar to that in the pores of top layer of 12% cyclohexane samples.

At bed heights of 1 and 1.4 cm, the quality of migration indicated by enrichment ratio is higher for 12% cyclohexane containing samples.

To have a more quantitative comparison of bitumen migration, a new migration formula was developed which took into account the weight of the top layer collected after the drying experiments along with the Bit.C% initially and finally. This new migration formula was termed 'Bitumen migration fraction'.

### 5.3.2 Bitumen Migration Fraction (BMF)

Bitumen migration fraction is defined as the ratio of mass of bitumen migrated into the top layer to the total mass of bitumen in the sample. A point to note is that the definition of bitumen migration fraction is symmetric i.e. the mass of bitumen

migrating into the top layer = mass migrating out of bottom layer. It takes into account both the enrichment ratio and the masses of top and bottom layers.

$$\begin{aligned}
 \text{Migration fraction} &= \frac{W_{bitTLF} - W_{bitTLi}}{W_{bitBLi} + W_{bitTLi}} \\
 &= \frac{(x_{TL} - x_i)}{(x_i - x_s)} * \frac{y_{TL}}{y_{TL} + y_{BL}}
 \end{aligned} \tag{16}$$

Where bitumen in the top layer initially and finally is given by  $W_{bitTLi}$  and  $W_{bitTLF}$  respectively. Bitumen in the bottom layer initially is given by  $W_{bitBLi}$ .  $y_{TL}$  is the weight of dried top layer,  $y_{BL}$  is the weight of the dried bottom layer. Hence the weight of dried sample is given by  $y_{TL} + y_{BL}$ . The numerator in the equation denotes the weight of bitumen migrated to the top layer. The bottom layer denotes the weight of bitumen in the sample initially. Though the formula mentioned here seems quite intuitive it involves a small error as it is a variant of the actual bitumen migration fraction (Refer Appendix C.1). The error is quite small though and scales with initial Bit.C% (*i.e.*  $x_i - x_s$ ) of the sample and is given by  $1.2 * (x_i - x_s)$  %. Because the maximum initial Bit.C % of reconstituted sample used in this study is 2%, the maximum error using the bitumen migration fraction formula is 2.4%. This error has been neglected in the calculations.

BMF greater than 0 indicates migration to have taken place to the top layer. Due to the nature of the equation developed, BMF values will always be  $< 1$ .

### 5.3.2.1 Bitumen Migration Fraction Comparison for Reconstituted and Extracted Gangue

BMF of extracted gangue (#1) and most comparable reconstituted gangue sample (#2) was compared, similar to enrichment ratio as shown in Table 7.

**Table 7. Bitumen migration fraction of extracted and reconstituted gangue.**

Sample name	Bitumen migration fraction
Extracted gangue	0.60
Reconstituted gangue	0.64

The BMF values as shown in Table 7 are also comparable.

Based on the drying results from Chapter 4 and the enrichment ratio and bitumen migration fraction comparisons for extracted and reconstituted gangue done here, it can be ascertained that reconstituted gangue reflects and imitates not only the drying but also the associated migration behaviour of extracted gangue.

### 5.3.2.2 Bitumen Migration Fraction for Reconstituted Gangue with Bitumen, Water and 12 or 8% Cyclohexane

BMF of reconstituted gangue samples with *12, 8% cyclohexane, 0.5-2% Bit.C and 3.7% water* has been determined. Comparison of BMF for the 12 and 8% cyclohexane containing samples at the different bed heights has been made in Figures 39, 40 and 41.

For the bed height of 0.6 cm, 2% Bit.C samples with 12% cyclohexane had a higher BMF compared to 8% initial cyclohexane samples. This was what was expected looking at their similar enrichment ratios but higher top layer weight of 12% cyclohexane samples. 0.5% Bit.C was the only other Bit.C% where 12% cyclohexane samples had a higher BMF. Reconstituted samples with 1 and 1.5 % Bit.C had similar BMF at the different solvent contents.

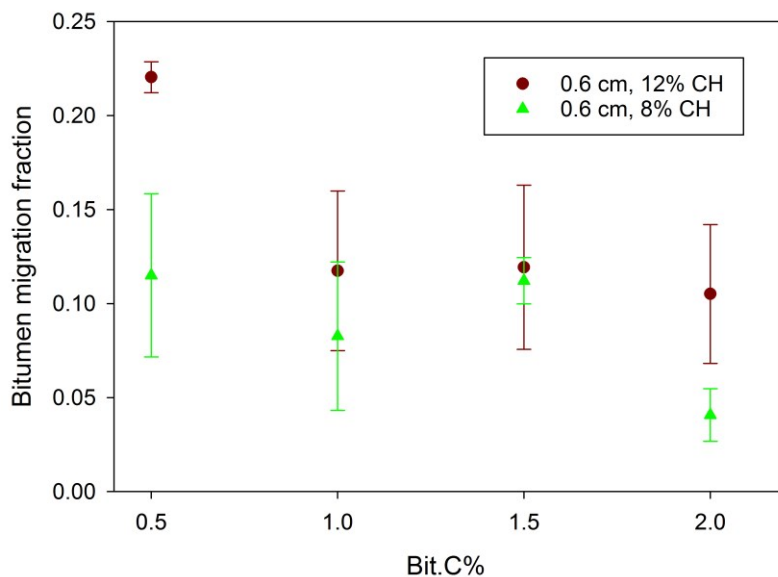


**Figure 39. Bitumen migration fraction comparison at different cyclohexane contents, bed height= 0.6 cm**

For bed heights of 1 and 1.4 cm, the BMF values of higher initial solvent samples was more for any Bit.C%. Hence it can be concluded that at these bed heights a higher migration occurs when the initial solvent content was 12%.

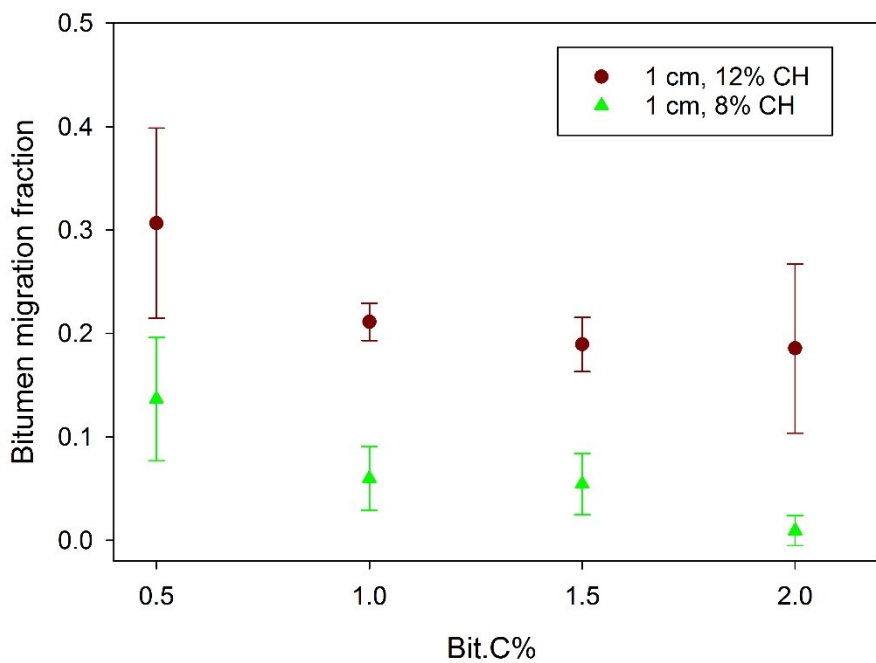


**Figure 40.** Bitumen migration fraction comparison at different cyclohexane contents, bed height= 1 cm

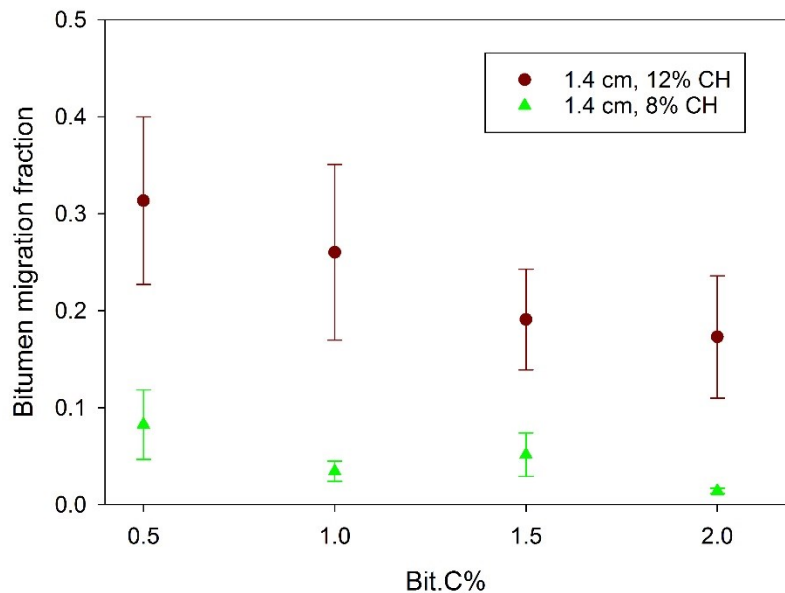


**Figure 41.** Bitumen migration fraction comparison at different cyclohexane contents, bed height= 1.4 cm

Bitumen migration phenomenon as stated before is largely dependent on capillary connectivity of cyclohexane from inside to the top of the bed (probably via liquid films). A higher bitumen migration can be said to be indicative of capillary connections to the top of the bed existing for a longer duration, hence allowing more bitumen from inside the bed to be deposited on the top. 12% initial cyclohexane containing samples seem to mostly have higher BMF compared to samples with 8% cyclohexane initially. It can be argued that a high BMF doesn't necessarily mean better liquid connectivity, but may indicate bitumen deposition at a faster rate for the same liquid connectivity.

Looking at Figs. 39, 40 and 41 we see that usually for any initial cyclohexane content, the BMF for 0.5% Bit.C samples was higher compared to 1.5 or 2% Bit.C samples. In Chapter 4, Figs 16 and 22 show how transition time increased with Bit.C% for samples with same initial solvent content. In the same chapter it was also concluded that most of the cyclohexane loss occurs prior to the transition time. A significantly shorter transition time for 0.5% Bit.C samples compared to 2% Bit.C samples and a reverse BMF trend in these samples (0.5% highest, 2% Bit.C lowest) possibly signifies a better sorptivity in the bed with 0.5% Bit.C. The sorptivity of the bed was investigated as a possible explanation to the reduced solvent drying times (lower transition time) and higher initial flux at lower Bit.C% in samples.

Before investigating the sorptivity though, it was checked if the reduction of initial flux in the 2% Bit.C samples compared to 0.5% Bit.C samples especially ones with initially 12% cyclohexane content was due to vapour pressure depression due to higher solute content in the cyclohexane-bitumen solution in the gangue bed.

## 5.4 Pure Cyclohexane and Cyclohexane-Bitumen Solution Drying

To study the effect of presence of bitumen on the drying of cyclohexane, 2 different wt. % of bitumen-cyclohexane solutions were prepared. The goal of this set of experiments was to validate if the almost 40% drop in initial flux for the 2% Bit.C samples with 12% initial cyclohexane and 3.7% water compared to 0.5% Bit.C samples with the same volatile composition was due to vapor pressure depression of cyclohexane . Samples were prepared assuming all the bitumen in the reconstituted gangue samples dissolved in the cyclohexane present initially. Realistically, not all of the bitumen present in the reconstituted gangue samples would dissolve in the initial cyclohexane present. Still this assumption of complete dissolution was expected to shed some light on vapor pressure depression, if present.

The solutions prepared contained about 5.30 and 15.70 wt. % of bitumen in cyclohexane initially (based on 0.5 and 2% Bit.C). Drying runs were performed for these samples in triplicates. Drying runs were also carried out with pure cyclohexane (n=6). The runs were performed in the fume hood balance chamber under the same conditions as reconstituted gangue drying runs but without the usage of lamps. Our objective was to see the trend in initial flux variation with increase in Bit.C% and not look into the absolute values attained and hence the non-usage of lamps shouldn't affect the observations.

While drying the cyclohexane bitumen solution an interesting observation was made. The picture below shows a petri-dish where the cyclohexane-bitumen solution is drying. The picture below taken after 15 min of cyclohexane bitumen solution drying shows a thick layer of bitumen (marked in the Figure 42) on the glass walls of the

petri-dish over a dark cyclohexane-bitumen solution. Figure 42 also provides a visual clue on what caused the bitumen to move to the walls of the glass petri-dish and deposit there.

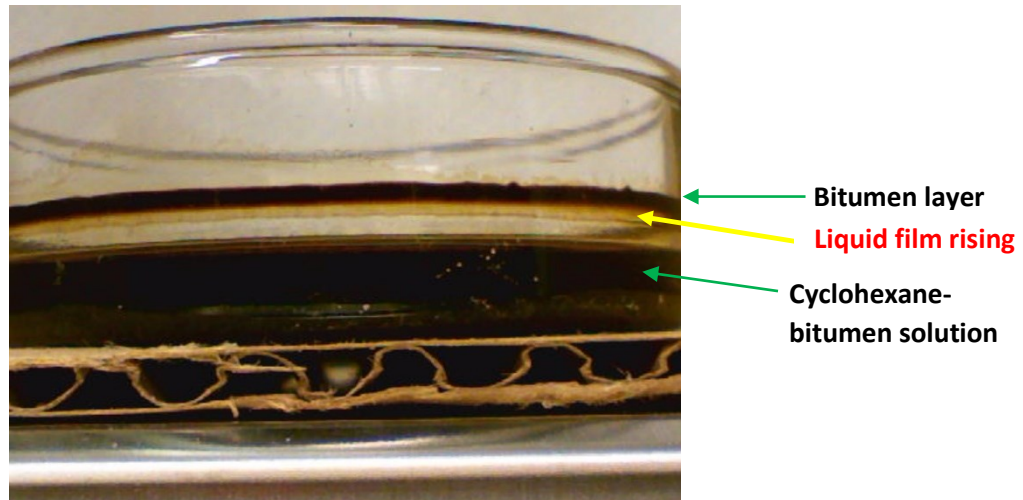


**Figure 42. Cyclohexane-Bitumen solution drying, showing thin liquid film rising**

The picture in Figure 42, makes it clear that the bitumen deposition on the walls of petri dish was made possible due to rising cyclohexane-bitumen films carrying the bitumen along the walls of the petri dish until the cyclohexane diffused into the air causing bitumen deposition. This observation was very crucial since it gave us a visual indication on how the bitumen migration might be occurring inside the gangue bed. We can expect a similar observation in the micro scale pores inside the gangue during drying. Capillarity driven solvent movement in the gangue via liquid films existing till the top of the bed as previously suspected seems to be what is causing the bitumen migration and deposition and validated by this observation made. Bitumen deposition in the pores though can significantly affect the drying behaviour (As will be discussed in Section 5.7) unlike in a petri-dish.

The drying curves obtained have been shown in Figure 43.

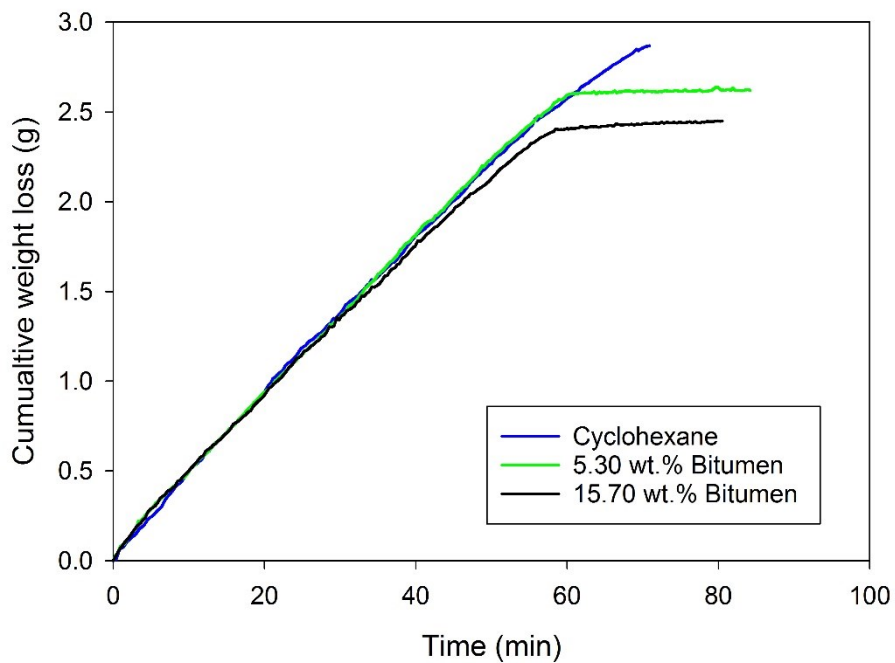


**Figure 43. Drying curves for cyclohexane, 5.30 and 15.70 wt. % initial bitumen**

About the same weight of solutions and pure cyclohexane were dried. Because 15.70 wt. % initial bitumen had more bitumen by weight in solution (black curve) we observe a breakpoint in it at a lower cumulative weight as compared to 5.30 initial wt. % bitumen-cyclohexane solution. The 5.30 and 15.70 initial wt. % bitumen samples both had an extremely slow drying stage (Though more evident in the case of 15.70 initial wt. % bitumen) following the breakpoint unlike pure cyclohexane drying which had no such stage. As can be seen above, the 5.30 and 15.70 wt. % initial bitumen content solutions have a very good overlap with the cyclohexane drying curve for the initial 40 min.

Looking at these representative curves it seems as if 15.70 wt. % initial bitumen samples might have a lower drying flux after 40 min of drying. The drying flux plots made in Figure 44 indicates that this lowering of drying flux was insignificant. The

drying flux was determined by linear fitting 5 min intervals of time and dividing by  $19.64 \text{ cm}^2$  i.e. the surface area of the petri dish. The drying flux values obtained for any interval was plotted vs the midpoint of that interval. There was a lot of fluctuation in the drying flux initially when the sample was loaded, probably due to uncontrolled airflow while setting up the experiment. Hence for the 1<sup>st</sup> 5 min, 2 linear fits were made at 2.5 min intervals.

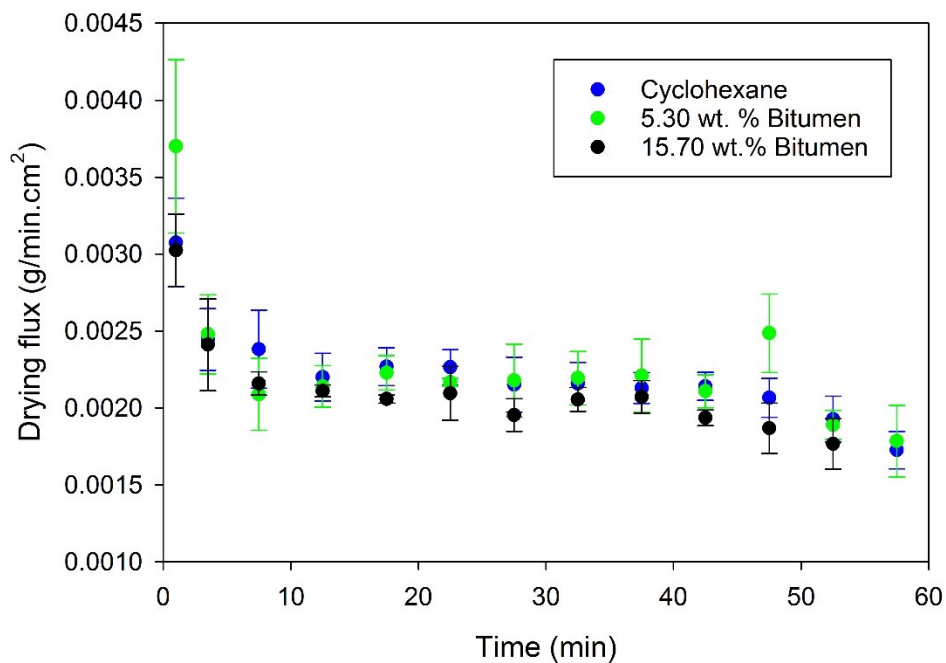


**Figure 44. Drying flux plots for cyclohexane, 5.30 and 15.70 wt. % initial bitumen**

The standard deviations shown in the plot is because the experiments were repeated three to five times. The drying flux for both the solutions and for pure cyclohexane drying was identical and almost constant from 5-57.5 min. Clearly this meant that there was negligible vapor pressure variation due to different wt. % of bitumen in the bulk solutions present inside the gangue. Hence vapor pressure depression due

to variable solute content in the bulk solution can't justify the variation in initial flux being observed at highest and lowest Bit.C%.

The slow drying stage obtained after the breakpoint though, in the bitumen-cyclohexane solutions needed more attention. For 15.70 wt. % initial bitumen solutions the drying flux during this stage was  $1.49 \pm 0.25 \text{ e-}04 \text{ g/min.cm}^2$  (By linear fit in this stage). Compared to the drying flux prior to the breakpoint (mean  $\sim 2.2 \text{ e-}03 \text{ g/min.cm}^2$ ) the drying flux in this post breakpoint stage was an order of magnitude lower. What this implied is that bitumen could be considered a strong resistance for the cyclohexane evaporation if cyclohexane was present in traces in the solution.

Next, pore blockage due to bitumen migration was investigated as the cause for reduction in initial flux and in the overall drying time in the 2% Bit.C samples compared to 0.5% Bit.C samples. This was suspected especially for *0.5-2% Bit.C, 12% cyclohexane and 3.7% water* samples which had higher BMF compared to *0.5-2% Bit.C, 8% cyclohexane and 3.7% water* samples. More on this study will be discussed in the following section.

## 5.5 Pore Volume Saturation with Bitumen

The BMF values for 0.5% Bit.C usually was higher compared to 1.5 or 2% Bit.C samples. From this information it might be misunderstood that the pores for 0.5% Bit.C samples will be more saturated with bitumen compared to 1.5 or 2% Bit.C samples. It needs to be kept in mind that BMF is a measure of the ratio of bitumen migrating into the top layer to the net bitumen in the sample and not the amount of bitumen present in the top layer. The calculations made as shown in Figure 45 was for samples with initially 12% cyclohexane. The pore volume saturation with bitumen

in the top layer as shown in Figure 45 was actually higher for 2% Bit.C (followed by 1.5% Bit.C) samples since they initially had much more bitumen in the pores compared to 0.5% Bit.C samples. Pore volume saturation % is actually a measure of the volume % of the pores occupied by the said solute/solvent.

The higher bitumen migration in 0.5% Bit.C samples cannot compensate for the initial high pore volume saturation with bitumen in the top layer for 2% Bit.C samples. The initial pore volume saturation with cyclohexane and water in 12% initial cyclohexane containing samples was close to 32% and 7% respectively throughout the bed. The initial pore saturation volume % with bitumen in Figure 45 refers to the initial pore saturation in the top layer with 0.5-2% Bit.C.

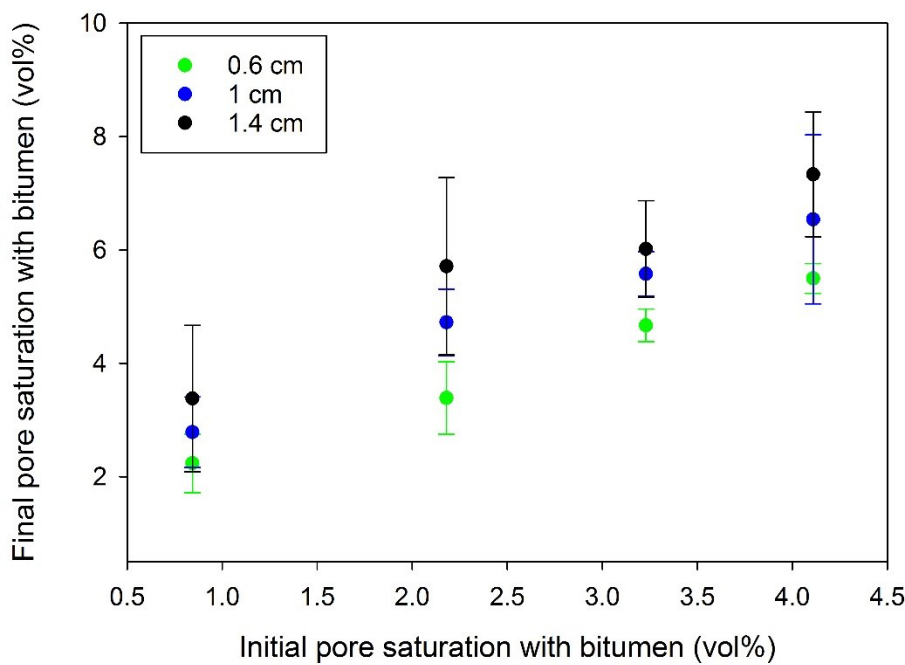


**Figure 45. Final vs initial pore saturation vol. % in the top layer with bitumen**

The calculations of final bitumen pore volume saturations for any sample actually represent the average bitumen pore saturation volume % over the entire top layer.

Assuming that the entire top layer would have a uniform pore saturation with bitumen though, is only valid when the sample hasn't start drying yet. This is because the sample prior to drying can be considered homogeneous. Bitumen migration could cause gradation in bitumen deposition leading to variable bitumen pore saturation volume % in the top layer. Because it was difficult to know how the bitumen saturation in the pores of the top layer varied, as a rough approximation the assumption of the entire top layer having the pore saturation volume % equal to the average value calculated was made.

From Figure 45 it can be concluded that the final saturation in the pores with bitumen increased with increase in Bit.C% (initial pore saturation volume). The maximum pore volume saturation % with bitumen after the drying was very low i.e. <10%. Pore blockage doesn't seem to be what was causing the drop in initial flux at higher Bit.C%.

Since samples with *0.5-2% Bit.C, 8% cyclohexane and 3.7% water* compared to 12% initial cyclohexane samples had much lower bitumen migration (At bed heights of 1 and 1.4 cm) hence the pore volume saturation would be lower and wasn't investigated.

Next the change in sorptivity of bed due to different concentrations of bitumen in bitumen-cyclohexane solutions inside the pores of gangue was investigated for causing possible reduction in initial flux in 2% Bit.C samples compared to 0.5% Bit.C samples with any solvent content and 3.7% water.

## 5.6 Sorptivity Studies

Sorptivity as mentioned before depends on both the material and fluid and is given by [46], [47] -

$$S = \left(\frac{\sigma}{\mu}\right)^{\frac{1}{2}} S' \quad (5)$$

Where  $\sigma, \mu$  are the surface tension of fluid (mN/m) and its viscosity (cP) respectively,  $s'$  is the intrinsic sorptivity of the material. A reduction in sorptivity implies a reduction in capillarity of the bed. For gangue samples with different residual Bit.C% we have assumed the intrinsic sorptivity to be constant. This estimate has been made considering that the solids (material) making up all the different gangue samples prepared was Soxhlet gangue (having a similar fines-coarse solids content due to being obtained from the same batch of oil sands ore). The fluid inside the gangue bed was the cyclohexane-bitumen solution.

The wettability of Soxhlet gangue and DSBS solids was determined by film flotation technique described in Section 3.8 and Appendix A.4. The critical surface tension of Soxhlet gangue was determined as  $34 \pm 7$  mN/mm. The critical surface tension of DSBS solids varied from  $29-32 \pm 5$  mN/m. There was no visible trend in critical surface tension with Bit.C%. In a gangue bed in actuality, part of this bitumen coating of DSBS solids would be dissolved in the cyclohexane to form the cyclohexane-bitumen solution. The wettability values mentioned above for the DSBS solids can be considered to be obtained if none of the bitumen dissolved i.e. the extreme case. The critical surface tension was measured for knowing if the wettability of the gangue bed

could be influenced by bitumen at these concentrations in gangue bed. As can be deduced looking at the values obtained, the critical surface tension of Soxhlet gangue and DSBS solids wasn't distinct.

The determination of sorptivity of the bed depends on the values of surface tension and viscosity of the fluid as stated in equation 5. The surface tension of cyclohexane is in the range 23.8-24.5 mN/m for the temperature range of 30-25 °C [58] .The surface tension of bitumen obtained from medium grade ore, Suncor and Fort McMurray sites has been reported to be in the range 23-28 mN/m at 23 °C [59]. Looking at these values for cyclohexane and bitumen, surface tension of cyclohexane-bitumen solutions with varying bitumen content was not expected to vary enough to cause a change in sorptivity.

Finally variation in viscosity of the cyclohexane-bitumen solution was investigated to look for changes in sorptivity in the bed if any. Previously, cyclohexane-bitumen solution viscosity variation had been determined for cyclohexane weight fraction 0-0.13 [60]. For higher cyclohexane weight fractions as would be expected in the bulk solutions inside the pores of gangue initially, the viscosity values hasn't been reported before. Instead of conducting a detailed study on the effect of higher cyclohexane weight fractions on cyclohexane-bitumen solutions viscosity, existing literature on toluene-bitumen solutions was examined. This viscosity relationship with varying weight fraction of toluene-bitumen solutions was approximated as an initial estimate/guess for what could happen with cyclohexane-bitumen solutions in the gangue initially.

Guan [50] determined toluene-bitumen viscosities for toluene weight fractions 0.05-0.60 at 27 °C and 1.2 atm. Models for predicting viscosity were also discussed and compared with the determined experimental values. The two mixing models that correlated well with the experimental data were power law model and Lederer model. The power law model was based on Kendall and Monroe [61] mixing model. For details about the various mixing models and their applicability please refer Guan [50].

Based on the assumption made in section 5.4, viscosity value variations for cyclohexane weight fractions of 0.84 and 0.95 (conversely bitumen weight fraction of 0.16 and 0.05) was of interest. For 8% initial cyclohexane samples assuming complete bitumen dissolution inside gangue bed, the viscosity variations for similar cyclohexane weight fractions of 0.8 and 0.94 needs to be determined. Neither of experimental or model predicted viscosity values for toluene-bitumen solutions at the same weight fractions were available. Hence in this work, Lederer model which worked well for the range 0.05-0.60 weight fraction of toluene was applied on the experimental data set to predict the viscosity values in the range 0.60-1.00 as shown in Figure 46 (Shown 0.30-1.00 toluene weight fraction).

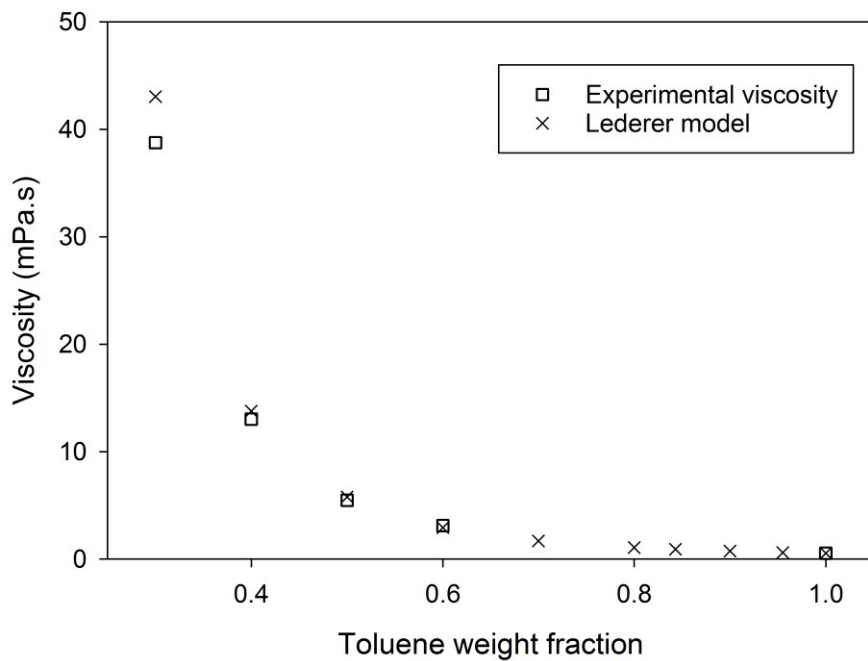


**Figure 46. Viscosity of toluene-bitumen mixture vs toluene weight fraction. The experimental viscosity values are from Guan [50]**

Based on the model predictions, the viscosity of toluene-bitumen solution at a weight fraction of 0.84 was nearly 1.5 times that at a toluene weight fraction of 0.95. This corresponds to the sorptivity at 0.95 toluene weight fraction being about 1.2 times the sorptivity at 0.84 weight fraction (assuming same intrinsic sorptivity of material making up the gangue bed, same surface tension of fluids). Hence assuming the conclusions made above is applicable for cyclohexane-bitumen solution in the reconstituted gangue bed, there is a definite sorptivity and correspondingly capillarity reduction in the bed for lower cyclohexane weight fraction initially. This capillarity reduction in the bed is going to affect the drying kinetics of the bed, possibly leading to the reduction in the initial flux. For now a model doesn't exist for drying cyclohexane-bitumen solutions in gangue and associated bitumen migration. Hence how this sorptivity variation will exactly translate to initial flux reduction can't be said.

## 5.7 Proposed Mechanism of Drying

In this section an understanding of the interaction of initial Bit.C% and cyclohexane in reconstituted samples and subsequent effect on initial drying flux and transition time will be developed. The conclusions made will be based on a bed height of 1 cm but will also be applicable for the bed heights 0.6 and 1.4 cm. As seen in Chapter 3, at bed height of 1 cm the residual cyclohexane content starts exceeding 260 ppm and hence should be the maximum operational bed height to achieve industrial requirements of solvent recovery.

In reconstituted samples with *12% cyclohexane, 0.5-2% Bit.C and 3.7% water* the bitumen deposition on the top is much higher compared to *8% cyclohexane, 0.5-2% Bit.C and 3.7% samples*. This is based on the BMF and enrichment ratio calculations as discussed before (especially for bed heights of 1 and 1.4 cm). 12% initial cyclohexane containing samples have capillary connectivity to the top of the bed (verified by the dark top bitumen layer formed). This capillary connectivity is maintained by liquid films. Near the top of the bed high concentration gradients might exist [26] for cyclohexane vapors. The high concentration gradient will lead to rapid cyclohexane loss and subsequent bitumen concentration at the top layer to increase at a fast rate. As bitumen starts getting concentrated on the top layer, the viscosity of the solution in this layer increases. The viscosity can increase rapidly with increase in weight fraction of bitumen as can be seen in Figure 46. Hence with an increase in concentration of bitumen in the top layer the sorptivity of this layer will be reduced. Due to this reduction in the ability to transmit fluids by capillarity, the solvent concentration in the top will drop rapidly and the liquid films would recede to being

just below the top layer. The liquid films also recede due to the reducing net solution content in the bed. The bitumen being migrated with the liquid films would start depositing lower now leading to an increase in thickness of the top bed as seen in Figure 32. This can also be an explanation for why the bitumen doesn't clog up the top pores but is spread up in a broader top layer leading to the low final pore volume saturations i.e. < 10% by volume as seen in section 5.5. This top bitumen layer due to rapid solvent concentration drop (leading to eventually high bitumen concentration) will have a very low solvent release flux as was observed during the later stages of cyclohexane-bitumen solution drying in section 5.4. Thus a local low flux region can be formed near the top limiting drying, similar to what has been reported before for concentrated salt solution drying [44]. For 2% Bit.C samples compared to 0.5% Bit.C samples, the pores in the top layer are more saturated with bitumen finally as was seen in section 5.5. The final top dark layer weight at a bed height of 1 cm for 0.5% Bit.C samples was  $2.96 \pm 0.44$  g and for 2% Bit.C samples was  $6.92 \pm 1.22$  g. So 2% Bit.C samples along with having higher bitumen concentrations at top also have a thicker top layer i.e. a wider region of local flux reduction.

In reconstituted samples with 8 % cyclohexane, 0.5-2% Bit.C and 3.7% water, there is a change in the overall drying behaviour as compared to samples with 12 % cyclohexane, 0.5-2% Bit.C and 3.7% water. This can be validated by looking at the values of initial flux of 12 or 8% cyclohexane, 0% Bit.C and 3.7% water from Figure 21. The initial flux for samples with 12% and 8% cyclohexane initially was  $3.71 \pm 0.02$  e-03 g/min.cm<sup>2</sup> and  $2.71 \pm 0.10$  e-03 g/min. cm<sup>2</sup> respectively. This 27% drop in initial flux implies a reduction in capillary connectivity in the bed expected with

reduced solvent content. The reduction in capillary connectivity of 8% cyclohexane containing samples has also been corroborated by the dark spots formed in the top layer as shown in Figure 35 B. These dark spots as mentioned before are the fine pores in the gangue bed. Hence the initial drying mechanism in reconstituted samples with 8% cyclohexane unlike in 12% initial cyclohexane containing samples is due to a combination of diffusion from the pores deep inside the bed and via liquid transport to top of the bed followed by diffusion of vapors. As in 12% cyclohexane containing samples the bitumen concentration in the hydraulically connected pores near the top would increase. This would lead to a similar reduction in sorptivity and liquid films in these pores receding. But unlike in the case of 12% cyclohexane containing sample the local flux reduction due to the top pores with bitumen should not significantly affect the overall local drying flux in the top layer region. This is because as said before drying in 8% cyclohexane sample even initially is partly limited due to diffusion from deep inside the pores (with no capillary connectivity to the top).

In 12% cyclohexane containing samples, thicker region for local flux reduction along with reduced initial sorptivity of bulk solution for 2% Bit.C samples compared to 0.5% Bit.C samples can explain the initial flux reduction. These two factors can also explain why the transition time (overall drying time of fast drying stage = overall time to remove most of cyclohexane) was higher for 2% Bit.C samples. For 8% cyclohexane containing samples, reduction in initial sorptivity seems to be the more dominant factor affecting the drying process.

## 6. Conclusions

A protocol was successfully developed to prepare controlled samples that could imitate the drying behaviour of rich grade gangue obtained from cyclohexane based extractions. The control samples were termed as 'reconstituted gangue' samples. With the reconstituted gangue samples the effect of varying initial solvent and residual bitumen contents on solvent removal from gangue was studied in a controlled way. The associated bitumen (solute) migration with solvent evaporation was also investigated. With gangue obtained from extractions due to their inherent variability in composition of cyclohexane and bitumen content it was not possible to perform such a controlled study.

Initially, non-aqueous extractions of rich grade oil sands ore were carried out with cyclohexane as the solvent to obtain two batches of extracted gangue samples. The CHNS analysis of the dried extracted gangue samples confirmed that the bitumen recoveries were higher than 95%. The gangue samples were dried inside a fume-hood under ambient conditions. The cyclohexane and water contents of these samples were estimated using a procedure described by Nikakhtari et al.[8]. Reconstituted samples were prepared using the protocol developed having similar composition as the extracted gangue. Bitumen migration during drying, led to the formation of 2 layers a top dark layer and a bottom relatively lighter colored layer. The drying and bitumen migration behaviour of the reconstituted and extracted gangue were found to be highly comparable.

Once the protocol's adequacy to prepare extracted gangue like samples i.e. reconstituted gangue samples was confirmed, samples with composition 0.5-2% Bit.C (Bitumen Carbon), 12 or 8% cyclohexane and 3.7% water (Cyclohexane free basis) were prepared. 0.5% and 1% Bit.C i.e. 0.6% and 1.2% residual bitumen respectively is the residual bitumen content corresponding to a recovery of 96% and 92% from a rich grade oil sands ore. Previously recoveries >92% have been achieved using cyclohexane on rich grade oil sands ore [8], [20]. One of the main motivations in the development of solvent based extraction technologies is the higher bitumen recoveries associated compared to the water based technologies. If the recoveries using solvent were <88% the economic viability of this process will be questioned. This is considering the typical 88-95% bitumen recovery in water based processes [1]. 1.5% and 2% Bit.C i.e. 1.8 % and 2.4% residual bitumen correspond to bitumen recoveries of 88% and 84%. Studying residual Bit.C% beyond 2% was without doubt unrealistic, since commercial solvent based extraction processes would probably recycle such gangue to obtain higher recoveries.

The critical surface tension for the Soxhlet gangue i.e. the extracted gangue sans bitumen, water and cyclohexane was measured and found to be higher than the surface tension of cyclohexane but lower than that of water. This implies that the reconstituted gangue would only be wetted by cyclohexane and not water. Hence only cyclohexane capillary films would exist in the gangue bed. Drying cyclohexane-bitumen solutions in a petri-dish showed liquid films rising up and depositing bitumen on the petri-dish walls. In the pores of gangue too liquid films might be causing the bitumen migration.

The reconstituted gangue samples were dried at three bed heights i.e. 0.6, 1 and 1.4 cm keeping the porosity of the bed constant. Packed-bed drying (as was studied here) or rotary drum drying are probable ways gangue would be dried up industrially. Lumps or agglomerates of gangue might be formed inside the rotary drum due to capillary binding forces [62] because of the wetting of sand particles by the solvent. Based on preliminary experiments with packed bed, it was expected that for any bed system a bed dimension of 1.4 cm should be the maximum for achieving solvent removal in 2 hr of drying. The packed bed system has the advantages of being easier to model. Though, modelling the process wasn't the objective of this work.

The drying studies revealed that the initial drying flux was affected by the residual bitumen content (i.e.  $1.2 * \text{Bit.C \%}$ ) in the gangue. This effect became pronounced with an increase in bed height (to 1.4 cm) and initial cyclohexane content. For initial cyclohexane content of 12% in the reconstituted gangue, the initial flux for samples with 2% Bit.C compared to 0.5% Bit.C was about 42% lower. For the case of initial 8% cyclohexane content in reconstituted gangue this drop was about 17% for the same bed height studied (i.e. 1.4 cm).

The typical drying curve obtained for gangue drying (reconstituted or extracted) could be divided into two stages, the fast drying stage and a slow drying stage. These two stages were separated by a breakpoint termed as transition time. This 'transition time' was determined using non-linear regression approach and its 95% confidence interval range was estimated using a statistical technique called bootstrapping.

The transition time marked the end of the fast drying stage. Based on the residual cyclohexane content after 2 hr of drying, it was concluded that if the transition time

was reached prior to the end of drying the residual cyclohexane content would be < 600 ppm in the bed. The fast drying stage hence can be said to be the stage where most of the cyclohexane in the bed was lost. The slow drying stage has been previously reported as a water dominant drying stage [8]. To test this, reconstituted gangue samples with 0.5% Bit.C, 12% initial cyclohexane with and without water along with water only samples were dried. The drying curves and flux during the slow drying stage revealed that indeed the slow drying stage was water dominant. The flux during the slow stage for reconstituted sample with 0.5% Bit.C and no water being an order of magnitude lower compared to what was observed for 0.5% Bit.C with water. Interestingly the flux during the same interval of time for the water only sample was the same as what was observed for 0.5% Bit.C samples with water.

The transition time for reconstituted samples with 12% initial cyclohexane like the initial drying flux was a function of Bit.C%. With an increase in Bit.C% the transition time was delayed indicating a slowing down of the solvent removal process. For reconstituted samples with 8% initial cyclohexane the transition time also seemed to be a function of Bit.C. The increase with Bit.C% though, was not gradual like in samples with initial 12% cyclohexane, but more like a step change in increase i.e. 0.5 and 1% Bit.C had similar transition time which was lesser than 1.5 (1 and 1.5% were comparable, though the mean for 1.5% was higher at bed height of 1 cm) and 2% Bit.C which had similar transition times.

When reconstituted gangue samples were dried in a packed bed of height 0.6 cm the time it took for removal of most of cyclohexane (i.e. the transition time) was always < 55 min and the residual cyclohexane content in the bed was < 80 ppm. The transition time and residual cyclohexane content seem to have a good correlation.

For transition times >80 min (i.e. duration of slow drying stage < 40 min) the residual cyclohexane content in the bed can exceed 260 ppm. Because the transition time increased with residual bitumen content and bed height, it was seen that such transition times when residual cyclohexane content was >260 ppm was when the Bit.C% was > 1.5 for a bed height of 1 cm. For 0.5% initial Bit.C% samples the residual cyclohexane content was always <200 ppm at this bed height. For every other sample like 0.5% Bit.C, the transition time was reached before the end of 2 hr of drying. At the bed height of 1.4 cm, transition time was reached only for the samples with 0.5% initial Bit.C% (5 out of 6) and 1 sample with initially 1% Bit.C. The reconstituted samples with initially 1.5 and 2% Bit.C never had their transition time reached at the end of 2 hr of drying. Their residual cyclohexane content was also very high i.e. >> 260 ppm. For optimizing cyclohexane recovery from gangue bed dimensions such as 1.4 cm should be avoided.

The bitumen migration analysis of samples with initial 8 and 12% cyclohexane were made using two ratios – i.e. Enrichment ratio and Bitumen migration fraction. 8% initial cyclohexane samples usually had lower enrichment ratio and bitumen migration fraction. Exception was at bed height of 0.6 cm, where enrichment ratio and bitumen migration fraction for 8 and 12% initial cyclohexane samples were identical. The lower migration in 8% initial cyclohexane sample could also be perceived visually. Dark discrete spots were formed with 8% initial cyclohexane samples compared to a dark top layer in 12% initial cyclohexane samples. The lower bitumen migration might be due to reduced capillary connectivity to the top of the bed, leading to lower bitumen deposition.

The reduction of initial flux and subsequent increase in duration of fast drying stage (transition time delay) in 12% initial cyclohexane samples with Bit.C% increase might be due to a combination of 1. Reduced sorptivity of bed due to increase in viscosity of bulk solution in the gangue and 2. Thicker top layer with higher pore volume saturation with bitumen. The thicker top layer can be considered as a zone of local flux reduction because of its very low sorptivity due to the highly viscous nature of solution present there as discussed in Chapter 5.6. The reduction in initial flux and step increase in transition time for 8% initial cyclohexane samples for now is thought to be mostly due to the reduced sorptivity of bed.

## Future Recommendations

Before commercialisation of a cyclohexane based extraction process, care needs to be taken to ensure that the grade of cyclohexane used is free from impurities. Cyclohexane is manufactured by catalytic hydrogenation of benzene. Unconverted benzene can be found in cyclohexane as an impurity [63] and is highly carcinogenic. It needs to be removed completely.

The experiments performed have shown conclusive evidence of the cyclohexane removal process from gangue becoming increasingly difficult with an increase in residual bitumen content (under ambient conditions). If bitumen recoveries with cyclohexane in the industry is similar to what has been achieved so far with the lab scale extraction process, the residual Bit.C% would be around 0.5%. This was the best case scenario for cyclohexane removal in the experiments performed here. It will be highly recommended for future scale up designs of the extraction process to

include more washing steps or mixing the gangue with the ore if needed so as to maintain high recoveries.

Based on the packed bed drying experiments performed here a model needs to be developed. This model should account for the effect of bitumen migration via liquid films during the drying. Modelling of the solvent drying process in a packed bed would help us understand how this process would translate to the drying in a rotary mixer where drying would be from lumps of gangue.

It is expected that a similar bitumen migration as was observed in a packed bed would be seen on the surface of the lumps. A small scale rotary mixer can be designed to study the formation of lumps and their drying by passing air over.

Transition time was found to be dependent on initial cyclohexane, residual bitumen contents and the bed height. Transition time prediction model can be developed from the available data to predict transition times for samples with 1.5 and 2% Bit.C at bed heights of 1.4 cm. Longer drying experiments i.e. > 2hrs can be performed to check for the model's validity.

The temperature in the fume-hood could be increased to study the effects of higher temperature in conjunction with variable bitumen content in the bed on cyclohexane recovery.

Finally, a similar study of variation of residual bitumen content on cyclohexane recovery can be carried out for low grade gangue. This would require preparation of reconstituted samples resembling the extracted low grade gangue samples. Low grade gangue has been reported to have a lumpy structure due to the large amount of water and fines binding the particles together. The bitumen migration possibly

takes place in these individual lumps [21]. It would be interesting to observe the effect of residual bitumen and initial solvent content variation on cyclohexane recovery in this far more complicated system.

## References

- [1] J. Masliyah, Z. J. Zhou, Z. Xu, J. Czarnecki, and H. Hamza, "Understanding Water-Based Bitumen Extraction from Athabasca Oil Sands," *Can. J. Chem. Eng.*, vol. 82, no. 4, pp. 628–654, 2004.
- [2] "Alberta's Oil Sands: The Facts," *Government of Alberta*. [Online]. Available: <http://www.energy.alberta.ca/OilSands/pdfs/AlbertasOilSandsFactsJan14.pdf>. [Accessed: 12-Oct-2015].
- [3] "Oil sands Facts and Stats," *Government of Alberta*. [Online]. Available: [http://www.energy.alberta.ca/OilSands/pdfs/FactSheet\\_OilSands.pdf](http://www.energy.alberta.ca/OilSands/pdfs/FactSheet_OilSands.pdf). [Accessed: 12-Oct-2015].
- [4] "Talk about SAGD," *Government of Alberta*. [Online]. Available: [http://www.energy.alberta.ca/OilSands/pdfs/FS\\_SAGD.pdf](http://www.energy.alberta.ca/OilSands/pdfs/FS_SAGD.pdf). [Accessed: 12-Oct-2015].
- [5] "Upgraders and Refineries: Facts and Stats," *Government of Alberta*. [Online]. Available: <http://www.energy.alberta.ca/Oil/pdfs/FSRefiningUpgrading.pdf>. [Accessed: 12-Oct-2015].
- [6] G. D. Mossop, "Geology of the athabasca oil sands.," *Science*, vol. 207, no. 4427, pp. 145–152, 1980.
- [7] "Athabasca River Conditions and Use," *ESRD*. [Online]. Available: <http://www.environment.alberta.ca/apps/OSEM/>. [Accessed: 13-Oct-2015].
- [8] H. Nikakhtari, L. Vagi, P. Choi, Q. Liu, and M. R. Gray, "Solvent screening for

non-aqueous extraction of Alberta oil sands," *Can. J. Chem. Eng.*, vol. 91, no. 6, pp. 1153–1160, Jun. 2013.

- [9] "Tailings Ponds - Oil Sands Today," CAPP. [Online]. Available: <http://www.oilsandstoday.ca/topics/Tailings/Pages/default.aspx>. [Accessed: 13-Oct-2015].
- [10] "The Facts On: Oil Sands," CAPP, 2015. [Online]. Available: file:///C:/Users/Siddhant/Downloads/270274.pdf. [Accessed: 13-Oct-2015].
- [11] "Facts and Statistics," *Alberta Energy, Government of Alberta*, 20-Jun-. [Online]. Available: <http://www.energy.alberta.ca/oilsands/791.asp>. [Accessed: 13-Oct-2015].
- [12] G. of Alberta, "Tailings," 10-Aug-2010. [Online]. Available: <http://www.oilsands.alberta.ca/tailings.html>. [Accessed: 13-Oct-2015].
- [13] F. W. Meadus, P. J. Chevrier, and B. D. Sparks, "Solvent extraction of athabasca oil-sand in a rotating mill Part 1. Dissolution of bitumen," *Fuel Process. Technol.*, vol. 6, no. 3, pp. 277–287, Sep. 1982.
- [14] Gordon Raymond Coulson, "Process for separating oil from bituminous sands, shales, etc.," US 2825677 A, 04-Mar-1958.
- [15] D. O. Hanson and F. T. Sherk, "Solvent extraction of tar sand," US 4139450 A, 13-Feb-1979.
- [16] deceased Neal Franklin Blaine and B. Geneva, "Solvent extraction of oil from tar sands utilizing a trichloroethylene solvent," US 4046669 A, 06-Sep-1977.
- [17] L. H. and P. R., "Solvent Extraction of Mined Athabasca Oil Sands," *Ind. Eng.*

*Chem. Fundam.*, vol. 24, no. 4, pp. 373–379, 1985.

- [18] J. Wu and T. Dabros, "Process for Solvent Extraction of Bitumen from Oil Sand," *Energy & Fuels*, vol. 26, no. 2, pp. 1002–1008, 2012.
- [19] A. Hooshiar, P. Uhlik, Q. Liu, T. H. Etsell, and D. G. Ivey, "Clay minerals in nonaqueous extraction of bitumen from Alberta oil sands," *Fuel Process. Technol.*, vol. 94, no. 1, pp. 80–85, 2012.
- [20] K. Pal, L. D. P. Nogueira Branco, A. Heintz, P. Choi, Q. Liu, P. R. Seidl, and M. R. Gray, "Performance of Solvent Mixtures for Non-aqueous Extraction of Alberta Oil Sands," *Energy & Fuels*, vol. 29, no. 4, pp. 2261–2267, 2015.
- [21] R. Renaud, *A study on the effect of temperature and pressure on the removal of cyclohexane from non-aqueous extraction gangue*. [2014], 2014.
- [22] "COMMERCIAL SCHEME Approval No. 8512D," *Energy resources conservation board (ERCB)*. [Online]. Available: [https://www.aer.ca/documents/oilsands/tailings-plans/ERCB\\_Approval\\_8512D.pdf](https://www.aer.ca/documents/oilsands/tailings-plans/ERCB_Approval_8512D.pdf). [Accessed: 13-Oct-2015].
- [23] R. Chandler, J. Koplik, K. Lerman, and J. F. Willemsen, "Capillary displacement and percolation in porous media," *J. Fluid Mech.*, vol. 119, no. -1, p. 249, 1982.
- [24] C. Lin and M. H. Cohen, "Quantitative methods for microgeometric modeling," *J. Appl. Phys.*, vol. 53, no. 6, pp. 4152–4165, 1982.
- [25] D. Wilkinson and J. F. Willemsen, "Invasion percolation: a new form of percolation theory," *J. Phys. A. Math. Gen.*, vol. 16, no. 14, pp. 3365–3376,

1983.

- [26] a. G. Yiotis, a. G. Boudouvis, a. K. Stubos, I. N. Tsimpanogiannis, and Y. C. Yortsos, "Effect of liquid films on the drying of porous media," *AIChE J.*, vol. 50, no. 11, pp. 2721–2737, Nov. 2004.
- [27] a. G. Yiotis, a. K. Stubos, a. G. Boudouvis, and Y. C. Yortsos, "A 2-D pore-network model of the drying of single-component liquids in porous media," *Adv. Water Resour.*, vol. 24, no. 3–4, pp. 439–460, 2001.
- [28] Y. C. Yortsos and A. K. Stubos, "Phase change in porous media," *Curr. Opin. Colloid Interface Sci.*, vol. 6, no. 3, pp. 208–216, 2001.
- [29] a. G. Yiotis, a. G. Boudouvis, a. K. Stubos, I. N. Tsimpanogiannis, and Y. C. Yortsos, "Effect of liquid films on the isothermal drying of porous media," *Phys. Rev. E. Stat. Nonlin. Soft Matter Phys.*, vol. 68, no. 3 Pt 2, p. 037303, 2003.
- [30] I. Tsimpanogiannis, Y. Yortsos, S. Poulopoulos, N. Kanellopoulos, and a. Stubos, "Scaling theory of drying in porous media," *Phys. Rev. E*, vol. 59, no. 4, pp. 4353–4365, 1999.
- [31] M. Prat and F. Bouleux, "Drying of capillary porous media with a stabilized front in two dimensions," *Phys. Rev. E*, vol. 60, no. 5, pp. 5647–5656, 1999.
- [32] N. Shokri, P. Lehmann, and D. Or, "Critical evaluation of enhancement factors for vapor transport through unsaturated porous media," *Water Resour. Res.*, vol. 45, no. 10, pp. 1–9, 2009.
- [33] N. Shokri, P. Lehmann, and D. Or, "Characteristics of evaporation from

partially wettable porous media," *Water Resour. Res.*, vol. 45, no. 2, pp. 1–12, 2009.

- [34] N. Shokri and D. Or, "What determines drying rates at the onset of diffusion controlled stage-2 evaporation from porous media?," *Water Resour. Res.*, vol. 47, no. 9, pp. 1–8, 2011.
- [35] P. Lehmann, S. Assouline, and D. Or, "Characteristic lengths affecting evaporative drying of porous media," *Phys. Rev. E - Stat. Nonlinear, Soft Matter Phys.*, vol. 77, no. 5, pp. 1–16, 2008.
- [36] N. Shokri and D. Or, "Drying patterns of porous media containing wettability contrasts," *J. Colloid Interface Sci.*, vol. 391, no. 1, pp. 135–141, 2013.
- [37] N. Shokri, "Pore-scale dynamics of salt transport and distribution in drying porous media," *Phys. Fluids*, vol. 26, no. 1, 2014.
- [38] M. Prat, "On the influence of pore shape, contact angle and film flows on drying of capillary porous media," *Int. J. Heat Mass Transf.*, vol. 50, no. 7–8, pp. 1455–1468, 2007.
- [39] N. Sghaier and M. Prat, "Effect of efflorescence formation on drying kinetics of porous media," *Transp. Porous Media*, vol. 80, no. 3, pp. 441–454, 2009.
- [40] O. Chapuis and M. Prat, "Influence of wettability conditions on slow evaporation in two-dimensional porous media," *Phys. Rev. E - Stat. Nonlinear, Soft Matter Phys.*, vol. 75, no. 4, pp. 1–11, 2007.
- [41] B. Camassel, N. Sghaier, M. Prat, and S. Ben Nasrallah, "Evaporation in a capillary tube of square cross-section: Application to ion transport," *Chem.*

*Eng. Sci.*, vol. 60, no. 3, pp. 815–826, 2005.

- [42] N. Sghaier, M. Prat, and S. Ben Nasrallah, "On the influence of sodium chloride concentration on equilibrium contact angle," *Chem. Eng. J.*, vol. 122, no. 1–2, pp. 47–53, 2006.
- [43] H. Eloukabi, N. Sghaier, S. Ben Nasrallah, and M. Prat, "Experimental study of the effect of sodium chloride on drying of porous media: The crusty-patchy efflorescence transition," *Int. J. Heat Mass Transf.*, vol. 56, no. 1–2, pp. 80–93, 2013.
- [44] Y. Zhang, X. F. Peng, a. Su, a. S. Mumjudar, and D. J. Lee, "Drying of Porous Medium Containing Concentration Sodium Chloride Solution," *Dry. Technol.*, vol. 25, no. 1, pp. 171–175, 2007.
- [45] N. Sghaier, M. Prat, and S. Ben Nasrallah, "On ions transport during drying in a porous medium," *Transp. Porous Media*, vol. 67, no. 2, pp. 243–274, 2007.
- [46] V. Brito and T. Diaz Gonçalves, "Drying Kinetics of Porous Stones in the Presence of NaCl and NaNO<sub>3</sub>: Experimental Assessment of the Factors Affecting Liquid and Vapour Transport," *Transp. Porous Media*, vol. 100, no. 2, pp. 193–210, 2013.
- [47] C. Hall and W. D. Hoff, *Water transport in brick, stone and concrete.* [electronic resource]. London : Spon Press, 2012., 2012.
- [48] T. Dang-Vu, R. Jha, S. Y. Wu, D. D. Tannant, J. Masliyah, and Z. Xu, "Wettability determination of solids isolated from oil sands," *Colloids Surfaces A Physicochem. Eng. Asp.*, vol. 337, no. 1–3, pp. 80–90, Apr. 2009.

- [49] C. Wang, M. Geramian, Q. Liu, D. G. Ivey, and T. H. Etsell, "Comparison of Different Methods To Determine the Surface Wettability of Fine Solids Isolated from Alberta Oil Sands," 2015.
- [50] J. Guan, "Physical Properties of Athabasca Bitumen and Liquid Solvent Mixtures." University of Calgary, Graduate Studies, Engineering, Chemical and Petroleum>, 2013-01-11., 2013.
- [51] H. Nikakhtari, K. Pal, S. Wolf, P. Choi, Q. Liu, and M. R. Gray, "Solvent removal from cyclohexane-extracted oil sands gangue," *Can. J. Chem. Eng.*, p. n/a-n/a, Dec. 2015.
- [52] H. Nikakhtari, S. Wolf, P. Choi, Q. Liu, and M. R. Gray, "Migration of Fine Solids into Product Bitumen from Solvent Extraction of Alberta Oilsands," *Energy & Fuels*, vol. 28, no. 5, pp. 2925–2932, 2014.
- [53] S. E. Ryan and L. S. Porth, *A tutorial on the piecewise regression approach applied to bedload transport data*. Fort Collins, CO : U.S. Dept. of Agriculture, Forest Service, Rocky Mountain Research Station, [2007], 2007.
- [54] R. S. Pindyck and D. L. Rubinfeld, *Econometric models and economic forecasts*. Boston, Mass. : Irwin/McGraw-Hill, c1998., 1998.
- [55] B. Efron and R. Tibshirani, *An introduction to the bootstrap*. Boca Raton, Fla. : Chapman & Hall/CRC, c1998., 1998.
- [56] R. Du and H. a Stone, "Evaporatively controlled growth of salt trees," *Phys. Rev. E*, vol. 53, no. 2, pp. 1994–1997, 1996.
- [57] D. S. Pasternack and K. a. Clark, "The Components of the Bitumen in

Athabasca Bituminous Sand and their Significance in the Hot Water Separation Process." 1951.

- [58] "Surface Tension of Cyclohexane from Dortmund Data Bank." [Online]. Available: [http://www.ddbst.com/en/EED/PCP/SFT\\_C50.php](http://www.ddbst.com/en/EED/PCP/SFT_C50.php). [Accessed: 12-Oct-2015].
- [59] E. I. Vargha-Butler, Z. M. Potoczny, T. K. Zubovits, C. J. Budziak, and A. W. Neumann, "Surface tension of bitumen from contact angle measurements on films of bitumen," *Energy & Fuels*, vol. 2, no. 5, pp. 653–656, Sep. 1988.
- [60] B. C. H. Fu and C. R. Phillips, "Plasticizing effectiveness of hydrocarbons in Athabasca bitumen," *Fuel*, vol. 58, pp. 554–556, Jan. 1979.
- [61] J. Kendall and K. P. Monroe, "THE VISCOSITY OF LIQUIDS. II. THE VISCOSITY-COMPOSITION CURVE FOR IDEAL LIQUID MIXTURES.1," *J. Am. Chem. Soc.*, vol. 39, no. 9, pp. 1787–1802, Sep. 1917.
- [62] C. E. Capes and K. Darcovich, "Size Enlargement," in *Kirk-Othmer Encyclopedia of Chemical Technology*, John Wiley & Sons, Inc., 2000.
- [63] "CYCLOHEXANE | C<sub>6</sub>H<sub>12</sub> - PubChem." [Online]. Available: <http://pubchem.ncbi.nlm.nih.gov/compound/cyclohexane#section=Methods-of-Manufacturing>. [Accessed: 21-Dec-2015].

## Appendix A

### Appendix A.1- Calculations for Reconstituted Gangue Preparation

We start with X g and 0.5\*X g of Soxhlet gangue and Cyclohexane respectively.

Bitumen contains about 83.3 % by weight of C [57] i.e.  $1.2 \times x_1$  g bitumen contains  $x_1$  g carbon. This  $x_1$  g carbon is referred to as bitumen associated carbon or Bit.C as the only way to add it to the Soxhlet gangue is by adding the  $1.2 \times x_1$  g bitumen. The formula used to determine the amount of bitumen needed to be added to obtain 0.5-2% Bit.C is:

$$\frac{x_1}{((1.2 * x_1) + X)} = \frac{(0.5 - 2)^+}{100}$$

<sup>+</sup> Some added Bit.C is lost during the sample preparations. Hence we have to add an extra 0.3-0.5 wt. % Bit.C to the required Bit.C wt. % to obtain the required final concentration.

Net weight ( $X_1$ ) =  $X + 1.2 * x_1$  g

2-4 wt. % water or ' $x_2$ ' g of demineralized water is added to the DSBS. In this work, 3.7 wt. % of water has been added throughout all the sample preparations.

$$\frac{x_2}{x_2 + X_1} = \frac{3.7}{100}$$

Net weight ( $X_2$ ) =  $X_1 + x_2$  g

8-12 wt. % of Cyclohexane or ' $x_3$ ' g of Cyclohexane is added to the WSBS to make the reconstituted gangue.

$$\frac{x_3}{x_3 + X_2} = \frac{(8 \text{ to } 12)}{100}$$

## Appendix A.2- Calculations for Ratio of Soxhlet Gangue: Cyclohexane-Bitumen Solution in Reconstituted Gangue

The calculated values shown below are assuming we have 100 g of reconstituted gangue. In our studies we observed that due to some solvent losses involved in the sample preparation and storage the actual cyclohexane content in reconstituted gangue was around 11 and 7.5% instead of the expected 12 and 8%. As explained previously, the 3.7% water in our samples is on a cyclohexane free basis. Hence on a net weight basis water content varies with the solvent content as can be seen in the table below.

**Table 8. Composition of Reconstituted gangue**

			<b>0.5% Bit.C</b>		<b>2% Bit.C</b>	
Re-G (g)	Cyclohexane (g)	Water (g)	Bitumen (g)	Soxhlet gangue (g)	Bitumen (g)	Soxhlet gangue (g)
100	11.0 (A)	3.29	0.51 (C)	85.20 (E)	2.05 (G)	83.66 (I)
100	7.5 (B)	3.42	0.53 (D)	88.55 (F)	2.13 (H)	86.95 (J)

**Table 9. Ratio of Soxhlet gangue: Cyclohexane bitumen solution in Reconstituted gangue**

Cyclohexane (g)	<b>0.5% Bit.C</b>	<b>2% Bit.C</b>
	Soxhlet gangue: solution	Soxhlet gangue: solution
11	7.40:1 (K)	6.41:1 (M)
7.5	11.02:1 (L)	9.03:1 (N)

$$K = \frac{E}{A + C}, L = \frac{F}{B + D}, M = \frac{I}{A + G}, N = \frac{J}{B + H}$$

### Appendix A.3 – Calibrations of QICMS

The MASsoft 7 software was operated in the Multiple ion detection (MID) mode to detect cyclohexane, water, oxygen and toluene in the inserted sample. The sample was connected to the mass spectrometer unit once the baseline reading was observed for cyclohexane. In order to analyze the response of the QICMS to the presence of a particular solvent (only cyclohexane in our case) it needed to be calibrated for that solvent. This was achieved by injecting known volumes of solvent to the QICMS and observing the response. Following this a calibration curve was created which came in handy when we needed to detect an unknown amount of solvent in a sample.

0.2-75 µl of cyclohexane was injected to 5g of dry soxhlet gangue present inside a glass tube with glass wool on both ends. The glass tube prior to cyclohexane injection was inserted into the heating unit and was connected on one end with the mass spectrometer unit and on the other end with the carrier gas supply.

Cyclohexane injections for any particular volume was repeated for 3-5 times. The mean response (mean peak integral) for the volume injected was plotted against the injection volume to obtain the following calibration curves.

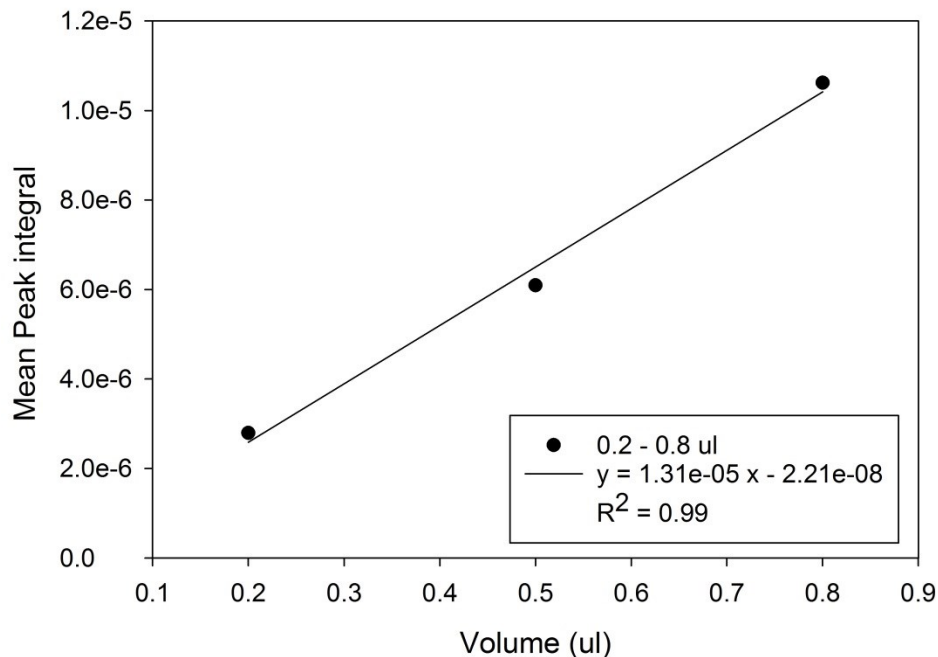


**Figure 47. Calibrations for volume in the range 0.2-0.8 ul**

0.2-30  $\mu$ l calibration range was actually used for the range 0.8 -30  $\mu$ l; for volumes lower than 0.8  $\mu$ l the previous range was used (i.e. 0.2-0.8  $\mu$ l). The calibration curve for 0.2-0.8  $\mu$ l was extrapolated in cases where measured volume was < 0.2  $\mu$ l (based on lower Peak integration value). For rare cases where volume was slightly greater than 75  $\mu$ l, the calibrations for 30-75  $\mu$ l was used by extrapolating it.

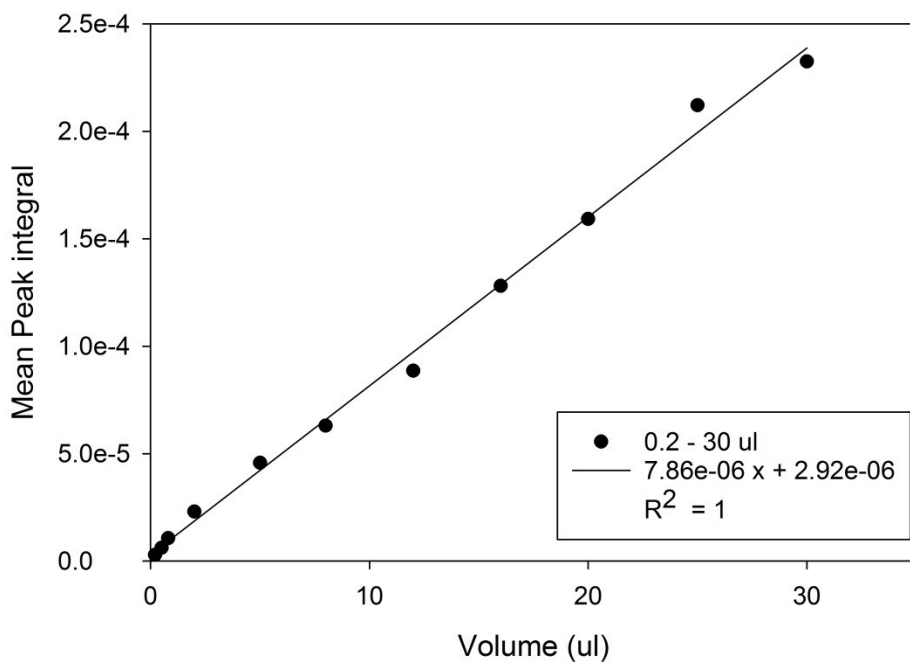


**Figure 48.** Calibrations for volume in the range 0.2-30 ul.

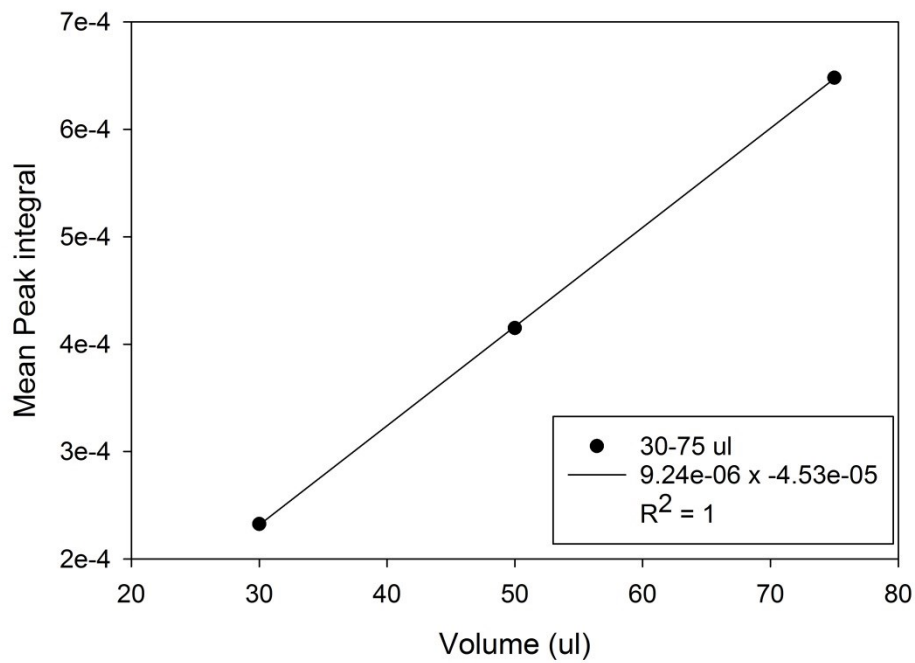


**Figure 49.** Calibrations for volume in the range 30-75 ul.

Operating the heating unit at near room conditions or at higher temperatures i.e. 50-80 °C didn't affect the peak integration values obtained from injection of any particular cyclohexane volume. Still it is recommended to operate the heating unit at near room conditions since leaks if any while making the connection of a tube can be fixed without losing much solvent to affect the final results.

#### Appendix A.4 – Wettability Determinations using Film Flotation Measurements

The wettability determination tests performed are as stated in Wang et al. [49]. Methanol and water solutions with surface tension in the range 22.5 – 72 mN/m were prepared and kept in a water bath at 25 °C. The different solutions prepared were each put into separate 50 mL glass bottles. 0.05 g of solids were sprinkled carefully on the surface of each solution. A filter paper was used for the collection of the floating solids on the solution surface after a 2 min wait time. The sunk solids were first dried and then weighed. The critical surface tension (cumulative) distribution was obtained by plotting the percentage of solids remaining floating on the solution surface as a function of the particles critical surface tension.

Mean critical surface tension of particles of solid ( $\gamma_p'$ ) is given by [48], [49] –

$$\gamma_p' = \int \gamma_p f(\gamma_p) d\gamma_p$$

Where  $\gamma_p$  is the solid particles critical surface tension and  $f(\gamma_p)$  is the function for the frequency distribution.

To determine the heterogeneity of particles surface or the standard deviation in the mean critical surface tension of the solids ( $\sigma$ ) the following can be used [49] –

$$\sigma = [\int (\gamma_p - \gamma'_p)^2 f(\gamma_p) d\gamma_p]^{0.5}$$

## Appendix B

### Appendix B.1 – Transition Time Interval Determination

A moving linear fit of 10, 20, 30 and 40 min was applied to the cumulative weight loss vs time data sets to observe the MSE (mean square error) around the interval where we expect the breakpoint/transition time to lie. Say we have 360 equally spaced data points representing 120 min of data. So we have cumulative weight readings at 0, 0.33, 0.66, 1 ..... 50.33, 50.66 ....120 min time points. A 30 min moving fit for this data will mean 0-30 min data fit linearly with MSE determination followed by the same for 0.33 min-30.33 min data and so on till the last 30 min range i.e. 90-120 min. The MSE values were then plotted against the start time for the model fit when the particular MSE value was obtained. For ex. if the MSE value obtained for 3.33-33.33 min in a particular data set was 1.30e-04, then the start time is 3.33 min and the corresponding MSE value is 1.30e-04. Sample plot of MSE vs start time is shown in Figures 51 and the corresponding cumulative weight loss vs time data is shown in Figure 50. The moving linear model fit and MSE determinations were performed with the help of MATLAB R2015a.

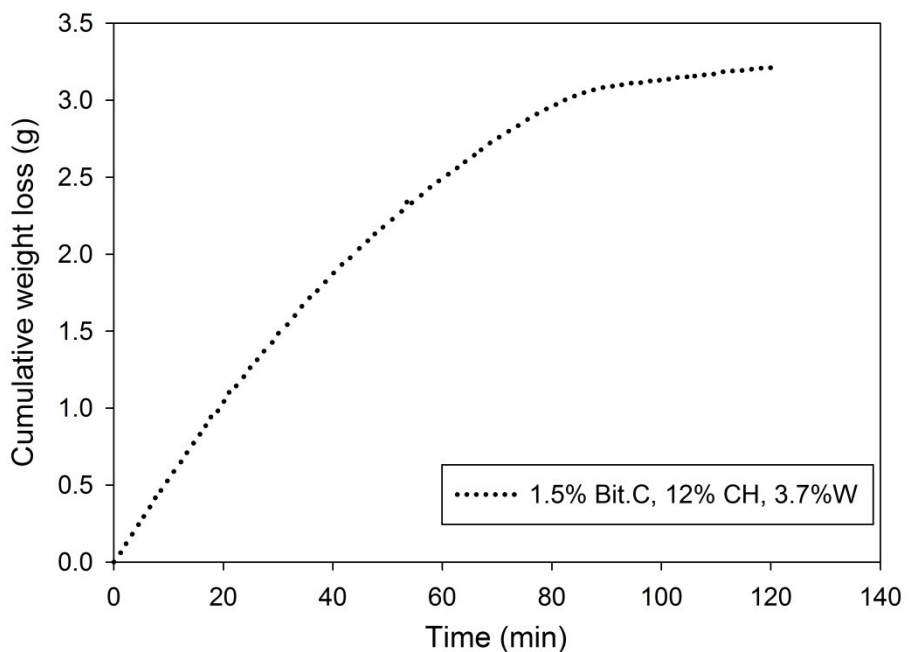


**Figure 50. Cumulative weight loss vs time plot**

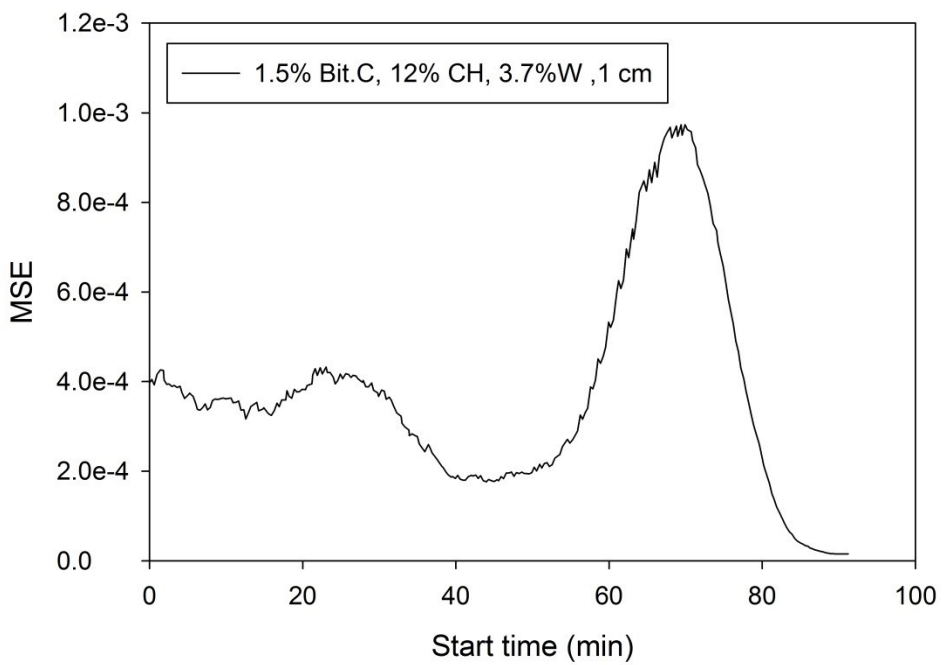


**Figure 51. MSE vs start time for a 30 min moving linear fit.**

Figure 51 shows MSE values to reach a maxima at a start time of around 70 min, and a very low value afterwards at start time of nearly 90 min. The linear models for 70-100 min and 90-120 min range were investigated further to observe what actually happened. Figure 52 and 53 shows the linear model fit for these 2 ranges.

As can be seen from Figure 52 linear fit model isn't the best choice for the range 70-100 min (MSE maxima). This is because of the fact that this range contains the transition time. The transition time signifies a change in drying flux from fast before to slow afterwards. Though other data ranges near the MSE maxima also contain the breakpoint, *the range where highest MSE is observed will be considered as the 'Transition time interval'*. This is because in this range the linear model fails the worst and there's a need for another model like the piecewise linear regression model to fit the data better.

Once the breakpoint has been crossed (MSE minima achieved), for ex. in Figure 53 the single linear model fits the data well.

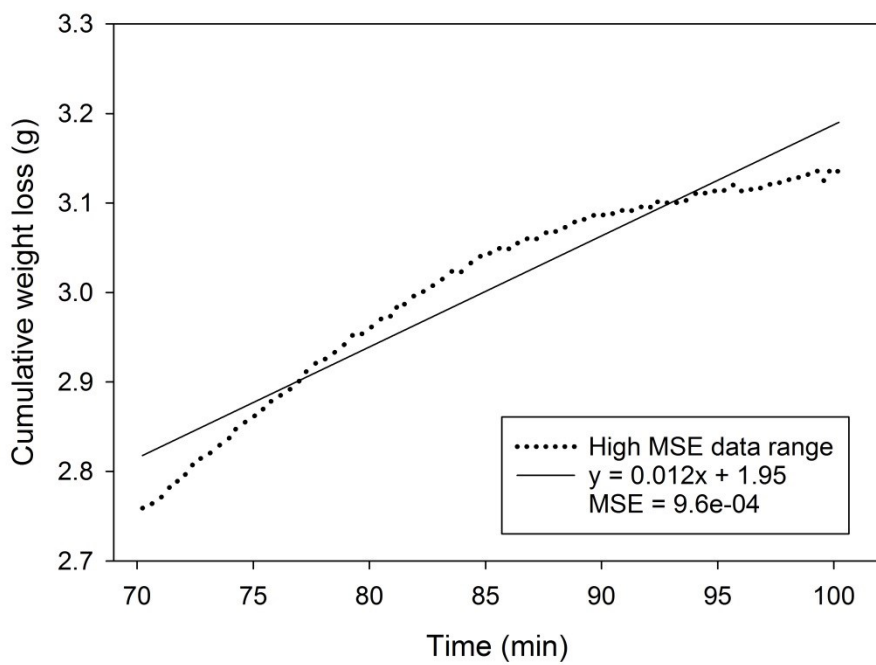


**Figure 52. High MSE data range (70-100 min).**

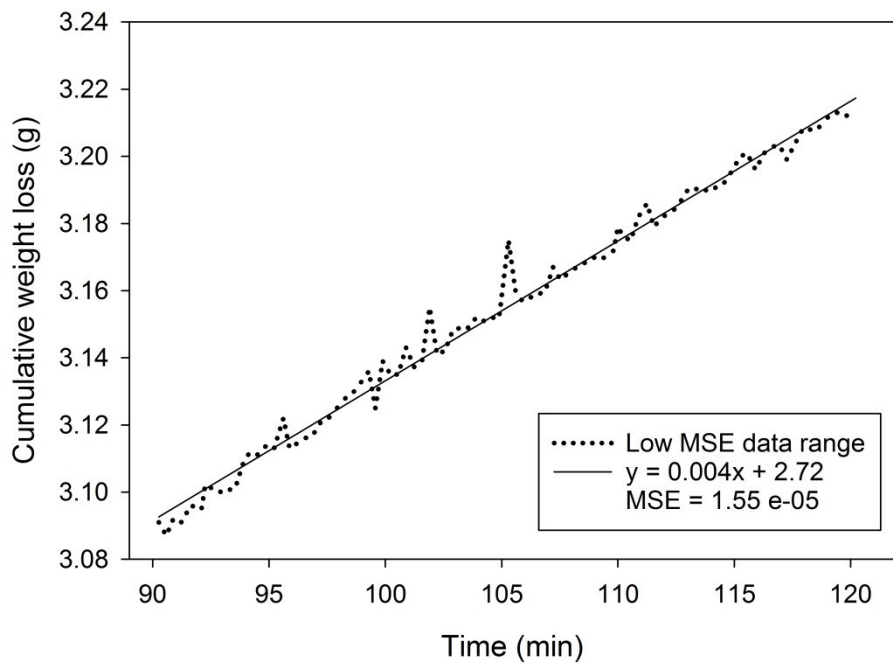


**Figure 53. Low MSE data range (90-120 min).**

As can be seen in Figure 56, MSE plot for a 10 min moving fit cannot help us identify the transition time interval. Both 40 and 20 min moving fit MSE plots work well to identify a transition time interval (MSE peak) in this particular example. The problem with using the 40 min fit for our data sets was that if the transition time was beyond 100 min, the MSE peak could not be observed. This was not the case when using 30 and 20 min moving fits since the time interval was shorter.

Either of the 20 and 30 min moving fits could be used for transition time interval determination. *In this work we define transition time interval as a 30 min data range (30 min) where linear regression fit had the highest MSE (maxima of the MSE peak).*

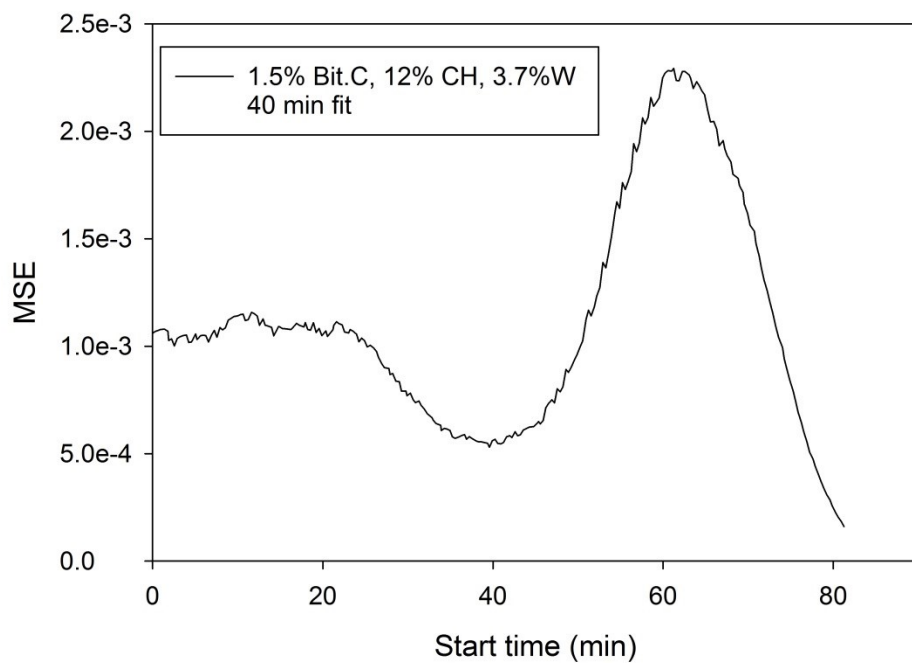


**Figure 54. MSE vs start time for a 40 min moving linear fit.**

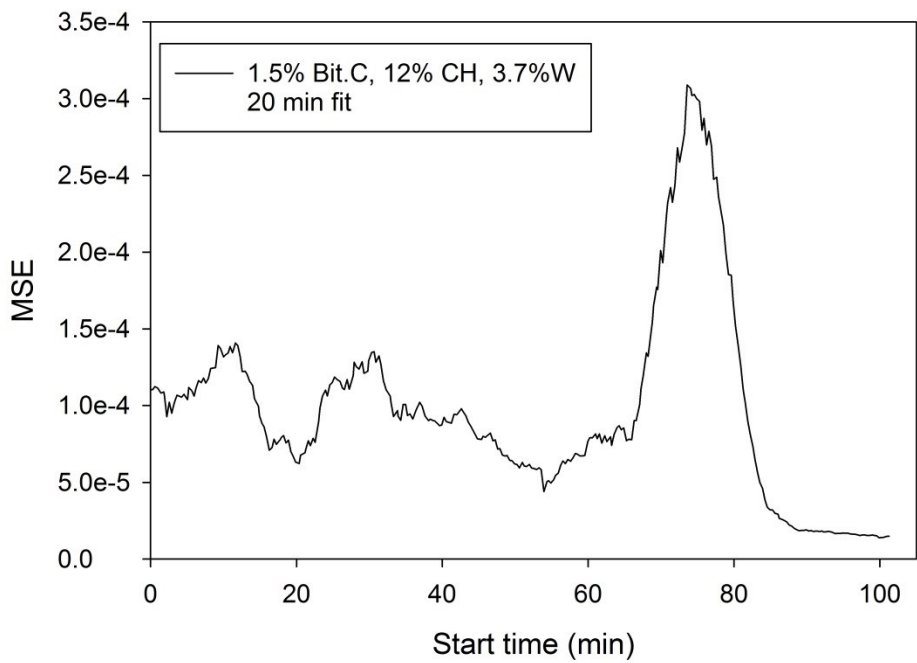


**Figure 55. MSE vs start time for a 20 min moving linear fit.**

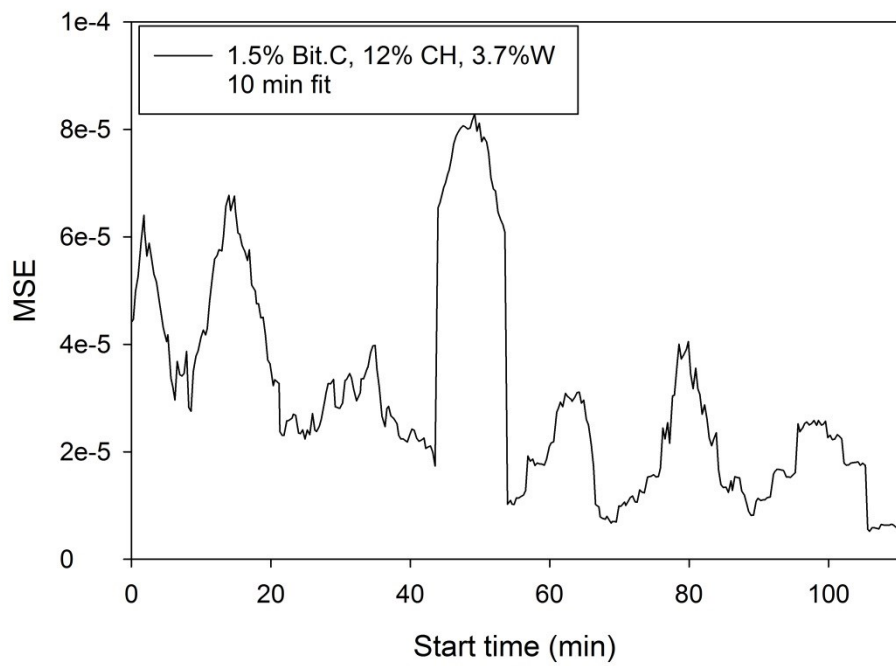


**Figure 56. MSE vs start time for a 10 min moving linear fit.**

If the maxima of the peak couldn't be determined due to the flat/broad nature of peak near the maximum value, that range was chosen which had a later start time.

The MSE vs start time plots were studied after 20-30 min from start of experiment in case of bed ht. of 0.6 cm and 40-50 min in case of bed ht. = 1cm. This is because we are not concerned with the variations in MSE in those time periods where we are sure that the breakpoint doesn't lie. Sometimes in these time periods MSE peaks with a greater maxima are observed than the one we observe near the transition time interval. This might be confusing and lead us to select the transition time interval incorrectly.

Now that the transition time has been identified, we need to apply piecewise regression approach to see if it can improve the fit.

## Appendix B.2 –Piecewise Regression Approach

The application of piecewise linear regression in the transition time interval involves using two linear regression lines instead of one to fit the data range.

$$y = m_1 + n_1x \text{ for } x \leq b$$

$$y = m_2 + n_2x \text{ for } x > b$$

At the breakpoint b,

$$m_1 + n_1b = m_2 + n_2b$$

The equation for  $x>b$  translates to:

$$y = m_1 + b(n_1 - n_2) + n_2x \text{ for } x > b$$

The above equations need to be solved to determine the transition time. These equations were solved using *nlinfit* function in MATLAB R2015a. This function uses nonlinear iterative least square regression technique to estimate the parameter values. For the initial estimate of the parameters the breakpoint time was assumed to be midway in the transition zone. Two discrete linear regression lines were fitted to the data, the first from the beginning of transition time interval till the assumed breakpoint time and the second from assumed breakpoint time till the end of transition interval. The initial parameters thus obtained were passed on to the *nlinfit* function as an initial guess. Figure 57 shows the piecewise regression fit obtained. Based on MSE value of 2.79e-05 obtained for piecewise regression fit compared to MSE value of 9.6e-04 for linear fit (Refer Figure 52 in Appendix B.1), piecewise fit appears to be an improvement over the linear fit.

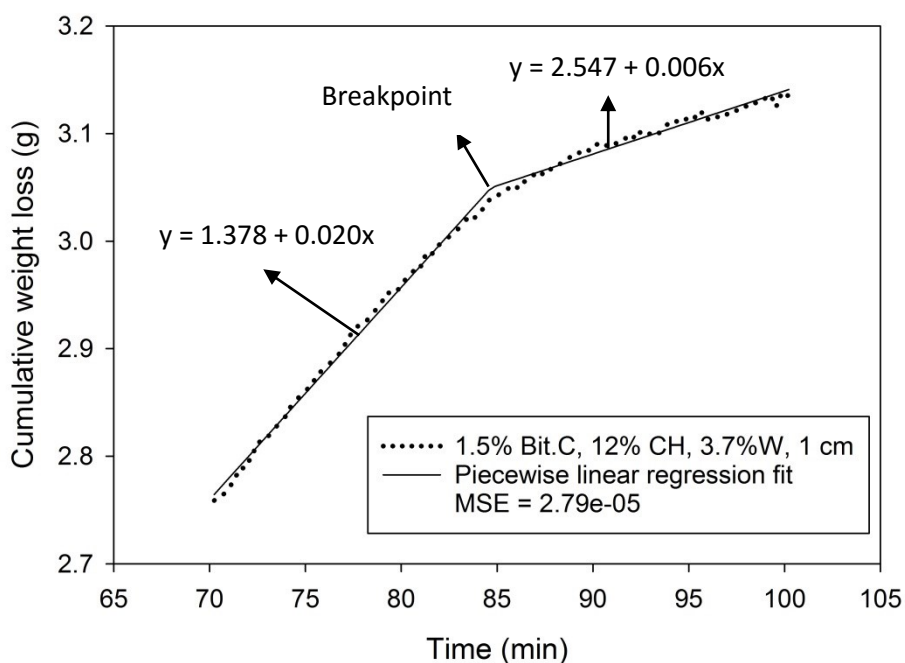


**Figure 57. Piecewise regression fit in the transition time interval. The transition time interval was obtained using the procedure given in Appendix B.1**

Similar transition time and 95% CI range are obtained using the 30 and 20 min transition time intervals. For ex. the transition time obtained using 30 min moving fit in the above data set was 84.7 min whereas that with the 20 min moving fit was 84.5 min. The 95% C.I obtained in the 30 min interval was 84.2-85.2 min and that in the 20 min interval was 84.1-85.1 min.

### Appendix B.3-Drying Comparison: Lamp and no Lamp Drying

The temperature rise in the chamber during the experiments performed in this work was  $3.5 \pm 0.5$  °C. An estimate of the temperature at the location where samples were kept was also made. The lamps were used for illumination purposes and were focused at the sample location, and hence this estimate was needed. This measurement was made by placing another temperature/humidity meter probe (Fisher Scientific™ Traceable™ Relative Humidity/Temperature Meters) at the location where a sample is kept during drying experiments. The lamps were switched on and the conditions maintained was similar to what was maintained during the drying experiments. The temperature rise at the location of sample placement was estimated as  $8 \pm 1$  °C. The temperature in the chamber initially was ambient room temperature of  $21 \pm 1$  °C.

Drying experiments with lamps had already been performed and compared in the previous section. To study this effect of using the two lamps on the overall drying process reconstituted gangue sample with *0.5% Bit.C, 12% cyclohexane and 3.7% water* was dried without lamps. The bed height studied was 1 cm, it being the intermediate height in the experiments.

Cumulative weight loss vs time plots for the without lamps run was plotted with the 2 most comparable lamp runs performed as shown in Figure 58 below.

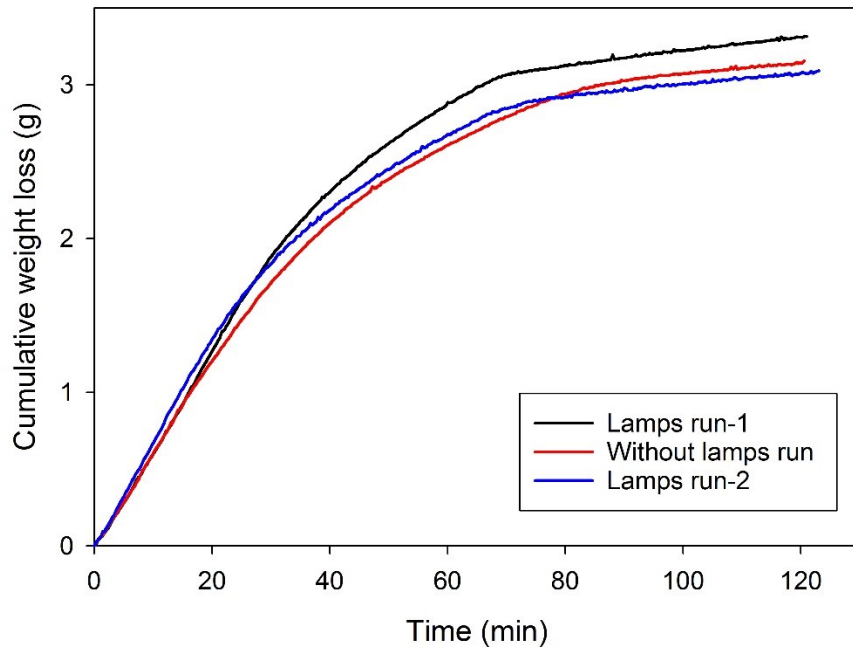


**Figure 58. Lamps and without lamps drying curves.**

All the drying curves seem to have a similar trend as can be seen from the above figure. To analyze the drying behaviour further, the initial flux, transition time and final flux was compared as shown in Table 10. The transition time was also compared (95% BCa confidence interval hasn't been shown). The lamps run was performed in triplicates and hence the standard deviations in values have also been reported. Other comparisons related to bitumen migration were also made and have been discussed.

**Table 10. Initial flux, transition time, final flux comparison (lamps and no lamps)**

Sample name	Initial flux	Transition	Final flux
	(g/min.cm <sup>2</sup> )	time (min)	(g/min.cm <sup>2</sup> )
0.5% Bit.C, 12% CH ,3.7% W – with lamps	3.70 ± 0.76e-03	68.9 ± 1.4	2.11 ± 0.33e-04
0.5% Bit.C, 12% CH ,3.7% W – without lamps	3.06e-03	82.6	2.10e-04

The temperature increase effect due to lamps wasn't enough to increase the initial and final fluxes as compared to the no lamps case. This can be seen from the table above which shows that the initial and final flux for no lamps run was in the range obtained for samples with the same composition but dried under lamps. Also the overall drying time for the fast drying stage was increased by < 20% (about 17%) based on the obtained transition times. Similar final flux values for no lamp run compared to with lamps experiments indicated that the water dominant drying stage was unaffected by the lamps.

The reconstituted gangue drying experiments performed in this work (Apart from the no lamps case discussed above) were under similar conditions (lamps). Because this temperature increase effect (albeit small) was present uniformly it has been ignored while comparing the effects of initial Bit.C% on drying and bitumen migration.

### B.3.1. Enrichment Ratio Comparison for Lamp and no Lamp Drying Runs

In the previous section the drying behaviour of *0.5% Bit.C, 12% cyclohexane and 3.7% water* sample for a bed height of 1 cm was compared. The enrichment ratio for the no lamp drying run compared to lamp drying runs ( $n=3$ ) performed has been shown in the table below.

**Table 11. Enrichment ratio comparison (lamps and no lamps)**

Sample name	Enrichment ratio
0.5% Bit.C, 12% CH ,3.7% W – with lamps	$3.29 \pm 0.72$
0.5% Bit.C, 12% CH ,3.7% W – without lamps	4.30

The enrichment ratio for no lamp drying run and lamp drying runs were both very high ( $>1$  indicates bitumen migration) and comparable.

### B.3.2 Bitumen Migration Fraction Comparison for Lamp and no Lamp Drying Runs

The enrichment ratio of *0.5% Bit.C, 12% cyclohexane and 3.7% water* samples for a bed height of 1 cm dried with and without lamps were found comparable indicating similar bitumen migration quality. The BMF for the no lamp drying run compared to lamp drying runs ( $n=3$ ) performed has been shown in the table below.

**Table 12. BMF comparison (lamps and no lamps)**

Sample name	BMF
0.5% Bit.C, 12% CH ,3.7% W – with lamps	0.31 ± 0.09
0.5% Bit.C, 12% CH ,3.7% W – without lamps	0.37

The bitumen migration fraction for without lamp run was in the range of that obtained with lamps. This verified that the net bitumen migration (quantitatively) for both the lamps and no lamps migration case was identical.

Both the drying and bitumen migration behaviour of without lamps drying case has shown that the lamps don't influence to a great deal the volatile loss and associated bitumen movement. The bitumen deposition in fact, in both cases resembled each other. The major purpose hence for the use of lamps was illumination as stated before.

## Appendix C

### Appendix C.1 – Development of the Final Equation of Bitumen Migration Fraction

$$\text{We know that, } \text{Migration fraction} = \frac{W_{bitTLF} - W_{bitTLi}}{W_{bitBLi} + W_{bitTLi}}$$

Terms to be used –

- $(x_{BL} - x_s) \rightarrow$  dried bottom layer Bit.C %
- $(x_{TL} - x_s) \rightarrow$  dried top layer Bit.C%
- $(x_i - x_s) = p \rightarrow$  initial bed Bit.C%, varies from 0.5-2

- Weight of completely dry TL (g)  $\rightarrow y_{TL}$
- Weight of completely dry BL (g)  $\rightarrow y_{BL}$
- Bitumen in BL initially and finally  $\rightarrow W_{bitBLi}$  and  $W_{bitBLF}$  respectively
- Bitumen in TL initially and finally  $\rightarrow W_{bitTLi}$  and  $W_{bitTLF}$  respectively

Now, the weight of Soxhlet gangue sand in Bottom layer is given by, Weight of dried bottom layer – Weight of bitumen in it =

$$W_{sox} = y_{BL} - \left[ 1.2 \left( \frac{x_{BL} - x_s}{100} \right) y_{BL} \right]$$

This Soxhlet gangue was mixed with p% Bit.C initially to form the reconstituted gangue,

$$\text{Hence, } \frac{100C}{1.2C + W_{sox}} = p$$

Here C is the amount of carbon in g added initially to get p% Bit.C.

Thus Bitumen in BL initially,

$$W_{bitBLi} = 1.2C = 1.2 \frac{W_{SOX} p}{100 - 1.2p}$$

Similarly,

Weight of Soxhlet gangue in top layer is given by, Weight of dried top layer – Weight of bitumen in it=

$$W_{soxTL} = y_{TL} - \left[ 1.2 \left( \frac{x_{TL} - x_s}{100} \right) y_{TL} \right]$$

As above,  $W_{bitTLi} = 1.2C_T = 1.2 \frac{W_{SoxTL} p}{100 - 1.2p}$

Finally,  $W_{bitTLF} = 1.2 \frac{y_{TL} \cdot (x_{TL} - x_s)}{100}$

Now, Migration fraction =  $\frac{W_{bitTLF} - W_{bitTLi}}{W_{bitBLi} + W_{bitTLi}}$

$$= \frac{y_{TL} \cdot (x_{TL} - x_s) - y_{TL}' \cdot (x_i - x_s)}{(x_i - x_s)(y_{TL} + y_{BL})}$$

$$\text{where } y_{TL}' = y_{TL} \frac{100 - 1.2(x_{TL} - x_s)}{100 - 1.2(x_i - x_s)}$$

$y_{TL}'$  is the initial weight of top layer i.e. before the start of experiment. To develop the formula for migration fraction in Section 5.3.2 of Chapter 5, the following assumption has been made,

$$y_{TL}' (x_i - x_s) \sim y_{TL} (x_i - x_s)$$

giving us,

$$\begin{aligned} \text{Migration fraction} &= \frac{W_{bitTLF} - W_{bitTLi}}{W_{bitBLi} + W_{bitTLi}} \\ &= \frac{(x_{TL} - x_i)}{(x_i - x_s)} * \frac{y_{TL}}{y_{TL} + y_{BL}} \end{aligned}$$

To calculate the error using this formula the ratio of actual bitumen migration fraction to the bitumen migration fraction calculated using the above formula has been determined.

The ratio is given by –

$$\frac{\text{Actual Migration fraction}}{\text{Migration fraction}} = k = \frac{(x_{TL} - x_s) - \frac{100 - 1.2(x_{TL} - x_s)}{100 - 1.2(x_i - x_s)} \cdot (x_i - x_s)}{(x_{TL} - x_i)}$$

$$= \frac{100}{100 - 1.2(x_i - x_s)}$$

$$\text{error\%} = \frac{\text{Actual Migration fraction} - \text{Migration fraction}}{\text{Actual migration fraction}} * 100$$

$$= \left(1 - \frac{1}{k}\right) * 100$$

$$\text{error \%} = 1.2(x_i - x_s)$$